Deanship of Graduate Studies
Al – Quds University

Geophysical and Hydrogeological Investigation of the Plio – Pleistocene Aquifer System and Potential artificial recharge sites
Jericho area

Mohammad Abdalleh Ali Sbeh

Master Thesis

Jerusalem – Palestine
1430/2009

Deanship of Graduate Studies
Al – Quds University

Geophysical and Hydrogeological Investigation of the Plio – Pleistocene Aquifer System and Potential artificial recharge sites Jericho area

Mohammad Abdalleh Ali Sbeh

Master Thesis

Jerusalem – Palestine
1430/2009

Geophysical and Hydrogeological Investigation of the Plio – Pleistocene Aquifer System and Potential artificial recharge sites
Jericho area

Prepared By:
Mohammad Abdalleh Ali Sbeh

B.Sc of Earth & Environmental Sciences in University of Al – Quds Jerusalem

Supervisor: Dr. Amer Marei

A thesis Submitted in Partial fulfillment of requirements for the degree of Master of Department of Applied Earth and Environmental science/Higher Studies/ Al – Quds University

1430/2009

Dedication

To my mother and father who give me the loyalty and hope in all my life time

To my life candle, my wife "Nisrin", you are all my reasons

To my brothers and sisters with love

To my friends who have been always supporting me

……..Mohammad

Environmental Studies
Department of Earth & environmental sciences
Deanship of Graduate Studies
Al – Quds University

Thesis Approval

Geophysical and Hydrogeological Investigation of the Plio – Pleistocene Aquifer System and Potential artificial recharge sites Jericho area

Prepared By: Mohammad Sbeh

Registration No. 20511019

Supervisor: Dr. Amer Marei

Master thesis submitted and accepted:

Names and signatures of examiners committee members are as following:

Head of committee:	Dr. Amer Marei	Signature: …….....
Internal Examiner:	Dr. Saed Al – Khayat	Signature: …….....
External Examiner:	Dr. Ziad Mimi	Signature: …….....

Jerusalem – Palestine
1430/2009

Chapter One

1. Introduction

Jericho city (Fig.1.1), the first human settlement and the oldest city in the world, it was settled by Mesolithic people of the Natufian age, 12,500 – 10,300 B.P (Neev,& Emery, 1995). The needs for water in Jericho area are critical since long time ago. Water was mainly used in the field of agriculture as the main economical sources; nevertheless, it is also used for the municipal uses. Site location and the unique climatic nature make the agricultural activities highly important in the future of Jericho economy. Nowadays, agricultural activities in Jericho area are facing major and critical issues in water sacristy; it is the main obstacle in any future sustainable development for the area. Water sacristy is reflected throughout the highly shortage in water quantities and the dramatic degradation of water qualities.

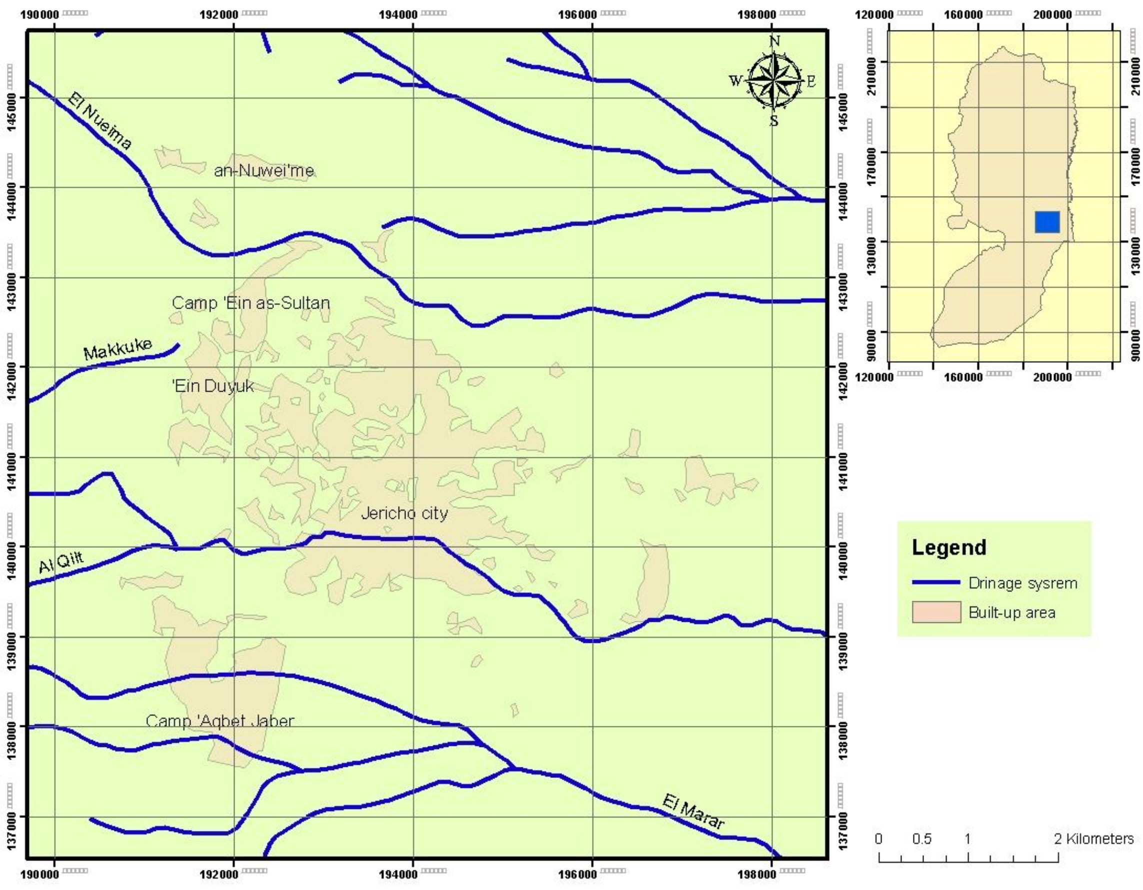

Figure 1.1 location of the study area.

Jericho district is located in the Palestinian side of the Jordan Valley. It lies in the eastern mountains foot of the mountain ridge. It bounded by the Dead Sea in the south, Marj Na'jah in the north, eastern mountain cliffs of the mountain ridge in the west, and Jordan River in the east (Fig.1.1). Jericho located between 100 – 350 meters below sea level (m.b.s.l). It is sited 10 km south of the Dead Sea and 7 km west of Jordan River (Fig.1.2).

A semi-arid climate characterized the metrological setting of the study area. The annual average precipitation rate ranging between 120 – 150 mm/a. the annual temperature ranges between 24 – 30 °C (Arad, 1967, ARIJ, 1995). Two winds direction affected Jericho area a long the day time, one comes from the Dead Sea with average speed of 3 m/s in the morning time, in the evening time a north – west wind blowing toward Jericho area within an average of 5 m/s, the maximum wind speed is measured at 15 m/s in the spring time (ARIJ, 1995).

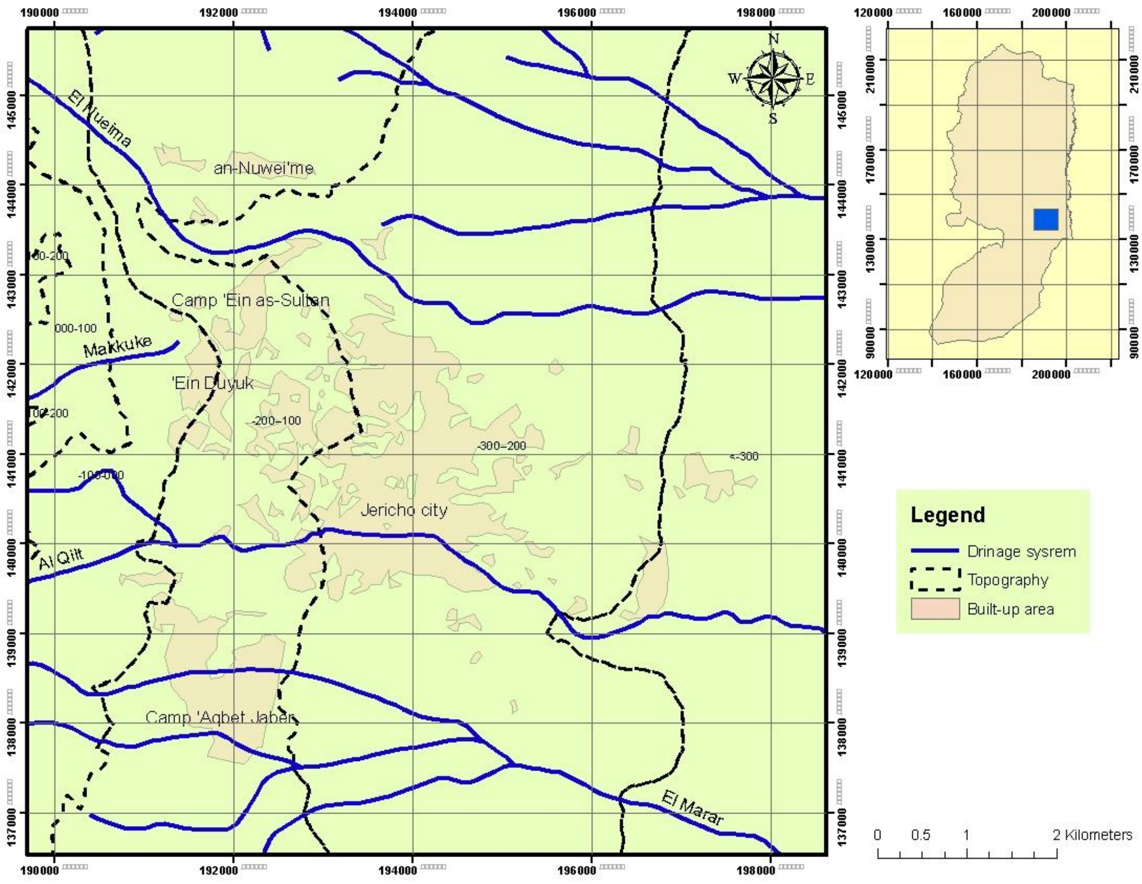

Figure 1.2 Topography of the study area.

Jericho district occupy about 35,330 hectares (353,300 dunums), there are six major build up areas which is Jericho city the only city in the district, the three villages are Dyouk, Nuwe'emah, and Auja. In addition there are Ein Sultan and Aqbet Jaber refugee camps (Fig.1.2). Cultivation activities in Jericho areas are mostly depending on the groundwater irrigation, spatially in the summer time. The total cultivated area in Jericho district is about 2419.4 hectares (Khayat , 2005).

Water resources in the study area (Jericho city) are coming from two main sources. The first one is the Surface water of the winter flooding wadis and the discharge of located springs. The second source is the groundwater which located in the local aquifer of Jericho city, this aquifer is mainly composed of alluvial deposits of the ancient wadis and the evaporated salts of the Lisan Lake. (Fig.1.3)

Surface water, includes the surface runoff of Wadi Al-Qilt and Wadi Nuwe'emah. In addition, the distributing channels of Sultan spring. Significant amount of water are coming from the surface water, nevertheless, the amount of useful water which could be driven to irrigation from this source is significantly small comparing to the groundwater useful volume. This is due to the high evaporation rate (2,085) (PCBS, 2007) and the absences of storing structures.

The estimated water volume coming from Wadi Al-Qilt only is ranging between 7 – 15 MCM/a. While less amounts comes from wadi Nuwe'emah. Sultan spring, Dyouk spring and Nuwe'emah spring. This water is distributed throw canal distribution network into the field of Jericho for irrigation. Some water volume of Sultan spring used for the municipal purposes.

Second water source is coming from the shallow groundwater Plio – Pleistocene aquifer, water have been abstracted from this aquifer since the early of sixties. Many wells were drilled all over the Jericho city. This aquifer is mainly recharged by the surface runoff of Wadi Al-Qilt (Marie, 2005). In addition, significant volume comes from the leached water of Sultan spring discharge and the Distributed network canal (Khayat , 2005).

1.1 Problem identification

Agriculture activities are the main income source in Jericho economy. Irrigated cultivation areas are heavily used, mostly in the summer time. Regarding the low precipitation rate (150 – 250 mm/a), irrigated water abstracted from the local aquifer (Arad, 1967, 1965. ARIJ, 1995).

Many wells were drilled since the late of 1960s. The depth of these wells are ranging between 80 to150 m. the total abstracted volume were estimated to be 3.5 MCM/a, this volume were abstracted throw 90 wells which located all over the Jericho city area.

A dramatic dropdown in the water table were identify in the last three decades, the total abstracted volume decreases to less than 2.0 MCM/a. Water table dropdown in many wells reaches more than 30 m and some wells already dried up.(PWA, 2002).

However, chloride content rose up to 2600 mg/l, which means that over pumping is not the main reason for salinization of the groundwater. (Marie, 2005) discussed the issue of the limited recharge possibility due to the limited recharge zones at the floor of Wadi Al-Qilt that cross the Plio – Pleistocene aquifer in 7 km along the Jericho area. (Gottman, 2005) suggest three sources for the high Cl concentration, anthropogenic effects of sewage inflow, agriculture backflow, and deep brine water and dissolution of salts from Lisan Layers.

Isotopes analysis summarized that the origin of water in this aquifer is meteoric with an age of less than 60 years. (Marie, 2005) hypothesize that during the last 100 years recharge took place at the same place available today and this water accumulated after drilling many wells during the sixties. Good water quality was abstracted at the beginning and then degraded continuously because of the limited recharge water. The reason for groundwater degradation is the limited annual recharge which could be less than 1 (MCM/a). there for the abstracted volume dropdown to less than 2 (MCM/a) from the Plio – Pleistocene aquifer.

1.2 Hypotheses:

In order to achieve the study goals the following hypotheses are developed, these hypotheses are constructed with referenced to the literature review and the pre - investigation of the currant problem among area. Hypotheses of the study are listed below:

1- The recharge mechanism through the floor of the wadi occurs in specific location with different chemical constituents and isotopes signatures.
2- Low recharge rates occurs due to the limited contact between the wadi floor and the aquifer.
3- Increase the recharged volume could be occurring through the increasing of the retention time for runoff water in definite sites.
4- New recharge gravel layers could be presents in the adjacent sites of the wadi which might be the old sediments of the old wadi trace.
5- The process of deep saline up coning which mentioned in the previous studies is controlled by a geological structure.

1.3 Objectives

Main objective

The overall objective of this study is to identify and investigate the potential recharge sites along the floor of Wadi Al – Qilt in order to select these sites for introducing the artificial recharge technique.

Specific objectives

1. To identify the aquifer (gravel) thickness and spatial distribution along the wadi.
2. To determine the recharge zones / zone along wadi.
3. To identify the depth and potentials of the rechargeable layer / layers.
4. To identify the most suitable site \ sites for implementing the artificial recharge.
5. To investigate the physical properties of the Wadi sediments

Chapter two

2- Literature review

The Dead Sea Rift Valley is the deepest inland depression on the earth, attaining a depth of about 800m (m.b.s.l) in the northern basin of the Dead Sea (Neav & Emery, 1967). Sediments accumulated in the Jordan Rift Valley depression are from the Dead Sea group and include evaporates, carbonates and terrigenous materials, Holocene and late Pleistocene fan-deltas are very common deposits along the western margin of the Dead Sea (Begin, 1974; Bender, 1974).

Recharge has been defined as "the entry into saturated zone of water made available at the water – table surface, together with the associated flow away from the water table within the saturated zone" (Freez and Cherry, 1979). Groundwater recharge is a key component in any model of groundwater flow or contaminant transport. (Healy and Cook, 2002). Accurate quantification of recharge rates is imperative to proper managements and protection of available groundwater resources. Water table fluctuation method (WTF) is utilized to estimate the recharge rate using water fluctuation data of the water table (Meinzer and Stearns, 1929). WTF method is applicable only to unconfined aquifers. Estimation of specific yield is also required (Bridget, 2002).

The conventional sounding techniques have been widely used in groundwater, civil engineering and environmental investigation since the twenties of the last century (Koefoed, 1979). A geo-electrical resistivity method was used to reveal subsurface structures and delineate the contaminated zones of groundwater (Arova, 1986; Mazak, 1987; Ilkisik, 1997; Monteiro, 1997, Salvany, 2004).

Resistivity methods could be utilized for groundwater investigations where good electrical resistivity contrast exists between the water bearing formation and the underlying rocks. Formations containing water of poor quality is characterized by lower resistivity compared with formation containing fresh water (Verma, 1980; Stewart, 1983; Abbas, 2004, Nowroozi, 1999).

The geological concept is of great importance for the interpretation of geo – electrical sounding curves (Flathe, 1976). Resistivity of natural water and sediments without clay may vary from 1 to 100 Ω.m while the resistivity of wet clays alone may vary from 1 to 120 Ω.m (Parasnis, 1986, Fouad, 2001). The resistivity of a layer saturated by saline water and some dissolved solids are in the range of 8 – 50 Ω.m (De Beuk & De Moor, 1969; Sabet, 1975; Zohdy, 1969, Claudia, 2003).

(Avihu, 1979) study the electrical sounding properties for Arava Valley south of Palestine, the resistivity of limestone was 150 Ω.m, also the resistivity of sand, marl – clay, gravel and saline water were 34-53, 5 – 10, 98 – 110, and less than 4 respectively.

Layer resistivity obtained by the inversion process is controlled by the resistivity of the pore water and resistivity of the host rock (Telford, 1990; Burger, 1992). 2D electrical surveys are the most practical economic compromise between obtaining very accurate results and keeping the survey costs down (Dahlin, 1996). Two – dimensional electrical imaging / tomography surveys are usually carried out using a large number of electrodes 25 or more connected to a multi-core cable (Griffiths & Barker, 1993).

(Wolfer, 1998) study the hydrochemistry of the Wadi Al – Qilt as the main drainage system between Jerusalem and Jericho. They discuses the influence of Plio – Pleistocene aquifer on the lower Cenomanian aquifer, they suggest that groundwater flow toward east. And this explains the extreme salt of the groundwater of the wells which is close to the Jordan Valley. (Tamimi, 2004; Marie & Vingosh, 2001) discuses the increase of salinity in Jericho Plio – Pleistocene aquifer. They suggest some mixing mechanism between the fresh and deep brine water.

Nonetheless, the leaching of salts within the aquifer and anthropogenic contamination of the agricultural return flow. (Hoetzl, 2005) used the hydrochemical tracer and tritium isotopes to study the salinity of the shallow aquifer of Jericho. The above conclusion were approved and discussed deeply.

Geographic Information System (GIS) provides powerful tool for Geo-electrical data analysis and interpretation (Ghayoumian, 2005). A GIS is defined as a system for input, storage, manipulation, and output of geographically referenced data, GIS provides a means of representing the real world through integrated layers of constituent spatial information (Corwin, 1996). GIS applications were applied and exercised in the field of hydrogeology, it used for groundwater data management and numerical modeling (Gogu, 2001).

Chapter three

3. Geology and hydrogeology

The geology of Jericho district is highly complicated, it is consists of three geological groups extending form west to east. Rammalh group located in western side of the Jericho area, Abu Dias group outcropped in the front of Rammalh group, and Dead Sea group are dominant in the rest of Jericho District (Fig.3.1).

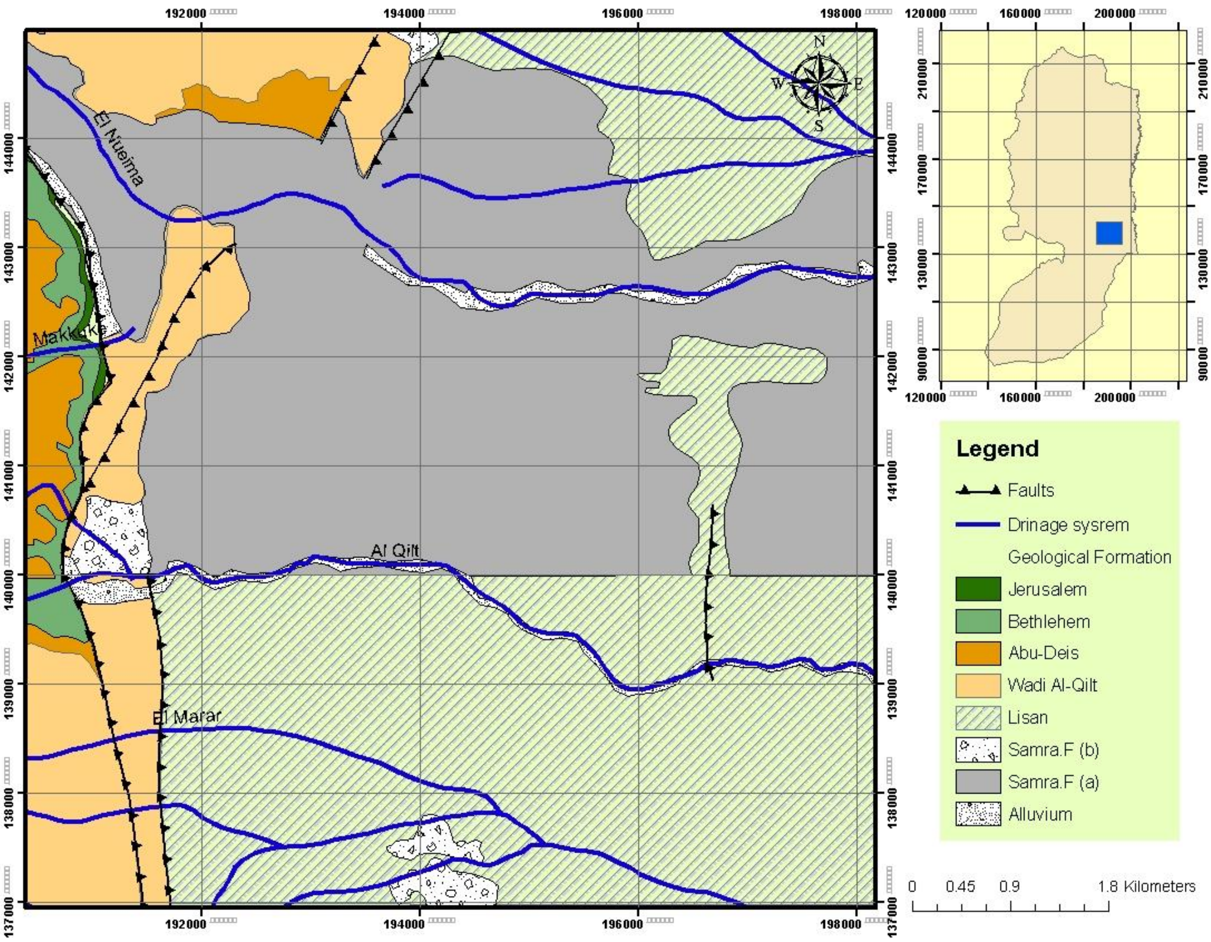

Figure 3.1 geological map of the study area (Begin, 1974, Roth, 1974).

3.1 Geological history of Jordan Valley

The study area located within Jordan Valley strike slip fault system, Jordan rift valley was generated due to the fault movement toward the north, since the Miocene age the Arabian plate has moved about 105 km relative to the Sinai plate, and formed the golf of Suez. (Neev and Emery, 1995).

Since the late Miocene Uplifting Rift shoulders bordering deep depression of the Jordan Valley Graben, it is filled with the young sediments, Upper Cretaceous carbonate, marl, clay, chalks and chart are exposed.

The geology of this study area began in the late Tertiary with Pliocene deposits, which is called the Samra formation, consisting of conglomerate, gravel, sand and some marl, this formation deposited in the wadi channel as lenses. Since the early Quaternary (Pleistocene), deposition of Lisan formation started due to the high evaporation rate of the Lisan Lake (Landmann, 2002). These deposits occupied the largest area in the Jericho basin. It consists mainly of sand, silts, marl, and gypsum (Bender, 1974; Begin, 1974). Ten thousand years ago during the Holocene age, alluvium deposits started to generate on both sides of the area's streams. (Begin, 1974)

3.2 Geological sitting of Jericho area

The lithostratigraphic units were described by (Rofe and Roffty, 1963), (Begin, 1974) (Abed and Wishahi, 1999), and (Kayat, 2005). It is characterized by the Jordan Rift Valley geological sitting. The lithostratigraphic units are described in (Table 3.1):

Table 3.1 Stratigraphic units of the study area.

Period	Epoch	Group (Israeli terminology)	Formation (Israeli terminology)	Formation (Palestinian terminology)	Hydrogeological Unit	Thickness (m)
Quaternary	Holocene		Alluvium			unexposed
	Pleistocene	Dead Sea	Lisan	Lisan		
Tertiary	Pliocene		Samra			
Upper Cretaceous	Campanian	Mt. Scopus	Mishash	Abu Deis	Aquiclude	100 -400
	Santonian - Campanian		Menuha			
	Turonian	Judea	Nezer	Jerusalem	Aquifer	90-100
			Shavta			
			Derorim			
	Upper Cenomanian		Weradim	Bethlehem	Aquitard	120 - 140
			Kefar shaul			

3.2.1 Rammalh Group

The total thickness of this group is about 700 m. the out cropping stratigraphic units are of the Upper Cenomainian – Turonian age. Two formations are outcropping in the study area:

3.2.1.1 Bethlehem formation

It is consists of well – bedded, hard dolomite and limestone with some Marl in the lower parts, forming a rugged morphology, it is crops out on gentle slopes. It is of the upper Cenomainian age. The thickness of Bethlehem formation ranging from 120 to at least 140 m (Rofe and Roffty, 1963).

3.2.1.2 Jerusalem formation

In general it is consists of hard, soft, karstic, and well bedded limestone, with some chalk and chert in the lower parts of the formation. In the lower parts of this formation limestone are colored yellow, red or gray. At the base there are chalk and nodular limestone rich with Ostried. Poorly preserved ammonites were found in the lower parts and it is marks the upper Cenomainian age (Rofe and Roffty, 1963).

The middle parts of this formation consist of dark – gray dolomite. Ammonites were found and marked the lower Turonian age. The upper parts of this formation consists of limestone, dolomite, and marl with some charts. The age of this formation is Turonian – Cenomainian. Thickness of the formation ranging from 90 to 100 m (Wolfer, 1998).

3.2.2 Mount Scopus group

During the Senonian, better circulation with the open sea was established (deepening), which indicated by the deposition of the pelagic chalk. It is of Santonian – Campanian age, mainly consists of chalk with absents of bedding. It is covers a large area of the West Bank, and also covers the western parts of the study area. It is composed of only Abu Dies formation (Rofe and Roffty, 1963, Wolfer, 1998).

3.2.2.1 Abu Dies formation

The lower parts consists of gray hard chalk and limey chalk, fossiliferouse and sometimes bituminous. The upper part consists of chalk and chart with some limestone and phosphates (Wolfer, 1998).

3.2.3 Dead Sea Group

This group crop out the majority of the study area. It is of Neogene and Quaternary age. It is mainly built of marine and continental clastic material, marine and limnic chalk, evaporites. This lthostratigraphic group composed of three distinguished formations:

3.2.3.1 Samra formation

It was deposited as marginal sediments along the Jordan Valley. The formation consists of conglomerates, sandstones and silts and is subdivided into two members Silt member with average thickness of 20 m mainly located in the western sides of Jericho city. It is composed of silt, sand, and clastic pebble lenses (Begin, 1974).

The coarse clastic member with average thickness of about 35 m, composing of sand and unconsolidated materials chiefly conglomerate and gravel. It is located near the ancient place called "Kherbet Al-Samra" to the north of Jericho city and also in the outlet of Wadi Al-Qilt (Fig. 3.1) (Begin, 1974).

3.2.3.2 Lisan formation

This formation is exposed in the eastern part of the study area as well as the whole Jordan valley rift and the Wadis. It consists mainly of laminated aragonite-chalk, gypsum and clay with some sandstone and pebble beds. The consecutive thin layers of clay and gypsum make it highly distinguishable. Lisan formation interfingers with conglomerates and silt beds of the above Samra formation. Sedimentation of the Lisan formation started 60,000 years ago (Kaufman, 1971).

3.2.3.3 Recent alluvium deposits

This formation covers the area adjacent to the Jordan Valley, nonetheless it is found in the adjacent sides of the study area streams. Ten thousand years ago during the Holocene age, alluvium deposits started to sediment on both sides of the area's streams. It is located all over the area mixing with the sub and top soils; the thickness of this formation is ranging between 5 to 12 m (Begin, 1974).

3.3 Hydrogeology

3.3.1 Upper Cretaceous carbonates aquifer

This aquifer is of Cenomanian to Turanian age. Composed of Karstified rocks, it is represents one of the most important water resources in the region. The thickness of the upper Cretaceous aquifer is about 170m in the western of the study area. It is composed of the stratigraphic formations Bethlehem Formation, and Jerusalem Formation (Table 3.1). The outlets of this sub-aquifer are in the Jericho springs and Wadi Al – Qilt Springs and Wadi Nuwe'meh Springs in the lower part of Wadi Makuk, close to the Jericho Fault (Wolfer, 1998).

3.3.2 Jordan Valley deposits [Dead Sea Group]

Two Dead Sea group aquifers are located in the Jericho area these are:

a) <u>The Holocene or sub-recent Alluvial aquifer</u>:

It is distributed mainly in the Jordan Valley and neighboring areas. It is built up of sub-recent terrigenous deposits formed along the outlets of major wadis. These alluvial fans are still under accumulation after large floods and consist of debris from all neighboring lithologies. The total thickness is maximum near the rift margins can reach up to high values, thinning out towards the centre of the rift basin. The alluvial aquifer often directly overlies the Pleistocene gravel aquifer and by that is hydraulically interconnected with this aquifer (Wolfer, 1998).

b) Pleistocene Lisan – Samra aquifer:

This includes three members [Samra coarse clastic, Samra silt and Lisan] of the Pleistocene Samra aquifer are a lateral facies succession from terrestrial/fluvial, to deltaic/limnic and limnic/brackish lake environments. They reflect the Plio-Pleistocene depositional conditions of the Lisan Lake. Lisan, the marl, gypsum and silt unit were generally considered an aquiclude. It is distributed mainly towards the middle of the graben. Samra formation consists of two members: A silt member underlying or interfingering with Lisan and a coarse clastic member further to the west that predominantly consists of gravel, interbedded with clay, sand and marl horizons (Khayat, 2005).

3.3.3 Hydraulic separation between the two aquifers

In the west of the Jericho , faulted blocks of the impermeable Senonian chalk (Abu Dies formation) prevent lateral flow of ground water from the Upper Cretaceous aquifer to the Plio-Pleistocene shallow aquifer system (Golani, 1972). However, the water from the Upper Cretaceous aquifer leak into the Plio-Pleistocene aquifer along the Dead Sea (GAVRIELI, 2001).

The Plio-Pleistocene aquifer shows piezometric level variation between -300 to -337. The groundwater flow from west to east and also toward southeast. Water level show general decrease toward east. The changes in aquifer hydraulic properties from west to east, as well as the high abstraction rate are the main results for the decline in the groundwater level (Khayat, 2005).

3.3.4 Wells

A large number of active boreholes have been drilled in the study area, mostly at two locations. The first location is locate along the foothills and on the mountain tops exploit water from the Regional upper Cretaceous Aquifers. The wells tap water from the calcareous aquifers and are characterized by low to moderate discharge [100-300 m^3/hr] and by deep static water levels (Guttman, 2005). These wells are located close to the recharge area and suffer from large water level fluctuation that sometimes [especially during drought periods] influence their discharge. The water is characterized by low salinity.

The second group of wells is located in the Jordan Valley abstract water from the Jordan Valley deposits. The wells are shallower than the first group. The average depth is around 100 meter. Their discharge is also smaller than the discharge of the first group and is only some tens of m^3/hr (ARIJ, 1995). The Jordan Valley deposits receive water from different sources such as lateral flows from the surrounding mountainous aquifers, infiltration of precipitation and flood water, irrigation return flows and ascending of saline water from deep aquifers.

The water level dropped and these saline water flows towards the pumped wells raising the salinity of the water (Guttman, 2005). Water table (2006) are shown in (Fig. 3.2), comparing the groundwater table in 2006 to the year 1997 which generated by (Khayat, 2005), it is clear that there is a general dropdown in the water table by more than 25 m.

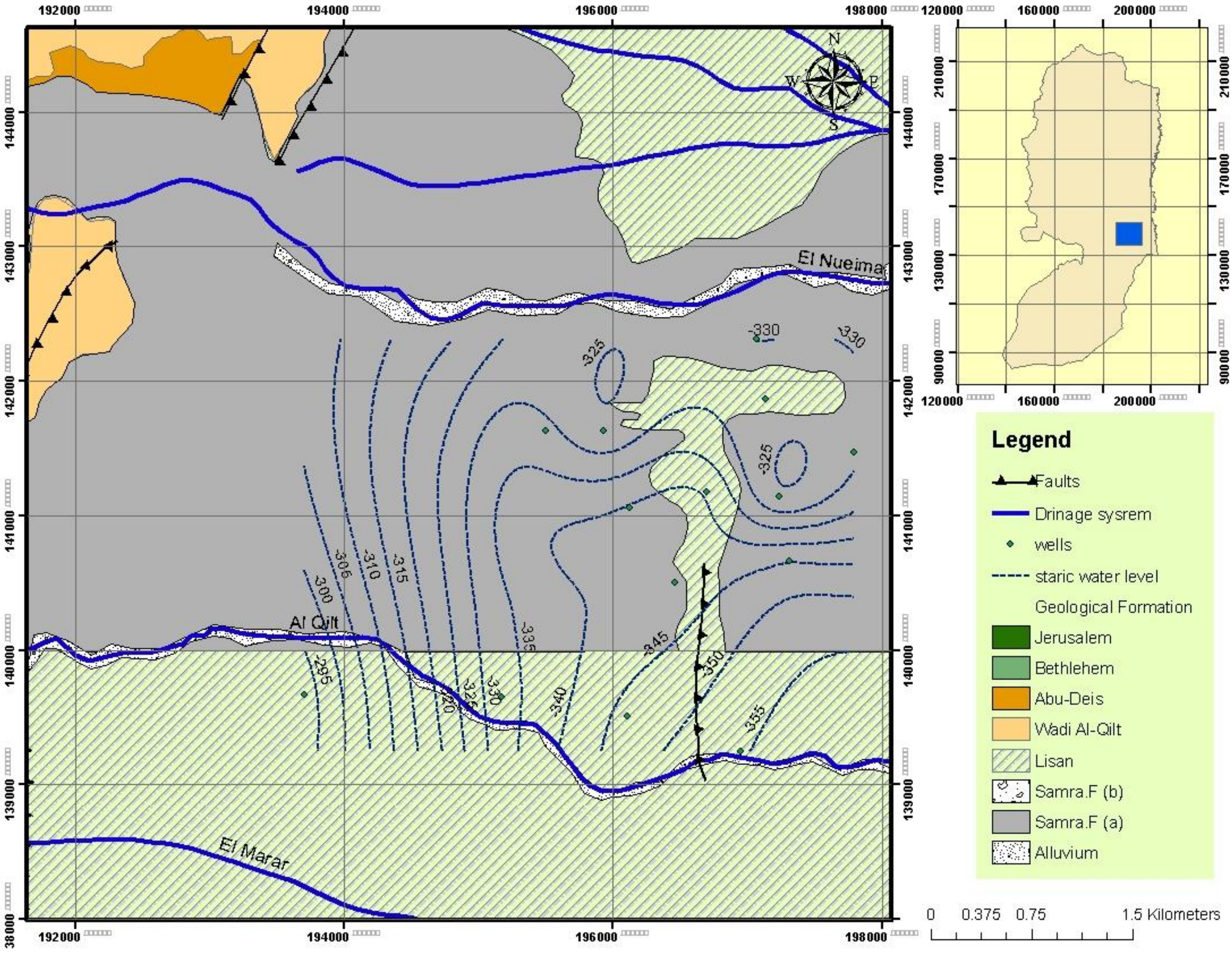

Figure 3.2 contour map of the static groundwater table (2008).

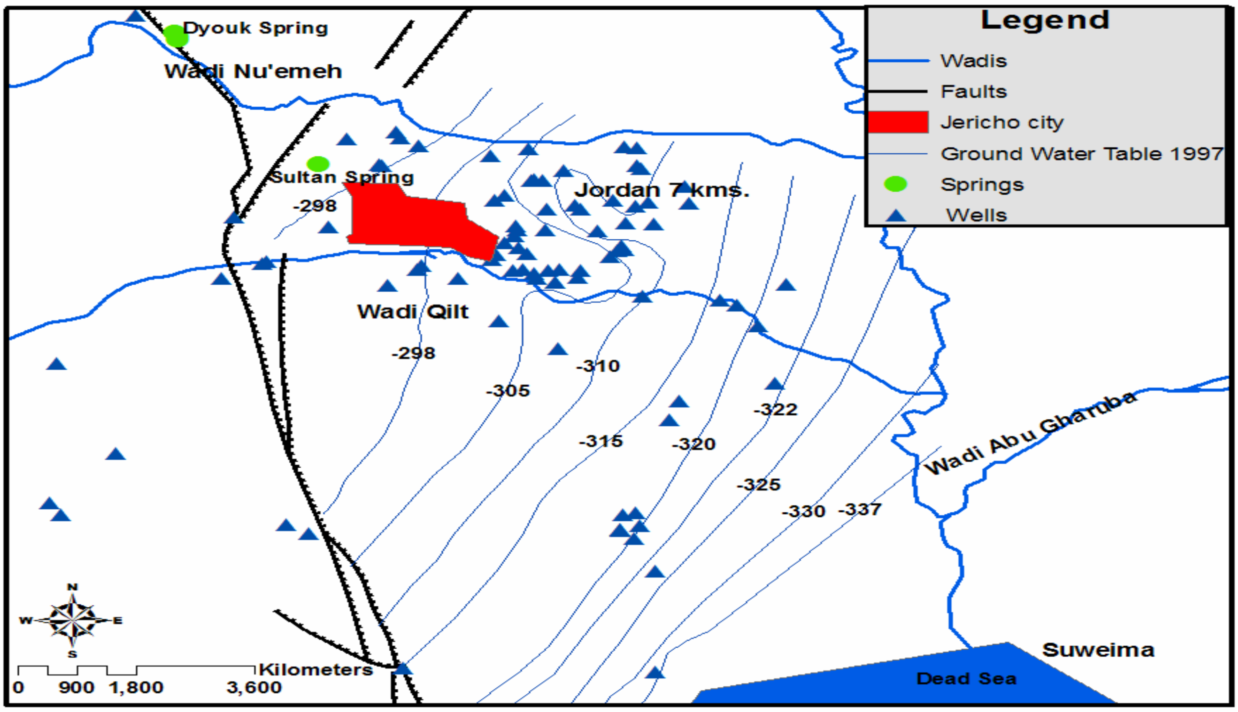

Figure 3.3 contour map of the static groundwater table (Khayat, 2006).

3.3.5 Springs

Four springs located within the study area of Jericho. It is Sultan spring, Duyuk Spring, Nuwe'meh Spring and Shosha Spring.

a) Sultan Spring

Sultan is located 2 km NW of Jericho and discharges at an elevation of -215m m.b.s.l. The spring was used for 10,000 years for domestic water supply of Jericho. The outflow of the spring is structurally controlled by a large SW-NE trending normal fault postulated by (Wolfer, 1998) and the spring can be classified as a fault spring. The mean annual discharge of Sultan spring is 5,780,000 m^3/year (Nuseibeh and Nasser Eddin, 1995).

b) Duyuk Spring, Nuwe'meh Spring and Shosha Spring

Discharges at the margin of the Eastern Slopes 3.7 km NW of Sultan spring. The system consists of three springs emerging at -110m m.b.s.l (BEINHORN, 2004). The outflow of these is collected in a concrete channel. The water is used by farmers for irrigation purposes. The average annual discharge of Duyuk spring is 5,000,000 m^3/a, while the average annual discharge for Nuwe'meh spring is ca. 2,700,000 m^3/a and for Shosha is about 668,000 m^3/a (Israeli Hydrological Survey)

Chapter four

4. Methodology and experiment design

Design of the conceptual experimental sequences of the thesis theory was goes throw four different investigation methods. These methods were used to investigate the storage capacity of Plio – Pleistocene aquifer. Wells hydrographs analysis using water table fluctuation method (WTF) (Meinzer and Stearn, 1929). The permeability of the gravel aquifer estimated by the pervious method for 10 years historical groundwater table data are used for the estimation of aquifer permeability's. Wells are randomly selected, the selection of these wells are mostly controlled by the data availability.

Geo-electrical investigation was curried out using 19 vertical electrical sounding points (VES) along Wadi Al-Qilt. This technique enables the construction of geo-electrical profile cross the wadi for identifying the electrical properties of the different lithology. Since the geo-electrical profile created the lithological profile, wells lithology is constructed including thickness of the different strata. Nevertheless, recharge volume and storage capacity calculated straightforward.

10 samples of soil were collected and sieve analysis was conducted. Chosen of Soil sampling sites were carried out with respect to the distance interval. Physical properties of the sub-surface soil calculated using sieve analysis technique. Runoff infiltration was calculated and compared along the Wadi.

Geo – chemical analysis were spatially distributed to generate the contour maps for EC, Cl, Na, SO_4^{-2}, and Tritium.

Raster model built up for (R) recharge rate spatial distribution among the study area using geographic information system (GIS), the model companies resulted hydraulic data of the Plio – Pleistocene aquifer. Layers of vector model created for wells, buildup areas, hydraulic network, topography, and geology. GIS site selection was used to determination the best site/sites for applying artificial recharge. Selection criteria determined from the hydraulic raster model.

4.1 Water Table Fluctuation method (WTF)

Recharge has bee defined as "the entry the saturated zone of water made available at the water – table surface, together with the associated flow away form the water table within the saturated zone" (Freeze and Cherry, 1979). Accurate quantification of recharge rates is imperative to proper management and protection of valuable groundwater resources.

WTF method conceder among the most widely applied method for estimating recharge rate. This is likely due to abundance of available groundwater – level data and the simplicity of estimating recharge rates from temporal fluctuations. It is applicable only for unconfined aquifers.

WTF method is based on the premise that rises in groundwater levels in unconfined aquifers are due to recharge water arriving at the water table. An estimation of specific yield is required in order to estimate the recharge rates. Recharge is calculated as:

$$R = (\Delta h/\Delta t) * Sy \quad \ldots\ldots\ldots\ldots\ldots\ldots (1)$$

Where:

R (m/h): recharge rate, Δh (m): water table height, Δt(h): time, Sy: specific yield.

$$\text{Recharge Volume} = \text{Surface area } (m^2) * R.R \text{ (m/day)} * \text{Flooding days} \quad \ldots\ldots\ldots (2)$$

Wells hydrographs generated for 14 wells all over the Jericho area. Long term hydrograph created for these wells, hydrograph starting from the hydrological year (1989-1990) and ending in (1998-1999) except in the wells 19-13/070, 19-13/029, and 19-13/012T due to the data availability, monthly records of water table and rainfall are plotted to calculate the recharge rates values and to estimate Lag time for each well.

4.2 Geo – Electrical Sounding (electrical resistivity)

The electrical resistivity method was applied in this investigation. This method is widely used for soil or rock lithology identification, groundwater investigation, and saltwater/freshwater interface definition. Application of the surface resistivity method requires that an electrical current be injected into the ground by a pair of surface electrodes. The resulting potential field (voltage) is measured at the surface by a voltmeter between a second pair of electrodes. The subsurface ground resistivity can be calculated by using the electrode spacing, geometry of the electrode positions, applied current and measured voltage. (Telford, 1990)

Earth resistivity measurements are reported in the units of ohm-meters. The depth of investigation of ground resistivity is related to the spacing of the electrodes and electrodes configurations (array type); it may also vary depending on the subsurface conditions.

The choice of the best array type for a field survey depends on the type of structure to be mapped, the sensitivity of the resistivity meter and the background noise level. Practically, the arrays that are most commonly used are (a) Wenner array, (b) Schlumberger array, (c) dipole – dipole array, (d) pole – pole, and (e) pole – dipole array (figure 4.2.1). Among the characteristics of an array that should be considered are (i) the depth of investigation, (ii) the sensitivity of the array to vertical and horizontal changes in the subsurface resistivity, (iii) the horizontal data coverage and (iv) the signal strength. (Loke, 2001).

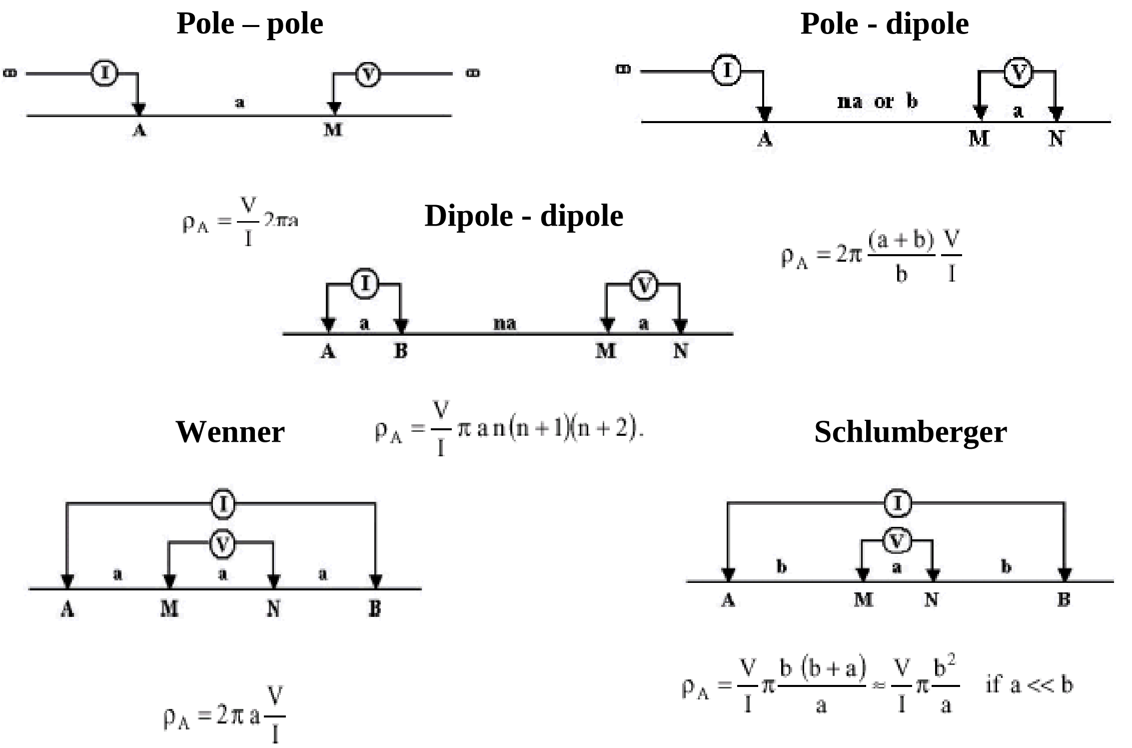

Figure 4.2.1 electrical sounding arrays.

The Wenner array is an attractive choice for a survey carried out in a noisy area (due to its high signal strength) and also if good vertical resolution is required. The dipole – dipole array might be a more suitable choice if good horizontal resolution and data coverage is important (assuming the resistivity meter is sufficiently sensitive and there is good ground contact).

Schlumberger array is a reasonable all-round alternative if both good and vertical resolutions are needed, particularly if good signal strength is also required. If the electrical system with a limited numbers of electrodes the pole – dipole array with measurements in both the forward and reverse directions might be a viable choice. For surveys that required small electrodes spacing and good horizontal coverage the pole – pole array might be a suitable choice (Loke, 2001).

Apparent resistivity of the layered rock can be obtained by the following equation:

$$\rho = k\,.\Delta V/I \;\ldots\ldots\ldots\ldots\ldots\ldots\ldots.\; (3)$$

Where:
ρ: apparent resistivity, k: geometrical factor, ΔV: potential or voltage differences, I: electrical current.

4.2.1 Vertical Electrical sounding (VES)

Also called depth sounding or electrical drilling. The method of vertical electrical sounding provides detailed information on the vertical succession of different conducting zones, their individual thickness and true resistivity.

Very simple theory stands behind this technique, which can be generalized by the electrical segregation of the successive lithological stratification. Electrical current passed throw the different geological formation, nevertheless it goes throw the different lithological strata's. Each lithological composition resisted the passing electrical current in different potential (Telford, 1990).

However, different lithological compositions resist the electrical current in a different manner; this is reflected in a different resistivity values given by the different lithological stratification (Loke, 2001).

Since each similar lithological composition marked with specific electrical resistivity the aquifer successive stratification could be easily differentiated. Vertical electrical sounding (VES) is one of the most used techniques in electrical sounding. (Keofored 1979), it has been used intensively in the groundwater and subsurface geological studies (Arova 1986, Solvay, 2004).

Vertical Electrical Sounding (VES) enabling the delineation of the aquifer lithological thickness. Nonetheless, the extinctions of the geological formation and the subsurface structures could be also determined by the above mentioned method. (Abbass, 2004).
The measurements are made with a four-electrode array, consisting of two current and two potential electrodes (Schlumberger array). The essence of VES is to expand the

electrode array from a fixed center. Current reached more depth by increasing the spacing between the outer electrodes; consequently the resistivity of the different successive horizontal rocks layers will be reached. Different lithological successive means different electrical response (different resistivity).

Geo – electrical profiling is constructed by correlating the different VES points. Matching the similar resistivity layers in many VES points to generate a horizontal resistivity profile.

4.2.2 Field experimental design

19 VES measuring points are accomplished in Jericho field using PASI instrument; the data which the instrument measure is ΔV, I, $\Delta V/I$. Schlumberger array is used in the 19 VES points. The distance between each VES points is about 650m. The array spacing distances are illustrated in (Table 4.2.1). IPI2win electrical sounding interpretation software is used to generate the geo – electrical profiles.

Table 4.2.1 Electrical sounding spacing.

Spacing number	AB/2	MN/2
1	1	0.2
2	1.5	0.2
3	2	0.2
4	3	0.2
5	4	0.2
6	4	1
7	5	0.2
8	5	1
9	7	1
10	10	1
11	10	2
12	10	1
13	15	2
14	20	2
15	30	2
16	40	2
17	30	10
18	50	2
19	50	10
20	70	10
21	100	10
22	100	20
23	150	10
24	150	20
25	200	20
26	300	20
27	400	20

4.3 Soil analysis

10 soil samples was sampled, all the samples was tacking at 40 cm depth form the sediments of Wadi Al-Qilt floor. The distance between sampling sites are about 650 m. Sieve analysis was applied to estimate the physical properties (permeability, effective grain size, uniformity coefficient) of the soil samples.

The weight of each soil samples is 500 gm. Each sample was dried to the room temperature for 24 hours. Sieve analysis was accomplished using 11 sieve mesh size, starting with 2.00 mm, 1.600 mm, 1.00 mm, 0.710 mm, and 0.500 mm, for the sand values. For the silt grain size the mish size was 0.250 mm and 0.200 mm. less than 0.200 mm mesh size is consider as clay, the mesh sizes for clay classification are 0.160 mm, 0.090 mm, 0.075 mm and 0.065 mm.

Laboratory sieve analysis is the most widely used method to determine grain size distribution. A sediment sample of 500 gm weights is placed in the top of a set of the 11 sieve with decreasing mesh diameters. The set is then placed in the mechanical shaker for up to 10 minutes; this will separate the sample into fractions which are retained at individual sieve.

The weight of each fraction is measured and expressed as percent of the initial (total) weight of the sample. The grain size distribution curve is plotted on a semi logarithmic paper. The cumulative percent coarser by weight is plotted on the vertical arithmetic scale, while sieve opening diameter is plotted on the horizontal logarithmic scale. The cumulative percent finer by weight can be used to plot the curve as well.

It is common practices to have two vertical arithmetic scales: one (usually on the right) with the cumulative percent coarser than the sieve diameter, and the other (usually on the left) with accumulative percent finer than the sieve diameter. Logarithmic scale of the grain size decreases from the left to right.

In order to calculate the permeability for the soil samples uniformity coefficient (U) should be determined by the equation:

$$U = d_{60} / d_{10} \ldots\ldots\ldots\ldots\ldots\ldots\ldots\ldots\ldots\ldots \quad (4)$$

Where:

U is the Uniformity coefficient, d_{60} is the sieve opening size (diameter) which allows 60 % of the sample by weight to pass and therefore retains 40 % of the sample. d_{60} is easily determine form the grain size curves (Fig.4.3.1). d_{10} is the sieve diameter which allows 10 % of the sample to pass, thus retaining 90 %.

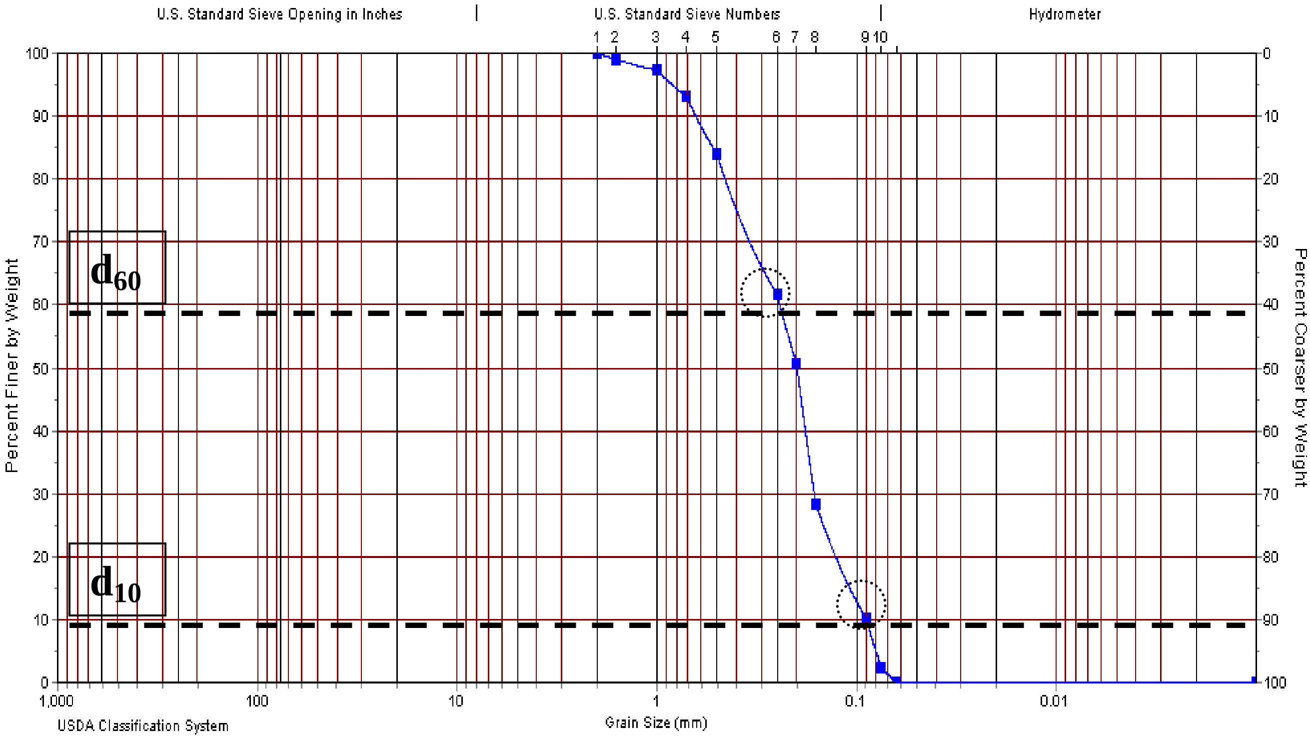

Figure 4.3.1 obtaining d_{60} and d_{10} by the grain size curve.

It is very easy to calculate the permeability after the obtaining of d_{60} and d_{10} values. Permeability was calculated in reference with three empirical formula, Breyer, Hazan, and Kozeny equations. The permeability was chosen according to the formula applicability. Hazen equation is applicable for sediments with coefficient of uniformity less than 5 (U<5) and effective grain size between 0.1 and 3 mm (0.1mm<d_{10}<3mm). Konezy equation is applicable for coarse sand, and Breyer equation is applicable for 1<U<20 and 0.06<U<0.6 which makes it useful for analyzing heterogeneous porous media. (Neven, 1997). In the study case, the most useful equation is the Breyer one, which is very good for the heterogeneous components of the Plio – Pleistocene aquifer.

Breyer equation:

$$K = (g/v)\, C_b\, d^2_e \ldots\ldots\ldots\ldots\ldots\ldots\ldots\ldots \quad (5)$$

Where:

K: hydraulic permeability, g: is the gravitational acceleration, v: is the kinematic viscosity of the fluid, C_b: is a dimension less coefficient which depend on the porous medium such as grain shape, structure, heterogeneity, etc…,d_e: is the effective grain size (usually d_{10}). C_b could be calculated by using the following equation:

$$C_b = 6 * 10^{-4} \log (500/U) \ldots\ldots\ldots\ldots\ldots\ldots \quad (6)$$

The results of the sieve analysis of Wadi Al – Qilt samples are tabled in chapter 5 (results), and the grain size curves were arranged in additional index in the end of this thesis. Following the permeability determination it is important to classify the texture of the sampling sediments, and correlate K values with the sitting texture of the sediments. TALwin software ver.4.2 was used to classify the sediments samples texture. USDA texture classification scheme is used in order to establish the sediments classification (Fig. 4.3.2).

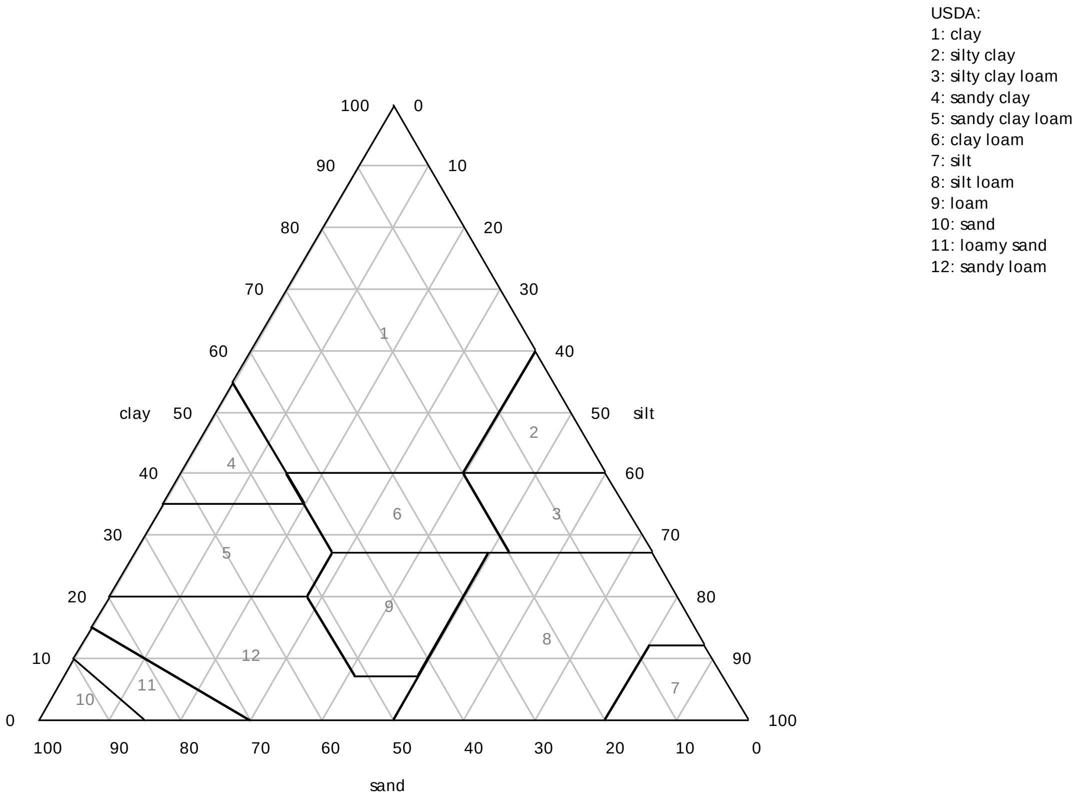

Figure 4.3.2 USDA soil classification scheme

4.4 GIS geo – data model and analysis

Geographic information system GIS has been used for data management and analysis. ARCGIS Ver.9.2 is choosing for data manipulation and analysis. This software provides power full tools for simulation and database management system to relate any data which related to a geographic location. Two types of data models are used. Vector data model and raster data model.

Vector data model is used in modeling the discrete features such as groundwater wells, VES measuring points, soil samples location, streams, rivers, and outcropping geology.

Raster data model is used in modeling the continuous phenomena such as, chemical distributions in groundwater, recharge rate distribution over Jericho Plio – Pleistocene aquifer, and soil permeability.

Chapter six

6. Discussion

Recharge tock place along Wadi Al – Qilt in different quantities. Many factors controlling the recharge volume along the wadi, such as the type of sediments in the wadi floor, the width of the wadi which filled with surface runoff during the flooding days, the runoff quantities, and the water depth in the wadi during the flooding time.

According to the recharge rate distribution map (Fig. 5.1.1), Wadi Al – Qilt (Jericho area) separated into three recharge rates. Intermediate recharge rate occurs in the first 3000 m of the wadi, highest recharge rate occurs in the middle part of the wadi along 2650 m, and at the last 1000 m of the study area the lowest recharge rate is occurs (Fig. 6.1)

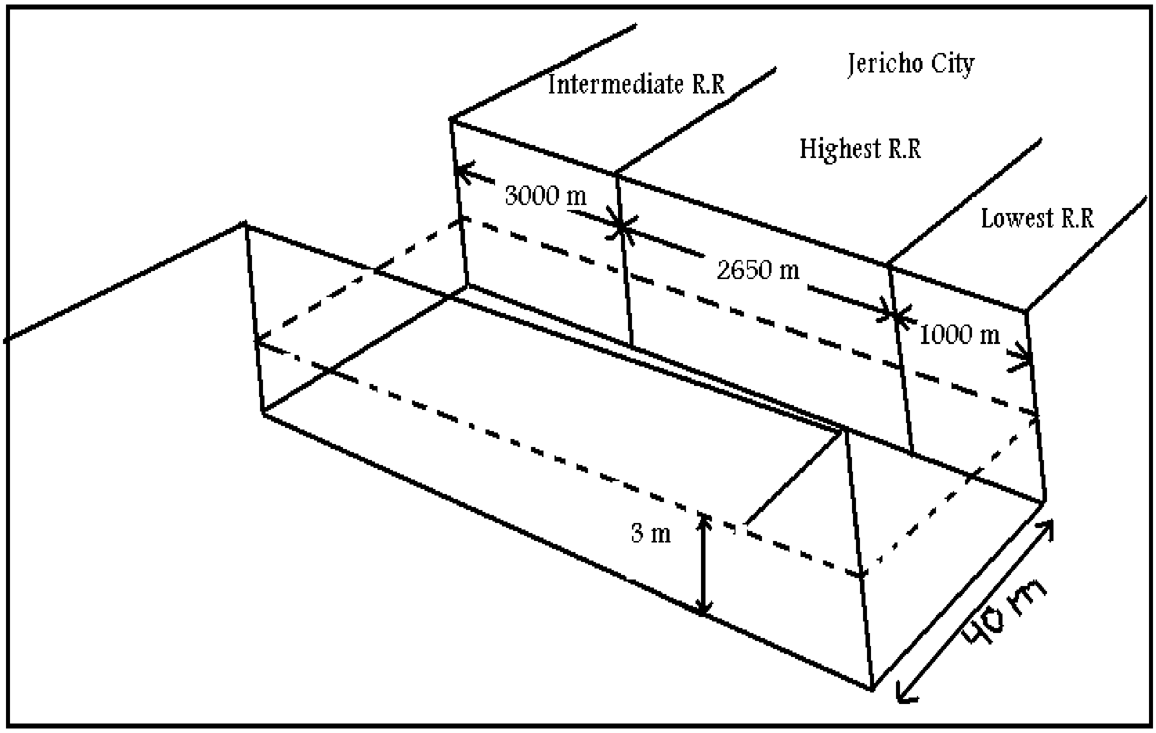

Figure 6.1 Wadi Al – Qilt (Jericho area) general dimensions and recharge rates.

Recharge volume is calculated according to the Wadi dimensions and different recharge rates which illustrate in (Table 6.1). The output recharge volume is multiply by the average flooding days which are estimated of 8 days / year.

Table 6.1 recharges volume of Wadi Al – Qilt.

Recharge rates	Wadi Surface area (m^2)	R.R (m/day)	R.V * 8 (m^3/a)
Intermediate	138,000	0.060	66,240
Highest	121,900	0.096	93,619
Lowest	46,000	0.002	736
Total			160,595

Recharge is occurs downward to the gravel layers. The upper most layers are consists of alluvium deposits with a thickness ranging between 5 m to 20 m. The alluvium layers is underline by silt layers with a thickness ranging between 20 m to 50 m. under the silt layers there are deep layers of gravel with a thickness ranging between 40 m to 100 m. Interfingaring occurs between these different layers and the Marl – Clay layers (Fig 5.2.2b). Fig. 6.2 shows the recharge diagram of Wadi Al - Qilt (Jericho area).

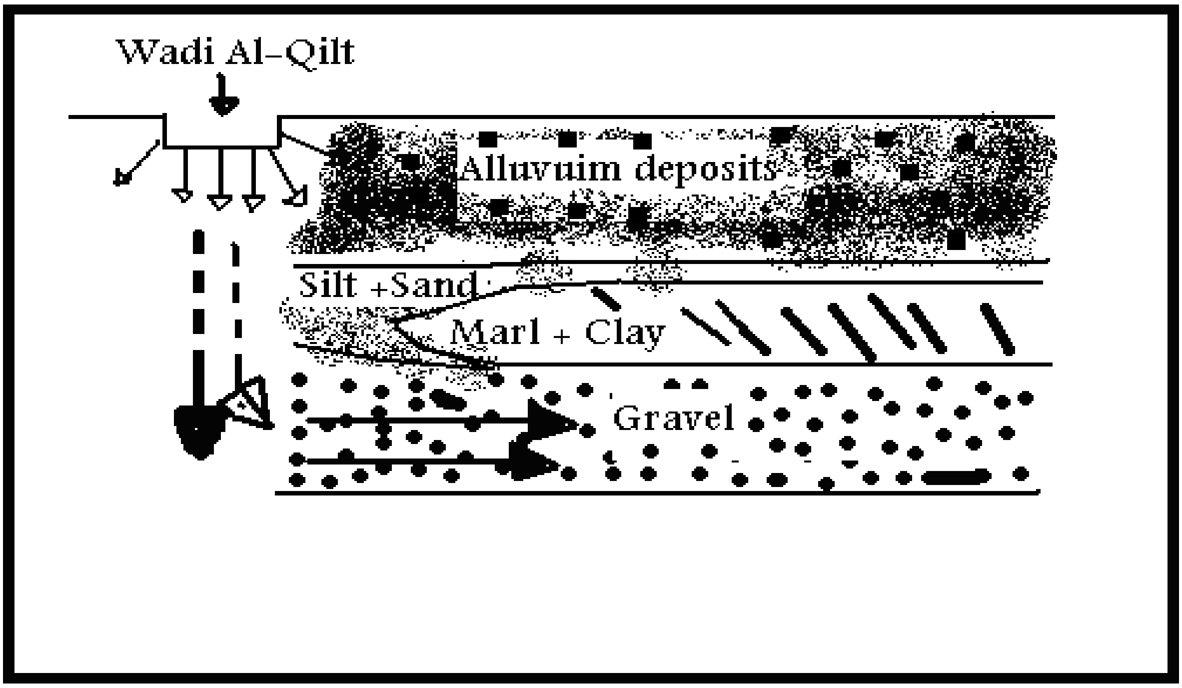

Figure 6.2 recharge diagram of Wadi Al – Qilt (Jericho area).

A new conceptual model is generating using the lithological profile of the study area. It is generated by combining the lithological profiles which resulted from the VES profiles. Many geological features are located within the study area. These geological features are:

1- Two faults are identifying within the study area (Fig.5.2.1). The first is located in the area of Aqbit Jaber camp with the following coordination 191,569 – 139,681. This fault is mapped by (Begin, 1974). It has north – south direction. The second fault is located in the area of Ketf Al- Wad. It has the following coordination 196,938 – 139,163. This fault is first time to be mapped (Fig. 5.2.1). It has north – south direction.

2- Old gravel deposits pathway (Fig. 5.1.15). This feature is buried at depth ranging between 40 to 70 m. and it has a width of ranging between 300 to 500 m. The gravel thickness of this pathway is ranging between 30 to 100 m. this theory is supported by the followings:

a) The recharge rate is the highest along the suggested pathway (Fig. 5.1.1). Recharge rates generating some type of leaner extension toward the east.

b) The gravel accumulations which identify by the geo – electrical sounding profiles (Figs. 5.2.3b, 5.2.4b, 5.2.5b). In these three lithological profiles there is a gravel mass accumulation at almost the same extent.

c) The geochemical mapping of the groundwater chlorides, Sulfates, Sodium, and Electrical conductivity shows some dilution area in the suggested gravel pathway. The concentrations of these constituents are extremely low comparing to the surrounding concentrations (Figs. 5.4.2, 5.4.3, 5.4.4, 5.4.5).

3- Saline groundwater body located in the area of Kitf Al – Wad. It is about 90 m depth. It has about 50 m thickness (Fig. 5.2.2b). This groundwater Saline body explains the suggested fresh – saline groundwater mixing phenomena (Marie & Vingosh, 2001). Mixing is occurs along the new identify fault.

The following block diagram (Fig. 6.3) is generated with supporting of the investigation information. It is clearly shows the two faults, the old pathway of Wadi Al – Qilt stream, and the saline groundwater body.

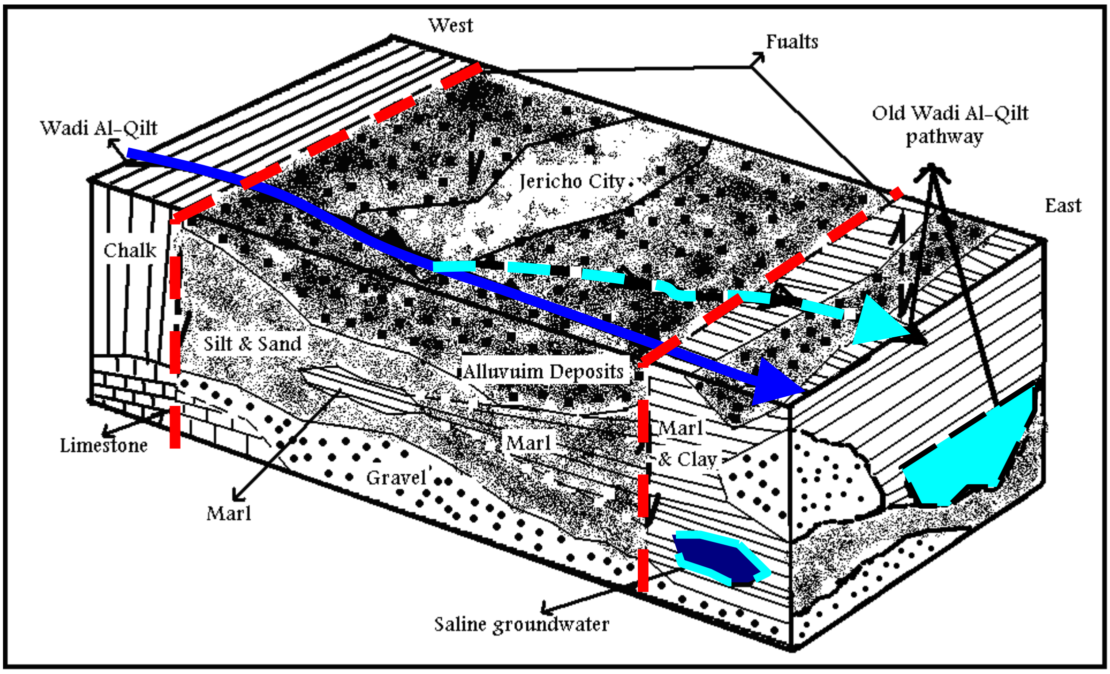

Figure 6.3 block diagram of Jericho area.

6.2 Artificial recharge site

Wadi surface sediments permeability is calculated in order to select the best artificial recharge site. It was combining with the highest recharge rates area. By the study investigation, the old Wadi Al- Qilt pathway is the highest recharge rate area (Fig. 6.3). The permeability Wadi Al – Qilt sediments is highly controlling the recharge quantities of the flooding water. Permeability of the Wadi Floor sediments is calculated using the grain size distribution curve (section 5.3.1).

The highest K values located between the sampling sites 6 and 7 (Table 5.3.3). The length of the recharging segments of the Wadi floor is 700 m. The targeted gravel sediments cover about 1,100,000 m^2. The average thickness of this gravel mass is 65m.

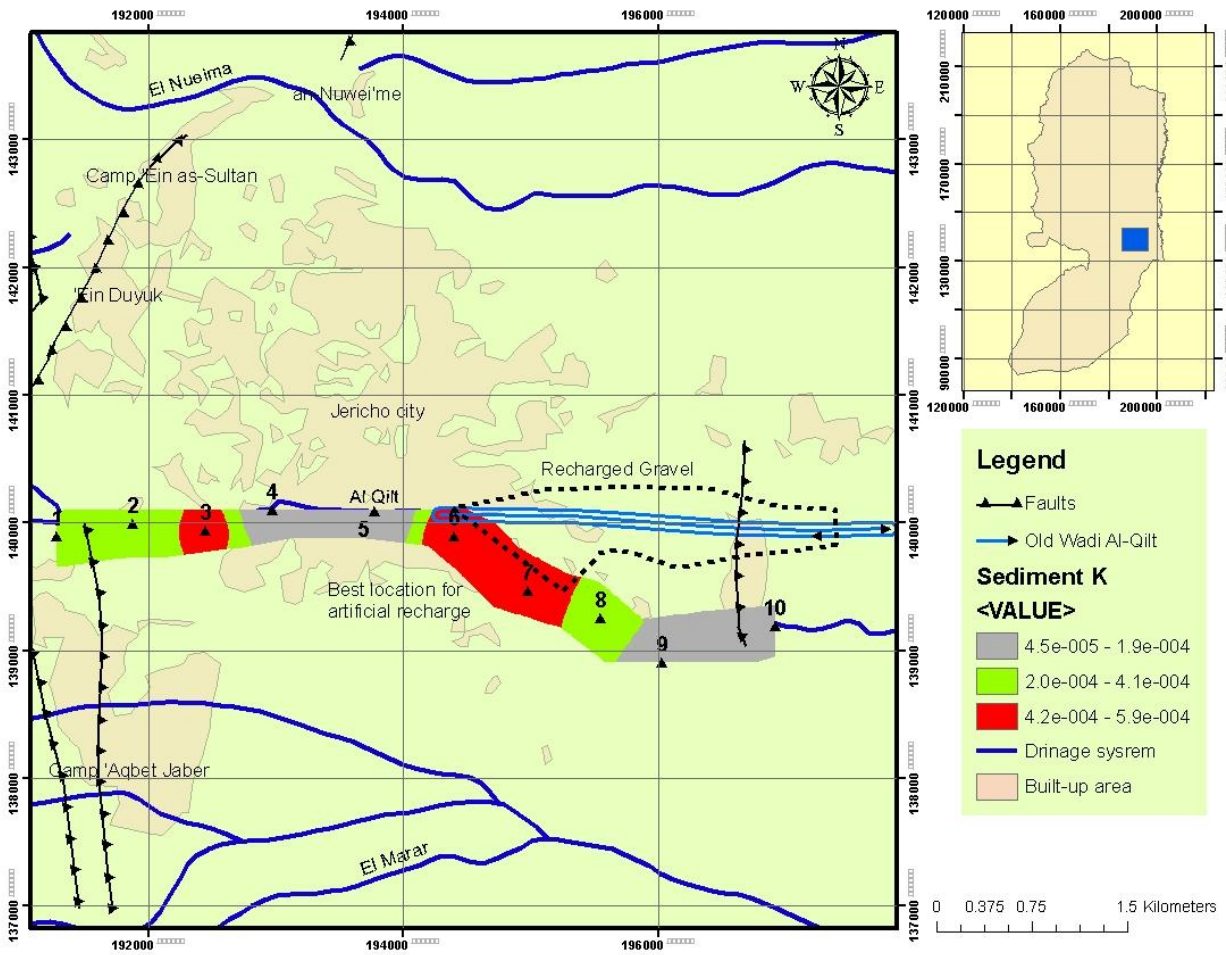

Figure 6.4 locations of best artificial recharge site and the gravel extension.

6.3 Hydrographs analysis conclusion

There are two groups of R.R values, 10^{-3} m/h indicating pure Samra gravel and sand lithology, and 10^{-4} m/h which point out the inter-fingering or inter – tanging of Lisan – Samra Lithology's. Raster model of the R.R value shows high values in Zone A and low values in Zone B (Fig. 5.1.1). By tracing the R.R value in zone A it suggest a gravel pathway which may be the resulted of raining periods of the Pleistocene age. In this period the alluvium sediments deposited in the mentioned Old Wadi Al-Quit pathway, there is 1 km shifting to the south in the new wadi.

This theory is also proved by the similarity of the water table hydrograph of the wells no. 19-14/019, 19-14/064, and 19-14/066, (Figs. 5.1.7, 5.1.9, and 5.1.10). Lag time is less than 150 days in the Samra gravel aquifer, it reaches about 410 days in the Lisan – Samra inter-fingering or inter – tanging areas.

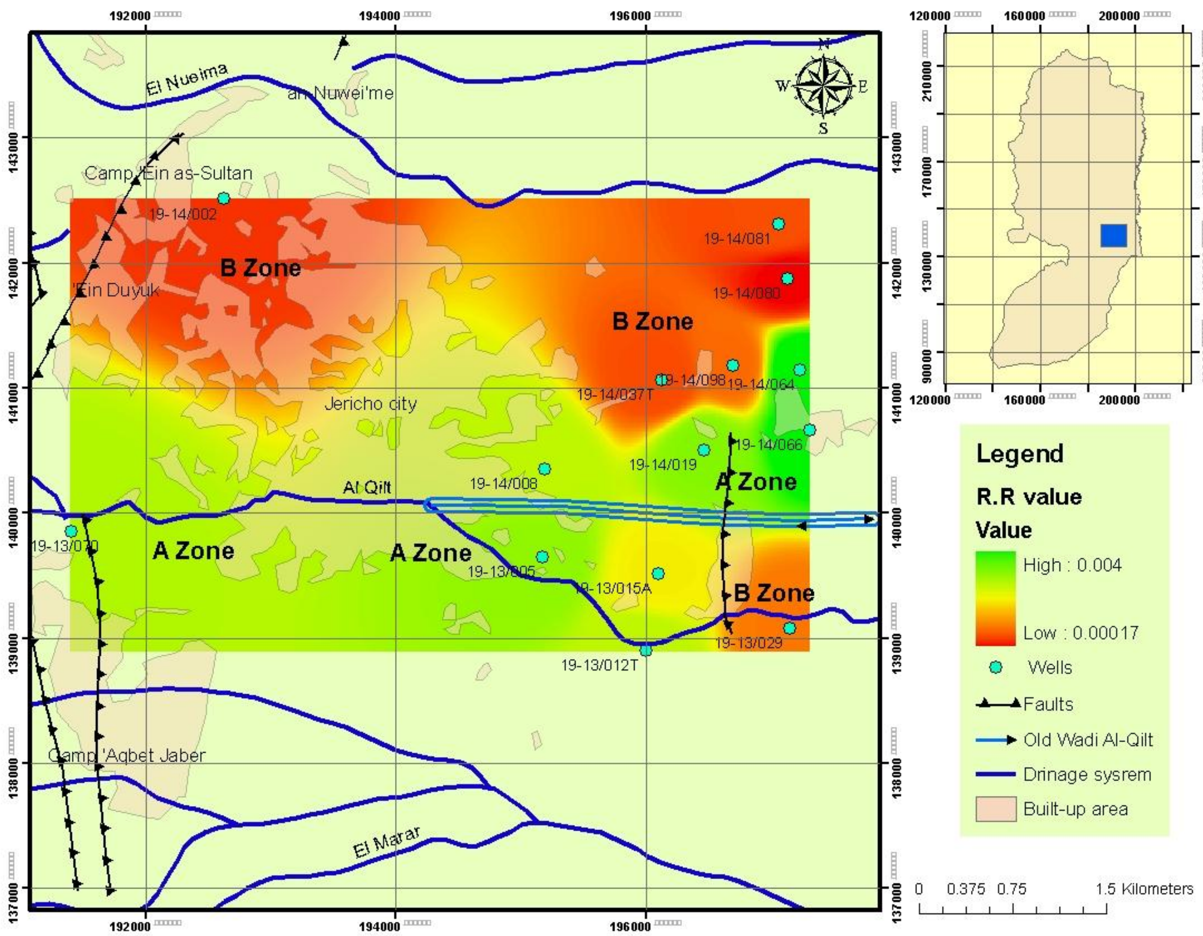

Figure 6.5 Recharge rate raster model and old Wadi Al-Qilt suggested pathway.

Chapter seven

7. Conclusions and Recommendations

7.1 conclusions:

The highest recharge rate is 0.096 m/day and the lowest recharge rate is 0.002 m/day. The high recharge rate indicating the Samra formation aquifer with gravel lithology. The intermediate recharge rate indicating the Samra silt formation. The low recharge rate indicating the Lisan Aquiqlued with marl lithology.

Large differences in electrical resistivity in the east site of Jericho (Fig. 5.2.2b), this indicating a fault structure extending north – south. The lithology is changing form silt and gravel to marl and clay along the fault.

The highest flooding velocity is 9 km/h and the discharge is about 51,800 CM/h. it was measured in 30/01/2008. Wadi Al – Qilt provides 160,595 m^3/a. this recharged volume is based on 8 flooding days/year.

Saline groundwater is discovered in the area of Ketf Al – Wad. It is located at depth of 90m. Electrical resistivity of less than 4 Ω.m in dicating the saline water. The extension and volume of this saline groundwater body need more investigations.

Sediments are varying in the permeability values along the Wadi floor, it is the highest (4.244E-04, 5.892E-04) between the soil sampling sites 6 and 7 indicating sandy Loam sediments. The lowest permeability values (4.705E-05, 4.530E-05) indicating clay and Clay loam sediments (Fig. 6.4).

The recharged zone length is estimated to 700 m. the recharge zone located with the coordinates of 194,246 – 140,061 and 195,237 – 139,471. The recharge gravel area is estimated to 1,100,000 m^2. The average thickness of the gravel layers are 65 m. Old pathway of Wadi Al – Qilt is discovered. It is starts with the coordinates 194,238 – 140,085, and still located in the coordinates 196,669 – 140,323.

7.2 Recommendations

- Increasing the flooding days from 8 to12 days. This should increase the recharge volume to about 240,000 m3/a.
- The new available water is estimated by 80,000 m3/a, with increase the recharge volume by 33%.
- Research project should be implemented in Wadi Al – Qilt (Jericho) to determine the number and diminutions of the suggested dames.
- Small dams should build along the intermediate and the high recharge zones.
- Drilling a deep injection wells in the new fault adjacent areas.
- Build a new numerical model based on the available data.

References

1- Abbas A M, Atya M A, Al-Sayed E A, Kamei H 2004. Assessment of groundwater resources of the Numeiba area at Sinai Peninsula, Egypt by using geoelectric data corrected for the influence of near surface inhomogeneities, Journal of Applied Geophysics, 56: (2004) 107-122.

2- Abed, A.M., and Wishahi, S.K. 1999. Geology of Palestine, West Bank and Gaza Strip, Palestinian Hydrology Group (PHG), Palestine, (in Arabic).461p.

3- Ali Nowroozi A, Stephen Horrocks B, Peter Henderson 1999. Saltwater intrusion into the freshwater aquifer in the eastern shore of Virginia: a reconnaissance electrical resistivity survey, Journal of Applied Geophysics, 42: (1999) 1-22.

4- Arad A, Michaeli A 1967. Hydrogeological investigation in the western catchment of the Dead Sea, Israel Journal of Earth – Sciences, Vol. 16, 1967, pp. 181 – 196.

5- Applied Research Institute – Jerusalem (ARIJ), 1995: Environmental profile for the West Bank, Volum 2: Jericho district. ARIJ, Jerusalem, October 1995.

6- Arora C L 1986. Geoelectric study of some Indian Geothermal areas. Geothermal 15(5/6): 677-688.

7- Avihu Ginzburg 1979. Resistivity surveying, geophysical surveys 1(1979) 325-355. Reidel Publishing Company, Dordrech-Holland.

8- Begin Z B, 1974. The geological map of Israel, Sheet 9-III: Jericho, 1: 50,000 Explanatory note, Geological survey of Israel.

9- Begin Z B, Ehrlich A, Nathan Y, 1974. Lake Lisan the Pleistocene precursor of the Dead Sea. Geological survey of Israel 63, 30.

10- Bender F 1974. Geology of Jordan Borntraeger , Berlin, 196 p

11- Burger H R 1992. Exploration Geophysics of the Shallow Surface. Prentice Hall, NJ, 485 pp.

12- Claudia Sainato, Griselds Galindo, Cristina Pomposiello, Horacio Malleville, Diego de Abelleyra, Losinno B 2003. Electrical conductivity and depth of groundwater at the Pergamino zone (Buenos Aires Province, Argentina) through vertical electrical soundings and geostatistical analysis, Journal of South American Earth Sciences, 16: (2003) 177-186.

13- Dahlin T 1996. 2D resistivity surveying for environmental and engineering application. First Break, 14, 275-284.

14- De Breuk E, De Moor G 1985. The water Table aquifer in the eastern coastal area of Belgium. Bull. Assoc. Sci. Hydro. 14, 137 – 155.

15- El Houcyne, El Idysy, Florimond De Smedt 2004. A geostatistical methodology to estimate the base of the Trifa aquifer (Morocco) with limited drilling and geo-electrical sounding data, Bull Eng Geol Environ (2004) 63: 345-351.

16- Fetter C W 2001. Applied hydrogeology. Fourth edition, Prentice-Hall,Inc.

17- Flathe H 1976. The role of a geological concept in geophysical research work for solving hydrogeological problems. Geoexploration, 14: 195-206.

18- Fouad F, Shaaban 2001. Vertical electrical sounding for groundwater investigation in Egypt: a case study in a coastal area, African Earth sciences 33: (2001)673-686.

19- Freeze R.A, Cherry J.A 1979. Groundwater. Prentice – Hall, Engle – wood Cliffs, NJ, 604 pp.

20- Ghayoumian J, Ghermezcheshme B, Feiznia S, Noroozi A 2005. Integration GIS and DSS for identification of suitable areas for artificial recharge, case study Meimeh Basin, Isfahan, Iran, Environmental Geology, 47: (2005) 493-500.

21- Giffiths D H and Barker R D 1993. Two-Dimensional resistivity imaging and modeling in areas of complex geology. Journal of Applied Geophysics, 29, 211-226.

22- Gogu R.C, Carabin G, Hallet V, Peters V, Dassargues A 2001. GIS – based hydrogeological database and groundwater modeling. Journal of Hydrogeology (2001) 9:555-569.

23- Golani, U 1972. Groundwater resources in Jericho region. Tech. rep., Tahal Report HR/72/016

24- Goldschmidt M J, Arad A, and Neev D 1967. The mechanism of saline springs in the Lake Tiberias Depression. Geol. Surv. Isr. Bull. 45

25- Guttman, 2005 GUTTMAN, J (2005): Geology and Hydrogeology of the Jordan Valley – Multi-lateral project, project 02WT9719 within the framework of the German-Israeli-Jordanian-Palestinian joint research program for the sustainable utilization of aquifer systems.

26- Healy R W, Cook P G 2002 Using groundwater levels to estimate recharge, hydrogeology Journal (2002) 10:91- 109.

27- Hoetzl, H. Tamimi, A. Ganam, M, Geyer, S. Ali, W, 2005. Using hydrochemical tracers and tritium isotopes to characterizing the groundwater from the shallow wells and springs, Jericho area, Palestine. Published online.

28- Ilkisik O M, Gurer A, Tokgoz T, Kaya C 1997. Geoelectrtromagnetic and geothermic investigation in the Ihlara valley geothermal field. J Volcanol Geotherm Res 78: 297-308.

29- Jundi. M, 2005. Hydrochemical and isotopic composition of groundwater in Jericho area, Master thesis, Jerusalem – Palestine. Al – Quds University.

30- Kaufman A, 1971. U – Series dating of Dead Sea basin carbonates, Geochem. Cosmochem. Acta, Vol.35, pp. 1269-1281.

31- Khayat S, 2005. Hydrochemistry and Isotopes Hydrogeology of Groundwater Resources in the Jericho Area/ Palestine PhD thesis. University of Karlsruhe, Germany

32- Koefoed O 1979. Geosounding Principles 1: Resistivity sounding measurements. Elsevier Science Publishing Company, Amsterdam.

33- Landmann G, Abu Qudaira G M, Shawabkeh K, Wrede V, Kempe S 2002. Geochemistry of the Lisan and Damia formations in Jordan, and implications for palaecolimate, Quaternary international 89: (2002) 45-57.

34- Lisa Shevenell 1996. Analysis of hydrograph in a karst aquifer: estimation of specific yield and continuum transmissivities, Journal of Hydrology 174 (1996) 331-355.

35- Loke M.H 2001. Tutorial 2-D and 3-D electrical imaging surveys.

36- Marei A, Al-Jundy M, Sbaih M, Weise S, Lange T 2005. The influence of Wadi el Quilt flooding on the groundwater quality of the Plio-Pleistocene aquifer System / Jericho, Jordan Valley.

37- Marie A, Vingosh A 2001. Source of salinity in groundwater from Jericho area, Jordan Valley, GROUNDWATER 39.No 2: 240-248.

38- Mazak O, Kelly W E, Landa I 1987. Surface geoelectrics for groundwater pollution and protection studies. J. Hydrol. 93: 277-294.

39- Meinzer OE, Stearns ND, 1929 A study of groundwater in the Pomperaug Basin, Connecticut, with special reference to in – tack and discharge. US Geol Surv. Water – Supply Pap 597 – B:73 – 146.

40- Monteiro Santos PA, Andrade AAR, Mendes VLA, 1997. Study of the Chaves geothermal field using 3D resistivity modeling. J. appl. Geophys 37: 85-102.

41- Moore G K 1992. Hydrograph analysis in fracture rock terrane. Ground Water, 30:390-395.

42- Nasser El Din, K. 1999. Upconning of salt water in the eastern part of Jericho area. M.Sc. thesis. An Najah National University, Nablus, West Bank.

43- Neev D, Emery K O, 1967. The Dead Sea. Depositional processes and environmental of evaporates. Geological Society of Israel Bulltetin 41, 147.

44- Neev D, Emery K.O, 1995. The destruction of Sodom, Gamorrah, and Jericho: geological, climatologically, and Archaeological background, Oxford Univ. Press, 1995. ISBN 0-19-509094-2.

45- Neven, K, 1997. Quantitative solutions in hydrogeology and groundwater modeling, Lewis Publishers, 1997. ISBN 0-56670-219-4.

46- Nuseibeh M, Nasser Eddin T, 1995. Palestinian Fresh Water Springs, springs disruption flow and water quality data (1970 – 1994), Palestinian Consultancy Group (PCG).

47- Parasnis D S, 1986. Principles of Applied Geophysics. Chapman & Hall, London, 402 pp.

48- PCBS, PALESTINIAN CENTRAL BUREAU OF STATISTICS (2002): Small area populations, 1997-2010, Ramallah, Palestine. (unpublished).

49- PWA (Palestinian Water Authority) 2002. Hydrogeological data base, West Bank - Palestine.

50- PWA (Palestinian Water Authority) 2008. Hydrochemical data base, West Bank - Palestine.

51- Richard W. Healy, Peter G. Cook 2002. Using groundwater levels to estimate recharge. Hydrogeology Journal (2002) 10:91 – 109.

52- Rofe and Roffty, 1963. Geological and hydrological report, Jerusalem and district water supply, Hashemite Kingdome of Jordan, Central water Authorities. 79p; Londen.

53- Roth. I, 1974. The geological map of Israel, Sheet 12-I: Wadi El Qilt, 1:50,000 Explanatory note, Geological survey of Israel.

54- Sabet M A 1975. Vertical electrical resistivity sounding locate groundwater resources: a feasibility study. Virginia Polytechnical Institute, Water Resources Bulletin 73, 63 pp.

55- Salvany J M, Carrera J, Bolzicco J, Mediavilla C 2004. Pitfalls in the geological characterization of alluvial deposits: site investigation for reactive barrier installation at AznalcÓllar, Spain, Quarterly Journal of Engineering Geology and Hydrogeology, 37: (2004) 141-154.

56- Stewart M, Layton M, Lizanoe T 1983. Application of resistivity surveys to regional hydrogeologic reconnaissance. Ground Water 21(1): 42-48.

57- Tamimi, A. Yellin, A. Inbar A. Haddad, H. Ganem, M 2004. Qualitative sustainability of groundwater in the Jericho area. German – Israeli – Jordanian – Palestinian joint research program. Second phase. Project Number 2WT 9179/177, 2004.

58- Telford W M; Geldart L.P; Sheriff R.E 1990. Applied Geophysical, Second Edition, Cambridge University Press.

59- BEINHORN, M., GUTTMAN J. S., SAUTER M., TOLL M., KOLDITZ O., April 2004. Groundwater modeling of the shallow aquifer in the Jericho area. In 5th Int. Symposium on the Eastern Mediterranean Geology, Thessaloniki, Greece, pp. 1483-1486.

60- USDA, 1993. Soil Survey Division Staff. Soil survey manual. USDA Handb. 18. U.S. Gov. Print Office, Washington, DC.

61- Verma R K, Rao M K, Reo C V 1980. Resistivity investigations for groundwater in metamorphic areas near Dhanbad, India. Ground Water 18(1): 46-55.

62- WOLFER, J. (1998): Hydrogeological Investigations along the Jerusalem – Jericho Transect (Wadi el Qilt), Israel, West Bank. - Diploma Thesis, University of Karlsruhe

63- GAVRIELI, I. YECHIELI, Y., HALICZ, L., SPIRO, B., BEIN, A. AND EFRON, D. (2001): The sulfur system in anoxic subsurface brines and its implication on brine evolutionary pathways: The Ca-chloride brines in the Dead Sea area. Earth Planet. Sci. Lett. 186, 199-213.

64- Zohdy A A R 1969. The use of Schlumberger and equatorial sounding on groundwater investigation near El Paso, TX. Geophysics 34, 713-728.

Appendix

Grain size distribution curve for estimation of d60 and d10. it is arranged from sample 1 to sample 10 respectively.

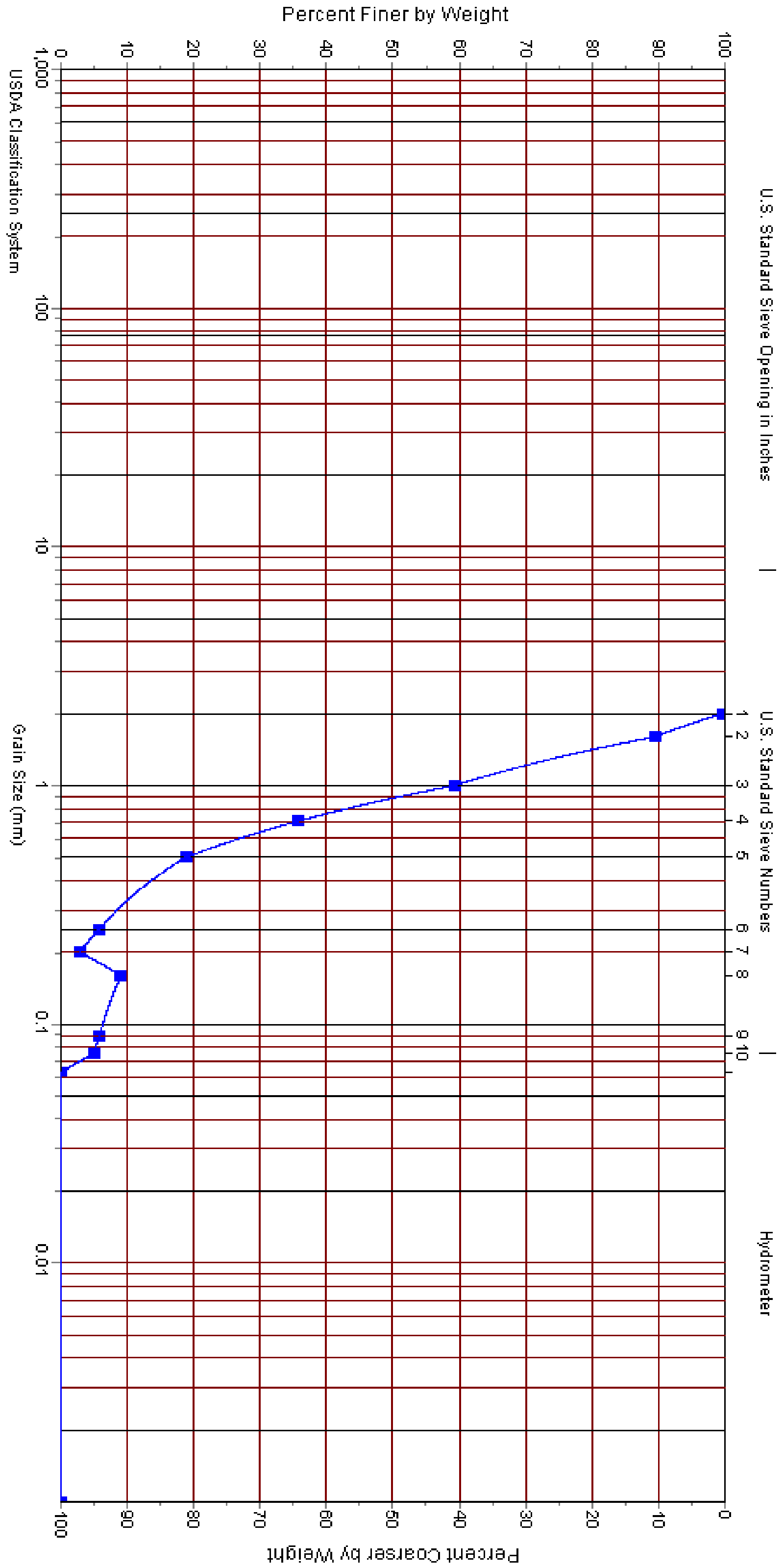

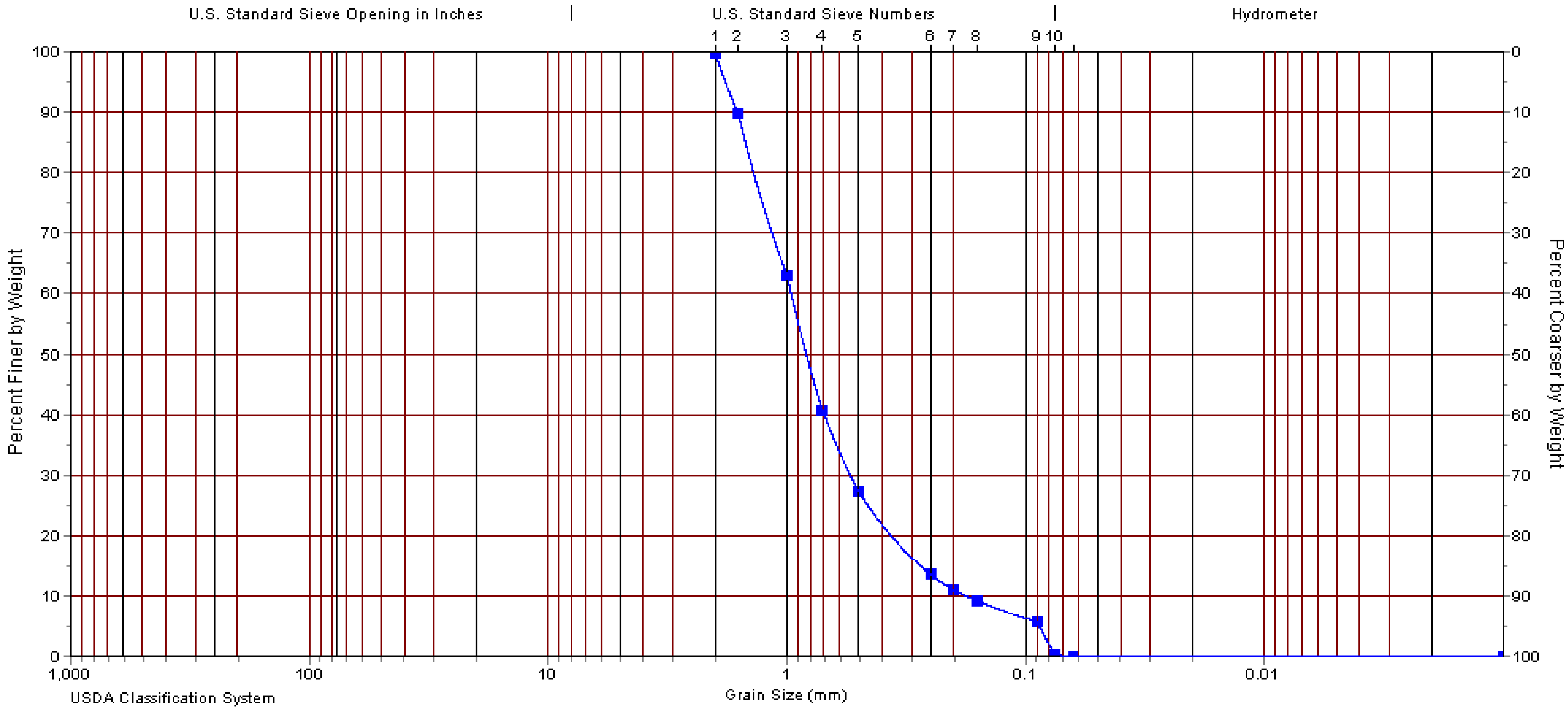
U.S. Standard Sieve Opening in Inches
U.S. Standard Sieve Numbers
Hydrometer
1 2 3 4 5 6 7 8 9 10
Percent Finer by Weight
Percent Coarser by Weight
1,000
100
10
1
0.1
0.01
Grain Size (mm)
USDA Classification System

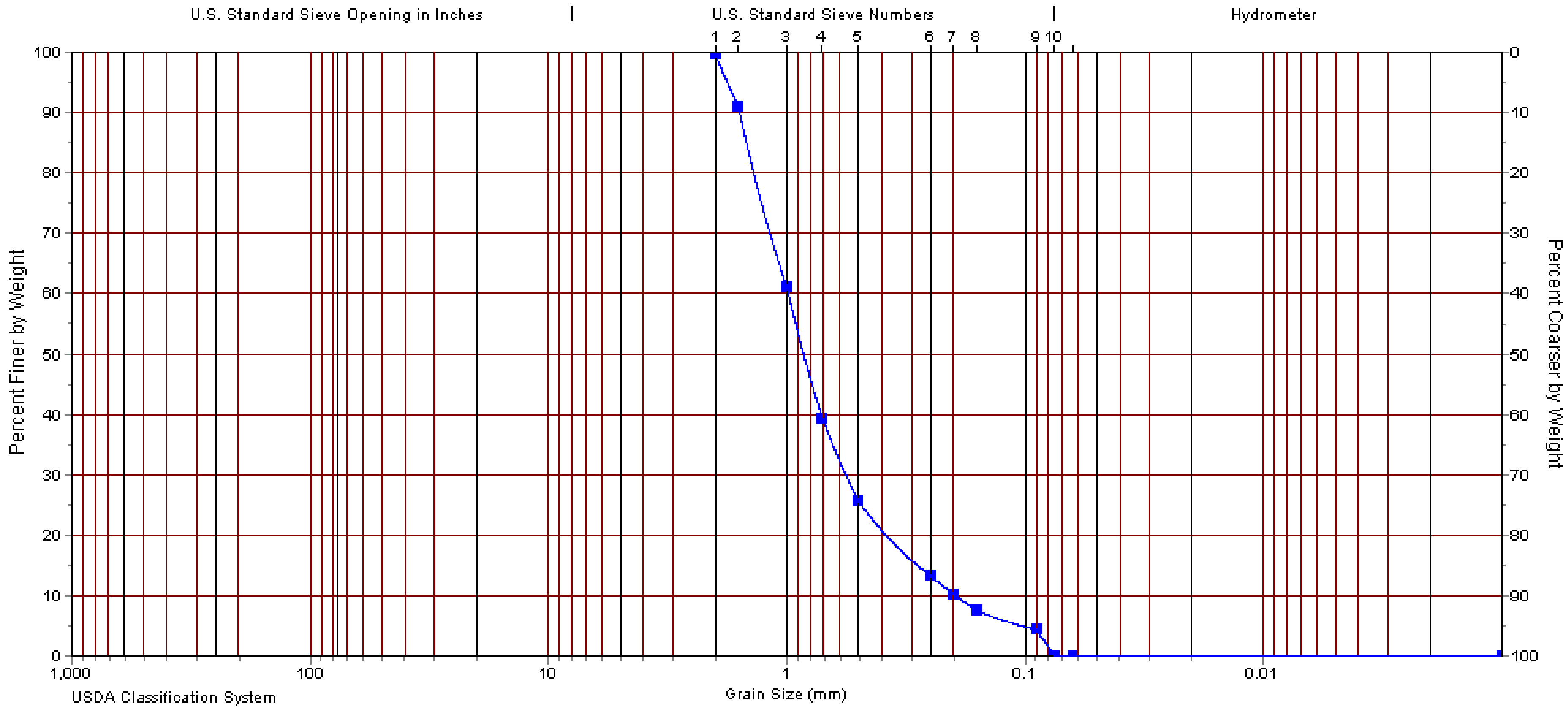

U.S. Standard Sieve Opening in Inches
U.S. Standard Sieve Numbers
Hydrometer
1 2 3 4 5 6 7 8 9 10
Percent Finer by Weight
0 10 20 30 40 50 60 70 80 90 100
Percent Coarser by Weight
1,000
100
10
1
0.1
0.01
USDA Classification System
Grain Size (mm)

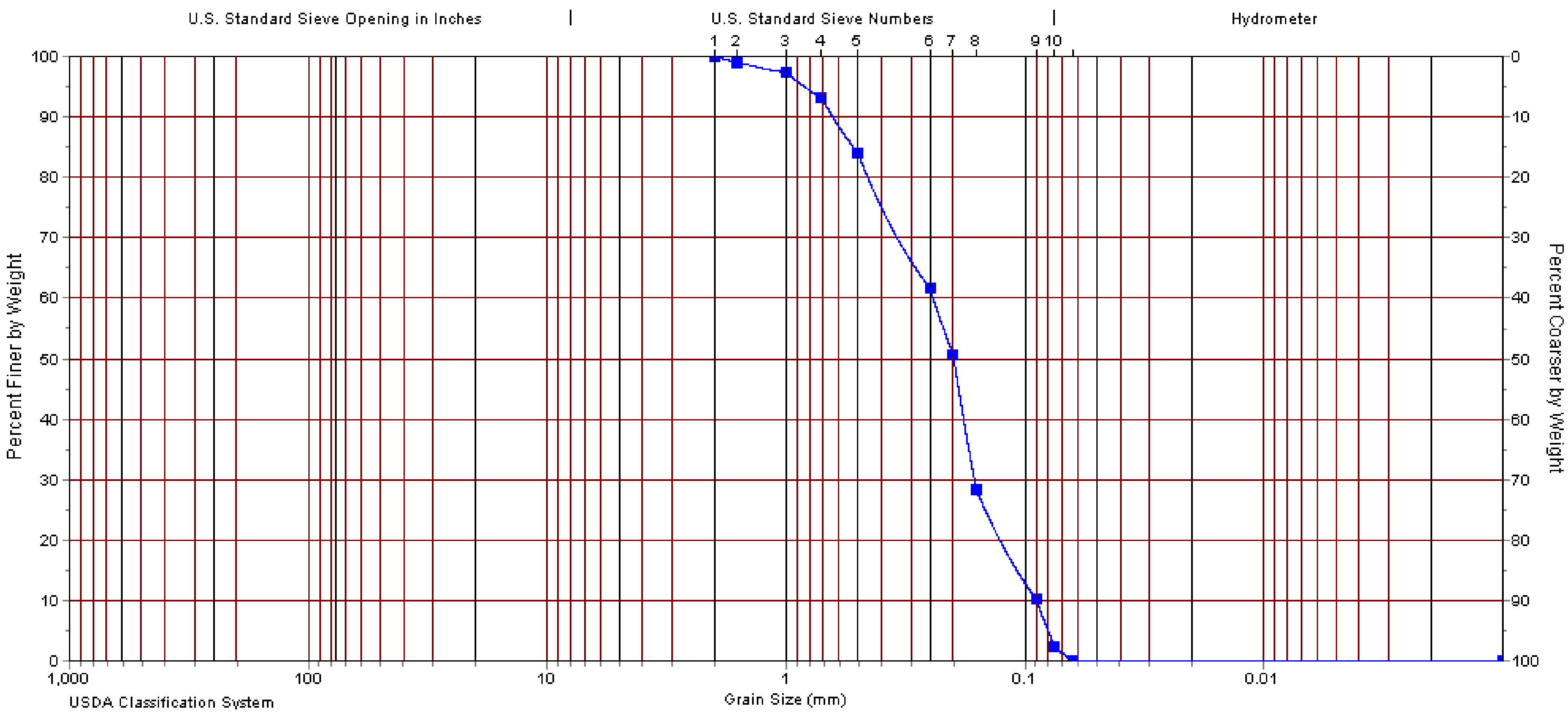
U.S. Standard Sieve Opening in Inches
U.S. Standard Sieve Numbers
Hydrometer
1 2 3 4 5 6 7 8 9 10
Percent Finer by Weight
Percent Coarser by Weight
100 90 80 70 60 50 40 30 20 10 0
0 10 20 30 40 50 60 70 80 90 100
1,000 100 10 1 0.1 0.01
Grain Size (mm)
USDA Classification System

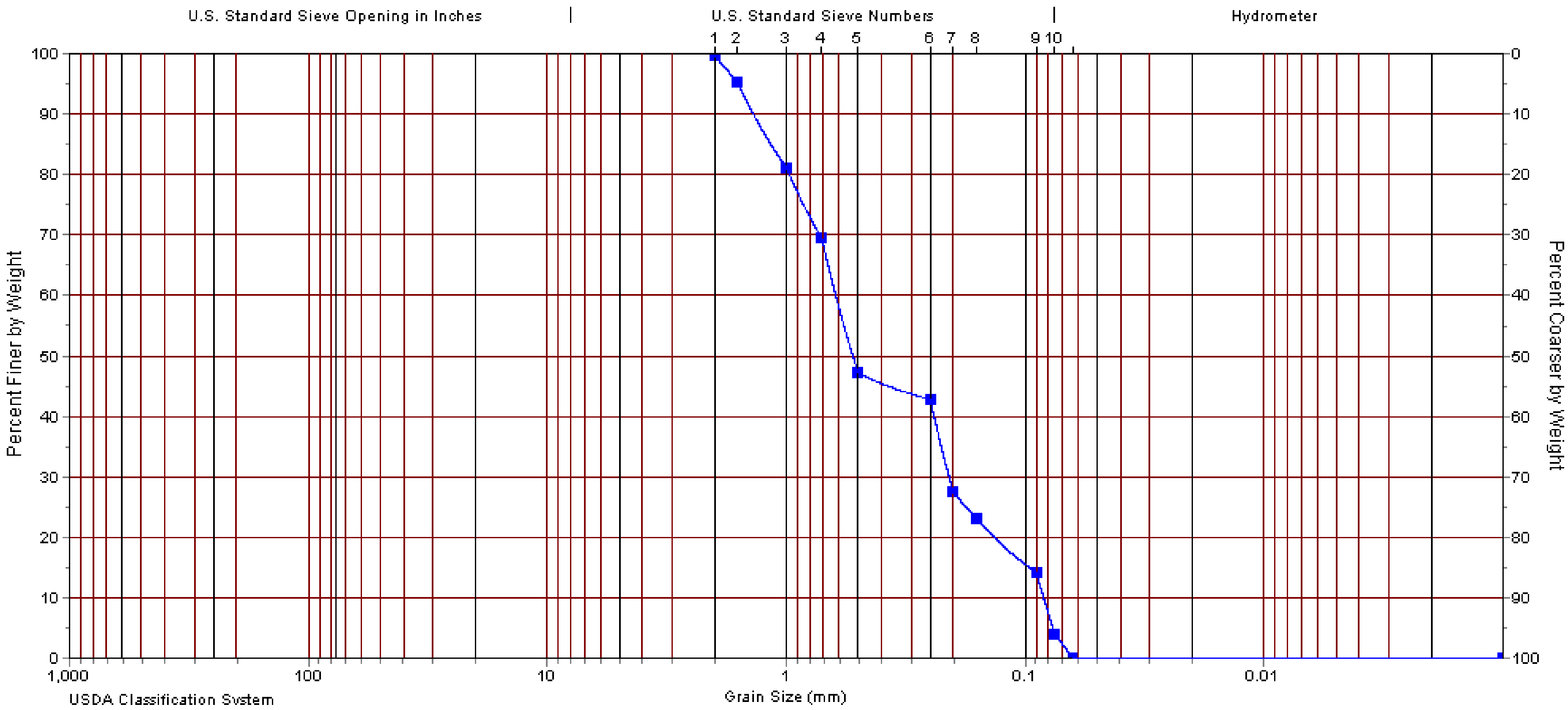

U.S. Standard Sieve Opening in Inches
U.S. Standard Sieve Numbers
Hydrometer
1 2 3 4 5 6 7 8 9 10
Percent Finer by Weight
Percent Coarser by Weight
100 90 80 70 60 50 40 30 20 10 0
0 10 20 30 40 50 60 70 80 90 100
1,000 100 10 1 0.1 0.01
Grain Size (mm)
USDA Classification System

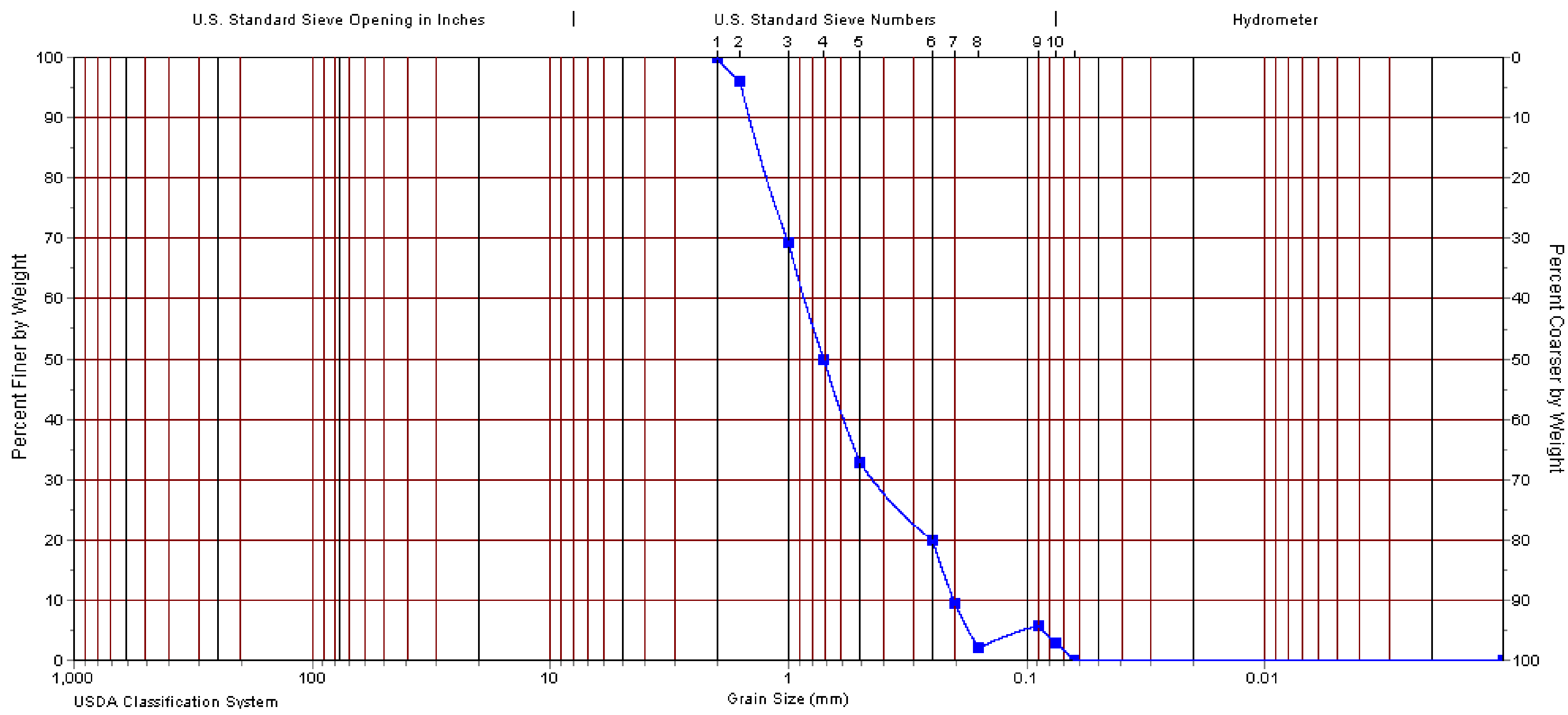
U.S. Standard Sieve Opening in Inches
U.S. Standard Sieve Numbers
Hydrometer
1 2 3 4 5 6 7 8 9 10
Percent Finer by Weight
Percent Coarser by Weight
100
90
80
70
60
50
40
30
20
10
0
1,000
100
10
1
0.1
0.01
Grain Size (mm)
USDA Classification System

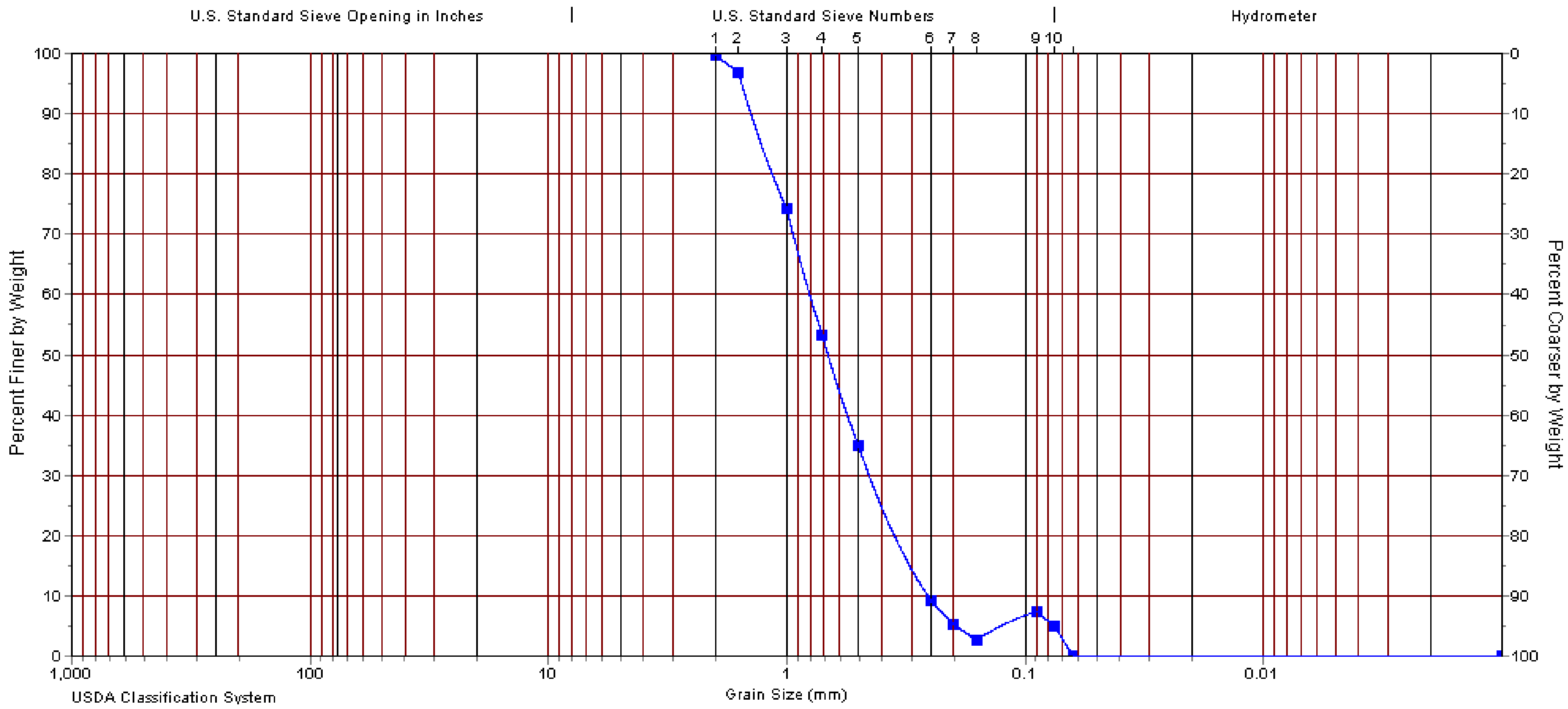
U.S. Standard Sieve Opening in Inches
U.S. Standard Sieve Numbers
Hydrometer
1 2 3 4 5 6 7 8 9 10
Percent Finer by Weight
Percent Coarser by Weight
1,000
100
10
1
0.1
0.01
Grain Size (mm)
USDA Classification System

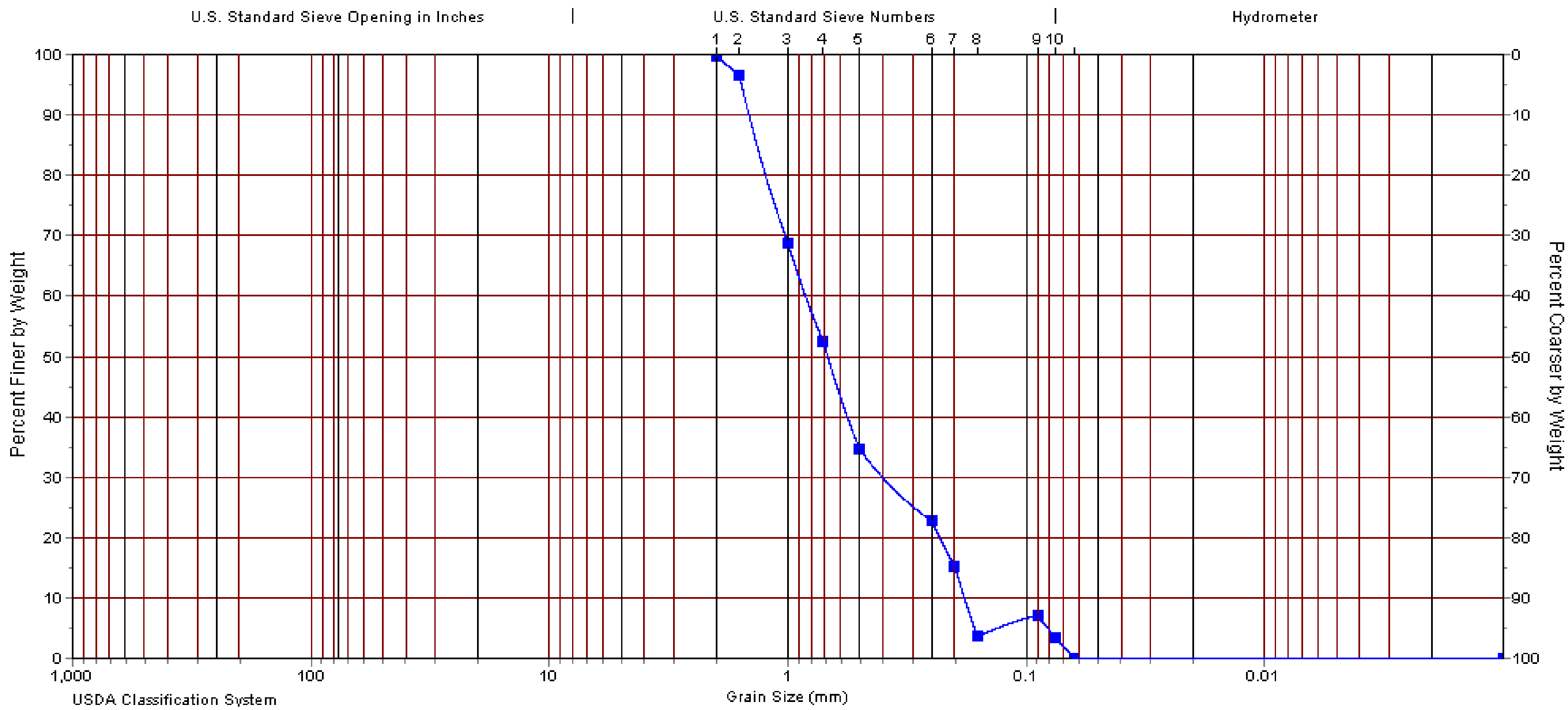

U.S. Standard Sieve Opening in Inches
U.S. Standard Sieve Numbers
Hydrometer
1 2 3 4 5 6 7 8 9 10
Percent Finer by Weight
100 90 80 70 60 50 40 30 20 10 0
Percent Coarser by Weight
0 10 20 30 40 50 60 70 80 90 100
1,000 100 10 1 0.1 0.01
Grain Size (mm)
USDA Classification System

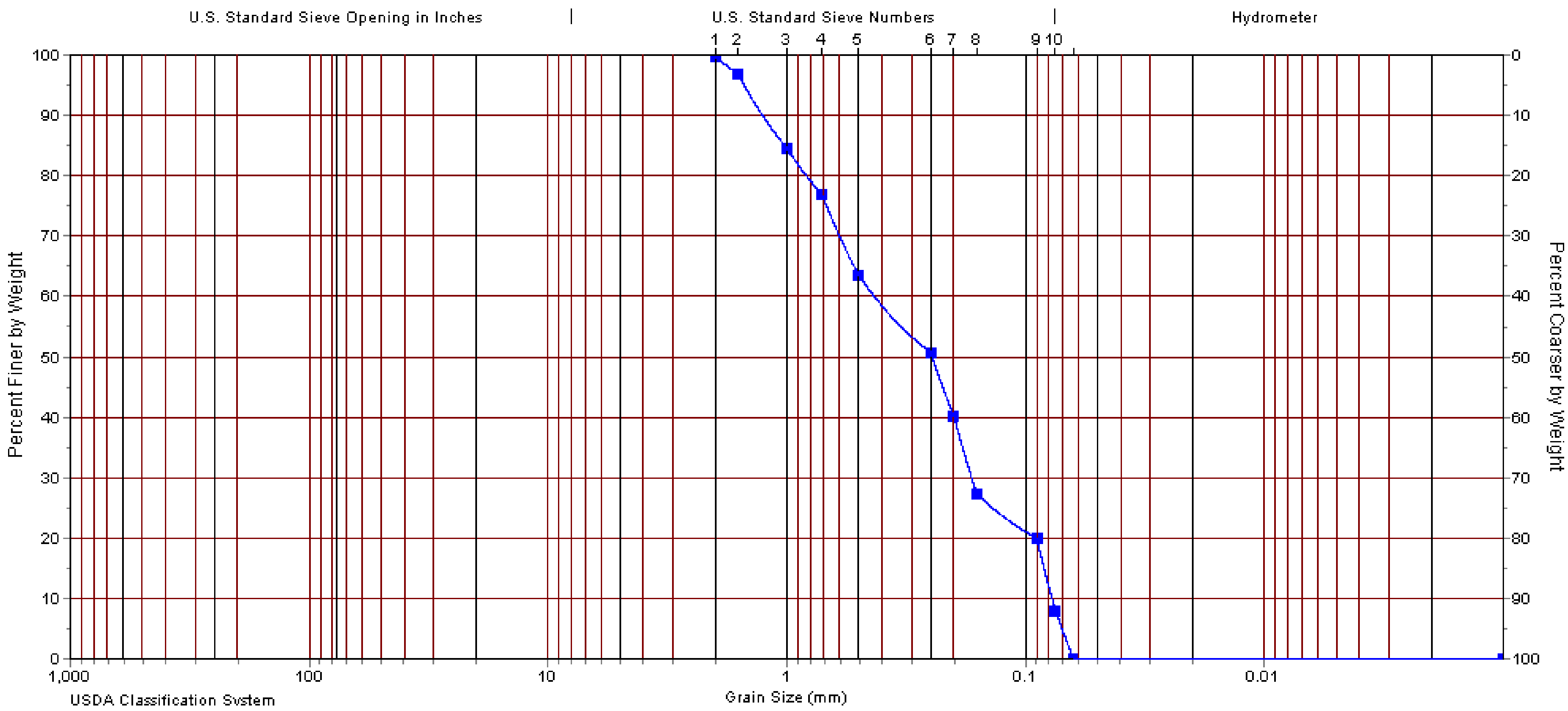

U.S. Standard Sieve Opening in Inches
U.S. Standard Sieve Numbers
Hydrometer
1 2 3 4 5 6 7 8 9 10
Percent Finer by Weight
100 90 80 70 60 50 40 30 20 10 0
Percent Coarser by Weight
0 10 20 30 40 50 60 70 80 90 100
1,000 100 10 1 0.1 0.01
Grain Size (mm)
USDA Classification System

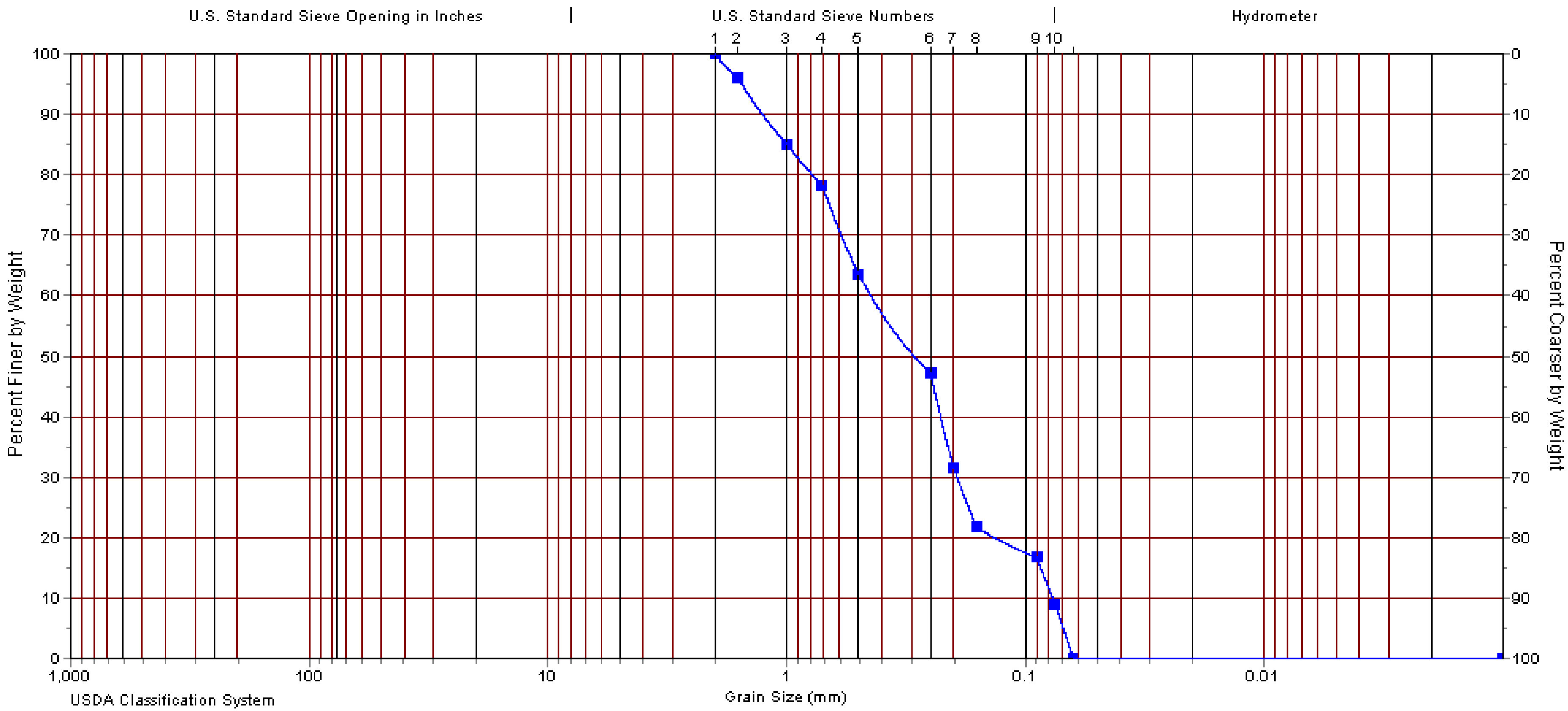
U.S. Standard Sieve Opening in Inches
U.S. Standard Sieve Numbers
Hydrometer
1 2 3 4 5 6 7 8 9 10
Percent Finer by Weight
100 90 80 70 60 50 40 30 20 10 0
Percent Coarser by Weight
0 10 20 30 40 50 60 70 80 90 100
1,000 100 10 1 0.1 0.01
Grain Size (mm)
USDA Classification System

Chapter five

5 Results

The results of the different field and laboratory experiments are shown below; it contains the well hydrograph analysis of the groundwater table, geo – electrical sounding profiles, physical properties analysis of the soil, lithological cross sections generated by boreholes lithological correlations, and geo – chemical analysis of the groundwater.

5.1 Water table fluctuation analysis

Water table fluctuation method (WTF) may be the most widely used technique for estimation recharge. It requires knowledge for specific yield and changes in water levels over the time; it is applicable only to unconfined aquifer, and the Plio – Pleistocene aquifer is unconfined

The recharge rate for the gravel aquifer estimated by the WTF method. 10 years historical groundwater table data are used for the estimation of recharge rate. Wells are randomly selected, the selection of these wells are mostly controlled by the data availability

R.R in the selected 14 wells ranges between $1.9 * 10^{-3}$ m/h to $1.7 * 10^{-4}$ m/h, a large difference between the R.R of the wells located within the Samra formation area and the others in the Lisan formation area. Analyzed wells are listed in (Table 5.1.1).

Table 5.1.1 Results of hydrograph analysis for the selected wells in Jericho.

Well #	**Well ID**	**R.R ($m/h.m^2$)**	**R.R ($m/day.m^2$)**	**Lag time (day)**	**Depth**
1	19-13/005	$2.9 * 10^{-3}$	0.069	135 •	80
2	19-13/012T	$2.5 * 10^{-3}$	0.060	90	137
3	19-13/015	$1.9 * 10^{-3}$	0.046	180 •	135
4	19-13/029	$8.8 * 10^{-4}$	0.021	X	130
5	19-13/070	$2.6 * 10^{-3}$	0.062	X	X
6	19-14/002	$3.6 * 10^{-4}$	0.009	165 •	150
7	19-14/008	$2.5 * 10^{-3}$	0.060	155 •	54
8	19-14/019	$3.0 * 10^{-3}$	0.072	210	67
9	19-14/037T	$6.6 * 10^{-4}$	0.016	165 •	83
10	19-14/064	$4.0 * 10^{-3}$ •	0.096	180 •	90
11	19-14/066	$3.9 * 10^{-3}$	0.093	180 •	33
12	19-14/080	$1.7 * 10^{-4}$	0.004	410 •	100
13	19-14/081	$5.4 * 10^{-4}$	0.013	210 •	100
14	19-14/098	$7.6 * 10^{-4}$	0.002	260 •	195

X: data not available, •: average lag time and R.R value.

Long term hydrograph created for the above wells, Hydrograph starting from the hydrological year (1989-1990) and end in (1998-1999) except in wells 19-13/070, 19-13/029, and 19-13/012T due to the data availability, monthly records of static water table and rainfall are plotted to calculate the R.R values and to estimate Lag time for each well.

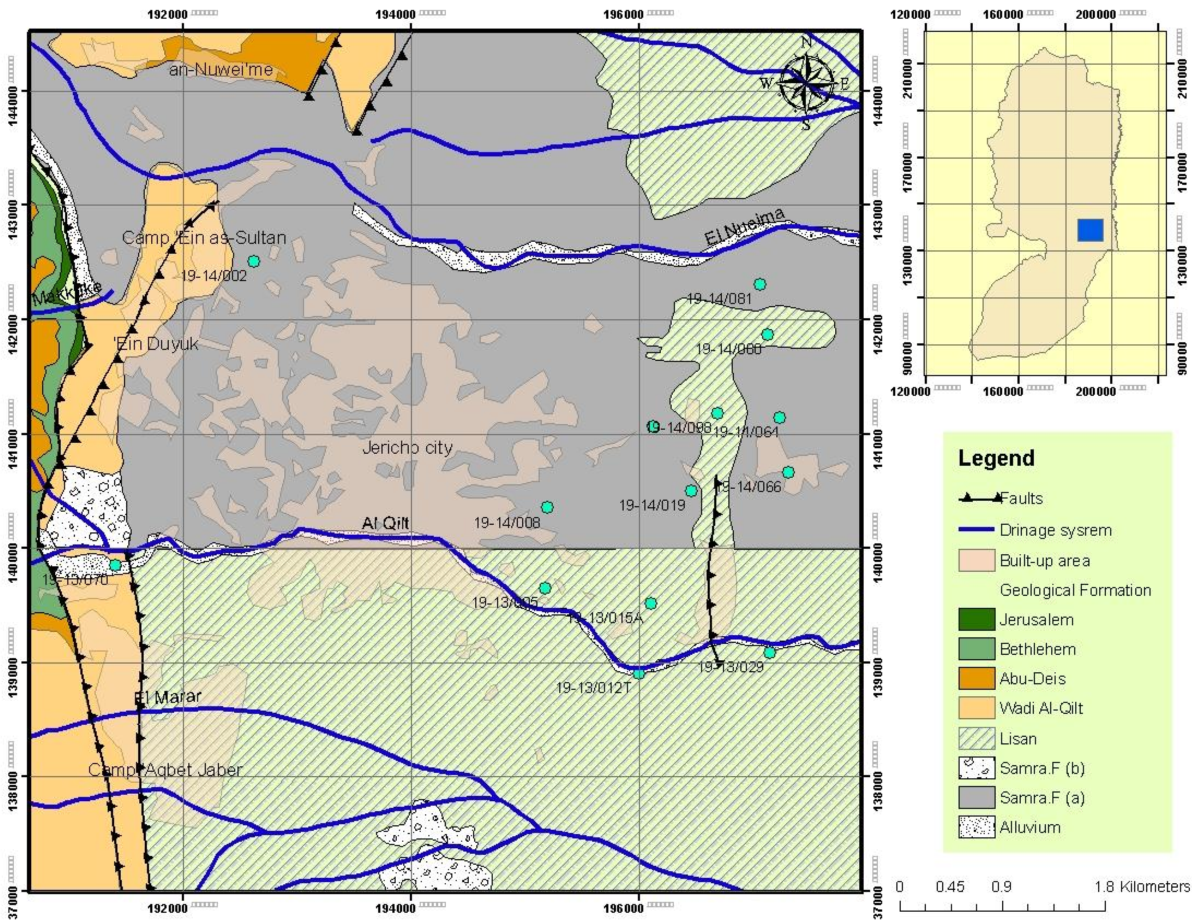

Figure 5.1.1: geology of the study area and wells location. (Begin, 1974)

1) Well 19-13/005:

Hydrograph analysis illustrated in (Fig. 5.1.2). This well located 177 m to the north of the Wadi. The depth of the well reaches 80 m; it is drilled within the out cropping of the Lisan formation. R.R value is $2.9 * 10^{-3}$ m/h; this value is a good indication of gravel aquifer. For Lisan formation R.R value should be less than this value, which means that the recharge tack place in the western upper area of Samra formation (Fig. 5.1.1). Nevertheless, Silt-gravel lenses of Samra formation spreading under the Lisan marl-clay layers.

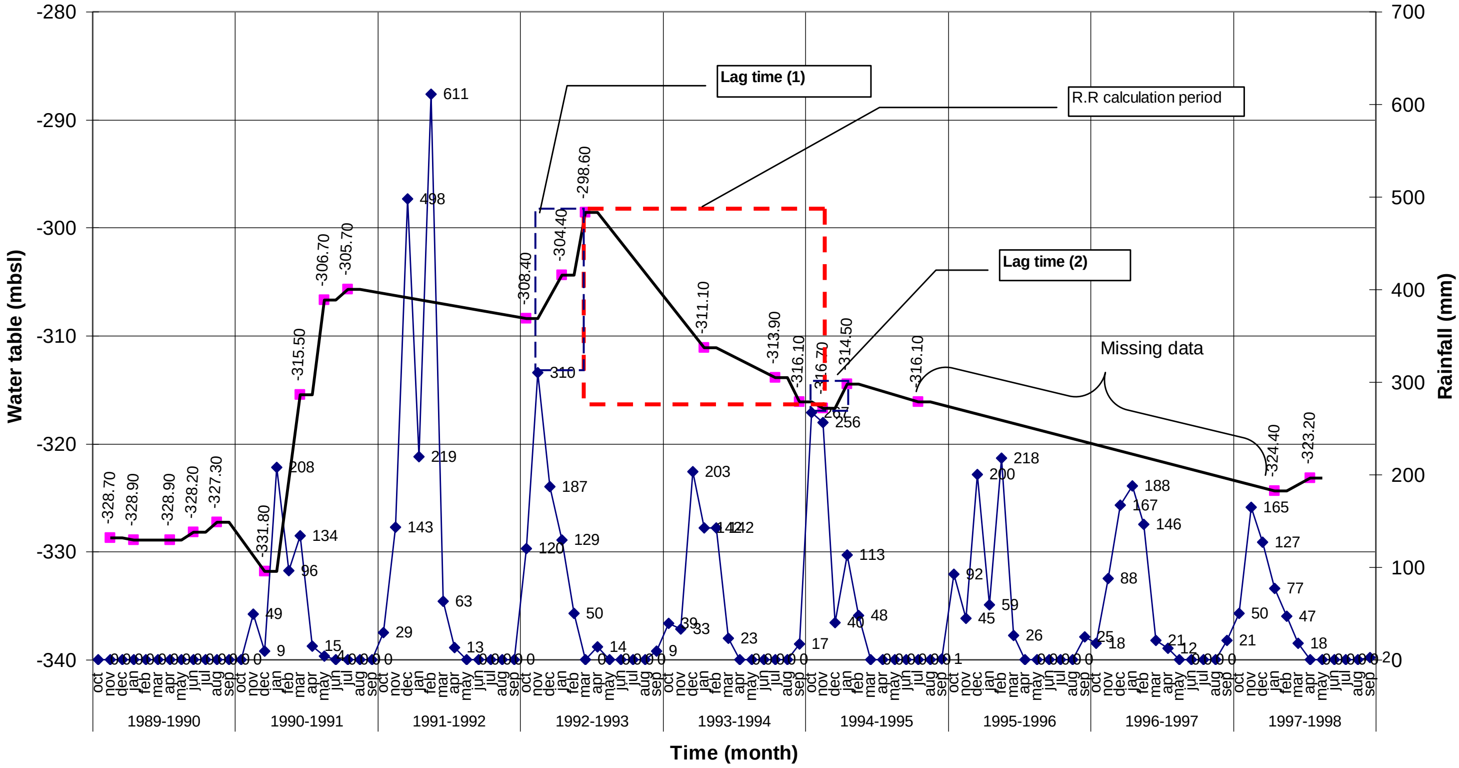

Figure 5.1.2 groundwater table hydrograph of the well 19-13/005.

2) Well 19-13/012:

This well is located 44 m far away from the Wadi. It is the closest well to the wadi, the location of this well is in the transaction area of the Lisan – Samra formations. High R.R value is $2.5 * 10^{-3}$ m/h, and the lag time was 90 days (Fig. 5.1.3). The depth of the well reached 125 m. The available data for this well is from 1989 – 1992 in both water table and rainfall.

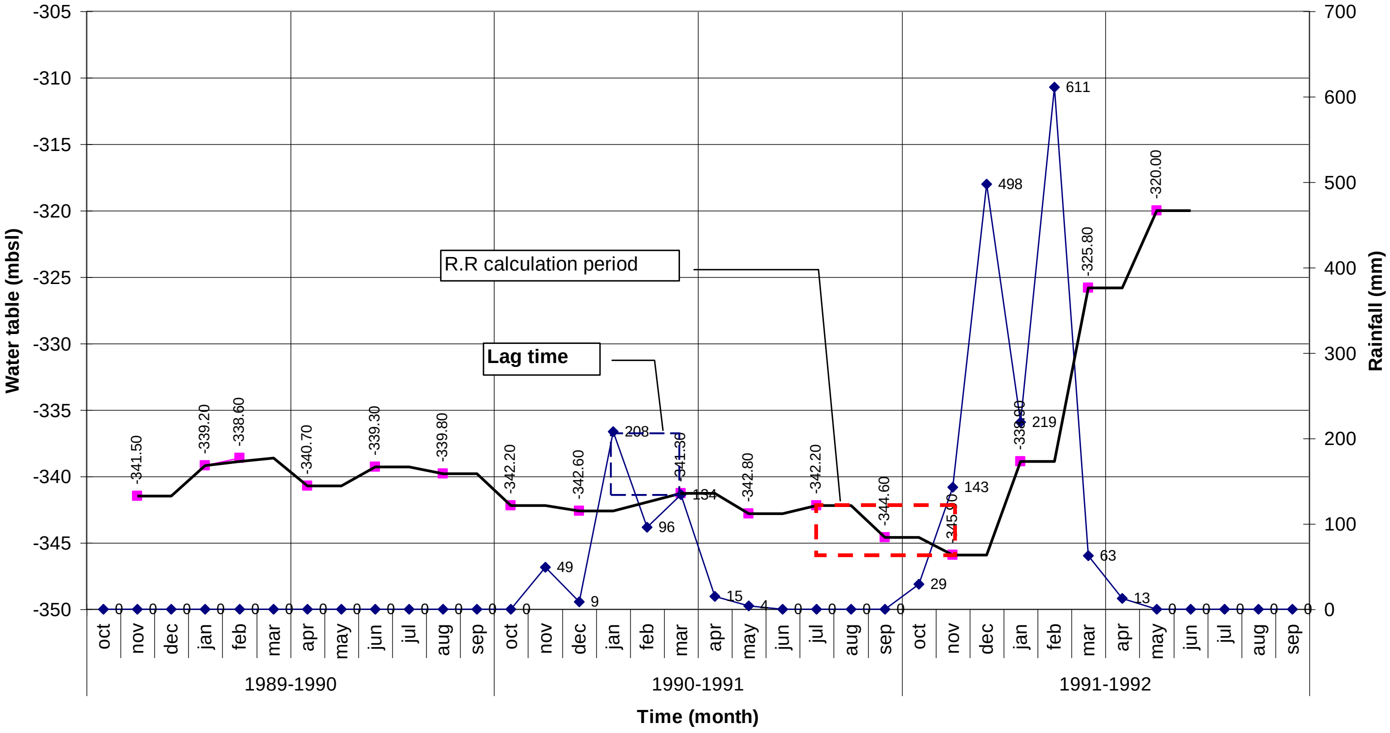

Figure 5.1.3 groundwater table hydrograph of the well 19-13/012T

3) Well 19-13/015:

This well is locate 590 m north Wadi Al-Qilt. It lays in the Lisan – Samra intersection area, inter-fingering in this area is will recognize. The R.R value is the highest, it reached 1.9 * 10^{-3} m/h (Fig. 5.1.4). This indicating a high connection to the outcropping of Samra formation, where recharge tacking place, also Lisan formation could be thin in the recharge area. Average lag time is 180 days; this value was estimated by two time periods (Fig. 5.1.4).

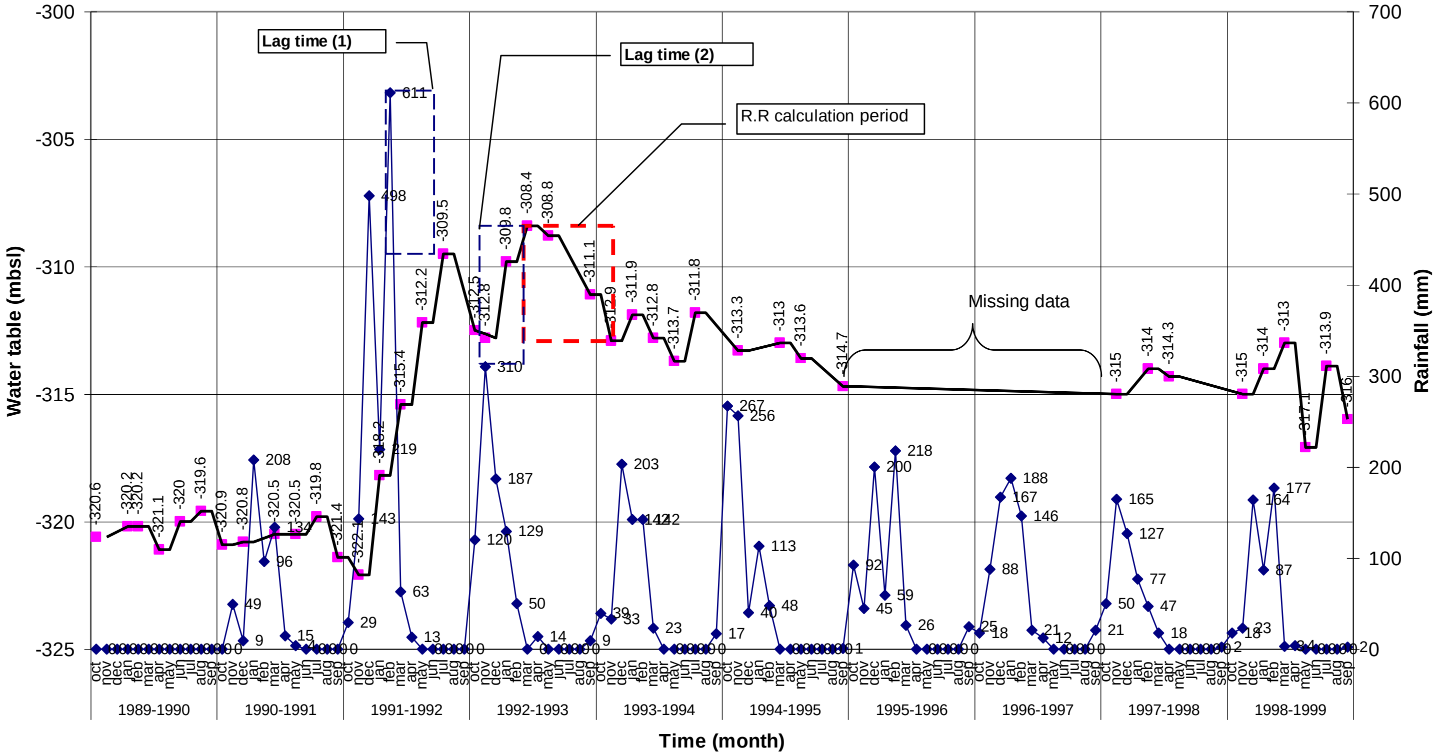

Figure 5.1.4 groundwater table hydrograph of the well 19-13/015.

4) Wells (19-13/029) and (19-13/070):

Historical data are used for evaluating the physical properties of these wells. Well no 19-13/070 locates in the out let of Wadi Al-Qilt. It lays 140 m south of the wadi out let. Well no. 19-13/029 locates in the eastern parts of Jericho city, with a depth of 105 m to the south of the wadi. The distance between the two wells is 6 km from west to east (Fig. 5.1.5), and (Fig. 5.1.6), Samra outcropping layers contributed to the well profile 19-13/070; on the other side Lisan thick layers contributed the lithology of the well no. 19-13/029.

The differences in lithologys logs could be noticed by R.R values of the two wells. In the well no. 19-13/070 the R.R was $2.6 * 10^{-3}$ m/h and in well no. 19-13\029 it decrease to $8.8 * 10^{-4}$ m/h. Significant differences in the behavior of the water table fluctuation by the two hydrographs can be noticed in (Fig. 5.1.5), and (Fig. 5.1.6). Lag time couldn't be calculated due to the absence of the rainfall data.

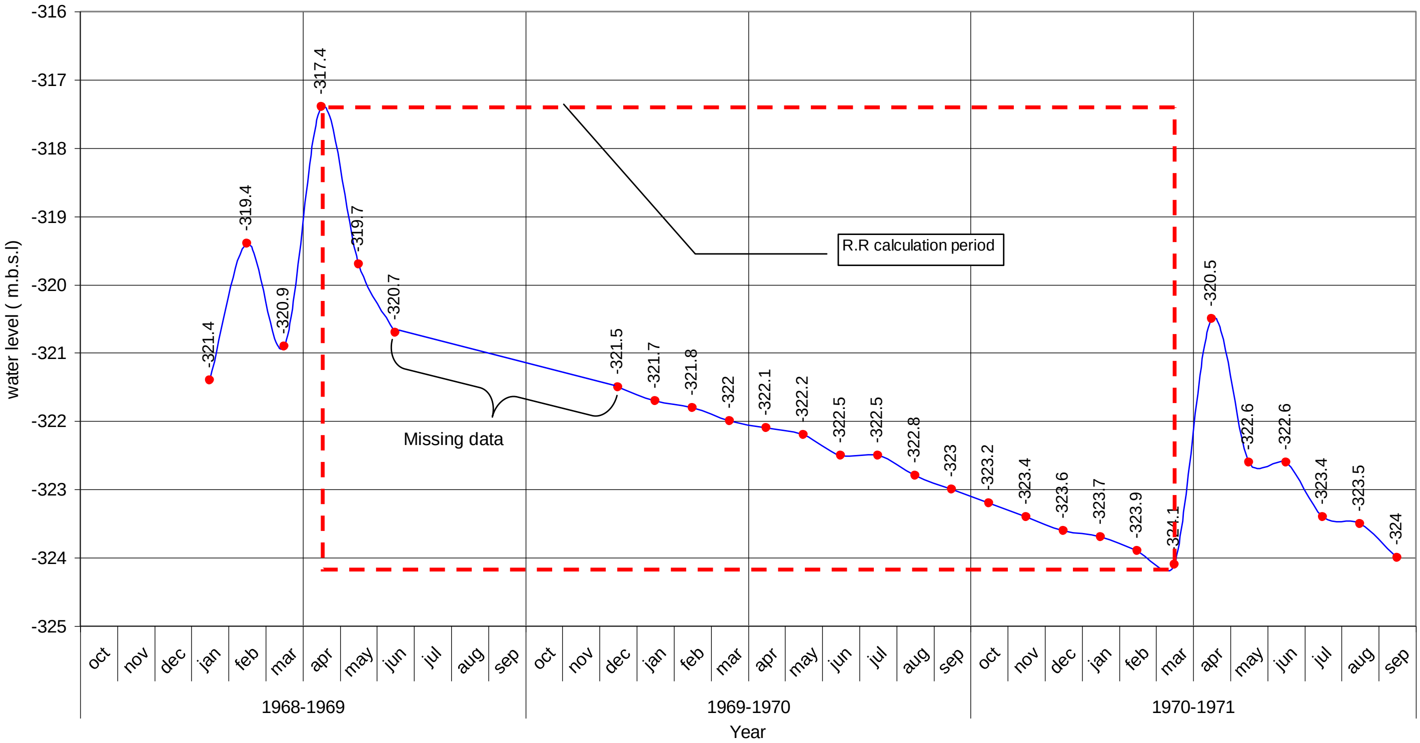

Figure 5.1.5 groundwater table hydrograph of the well 19-13/029.

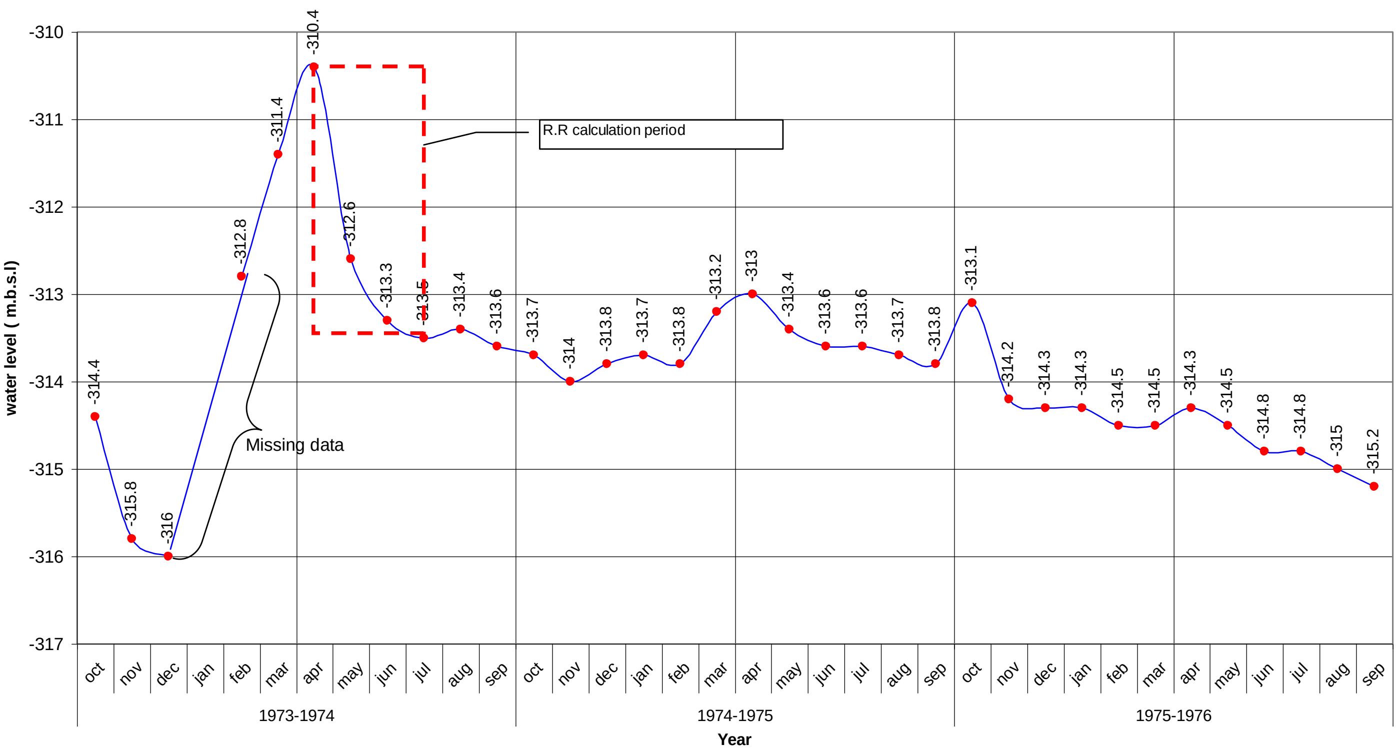

Figure 5.1.6 groundwater table hydrograph of the well 19-13/070.

5) Well 19-14/002:

This well located 2,346 m to the northwest of Wadi Al-Qilt near Sultan spring. (Fig. 5.1.1). The out cropping formation is mainly composed of sand, silt and gravel of Samra formation. This well has a depth of 150 m. This well mainly recharge from the underground seepage of Sultan spring water, also from the surface runoff of wadi New'emah. It is very close to the Sinomanian chalk formation (Abu-dies Formation). Consequently, the recharge rate should be very low. This idea is supported by the R.R value of the well which is 3.6 * 10^{-4} m/s. the average lag time estimated to be 165 days. (Fig. 5.1.7).

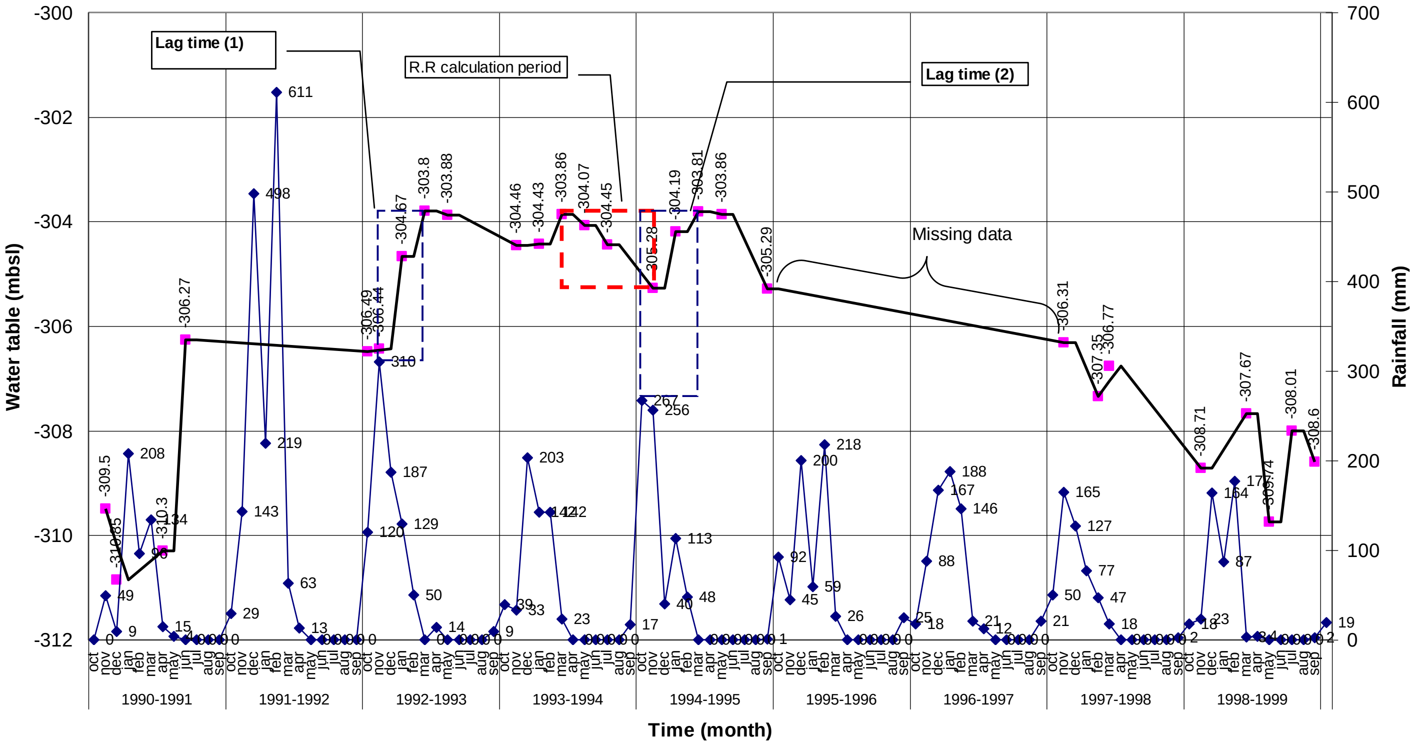

Figure 5.1.7 groundwater table hydrograph of the well 19-14/002.

6) Well 19-14/008:

This well locates 770 m by the north of Wadi Al-Qilt drainage system. It is drilled in the Samra outcropping formation. The depth of this well reaches 54 m. R.R was calculated based on the period of Mar/1993 to May/1994. The R.R value was 2.5 * 10^3 m/h and the average lag time was 155 days (Fig. 5.1.8). The short lag time is due to the direct recharge of Samra gravel layers, the extending of these layers intersecting with the Wadi's surface.

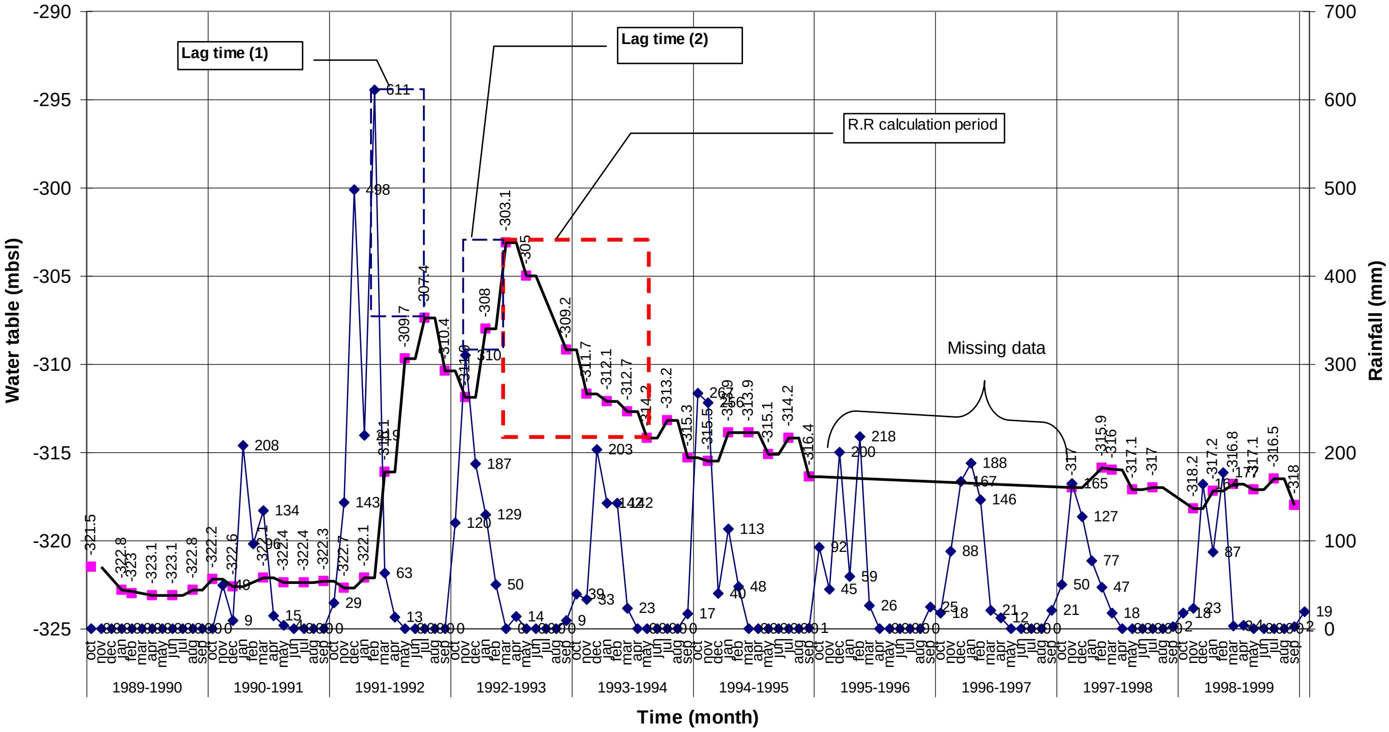

Figure 5.1.8 groundwater table hydrograph of the well 19-14/008.

7) Well 19-14/019:

This well locates in the core of Jericho field area. It lies by 1,555 m to the north of the Wadi, with total depth of 67 m. This well was drilled within the outcropping of Samra formation (Fig. 5.1.1). The lag time was estimated to be 210 days, and the R.R value is 3 * 10^{-3} m/h, and classify as high group of Samra gravel lithology (Fig. 5.1.9)

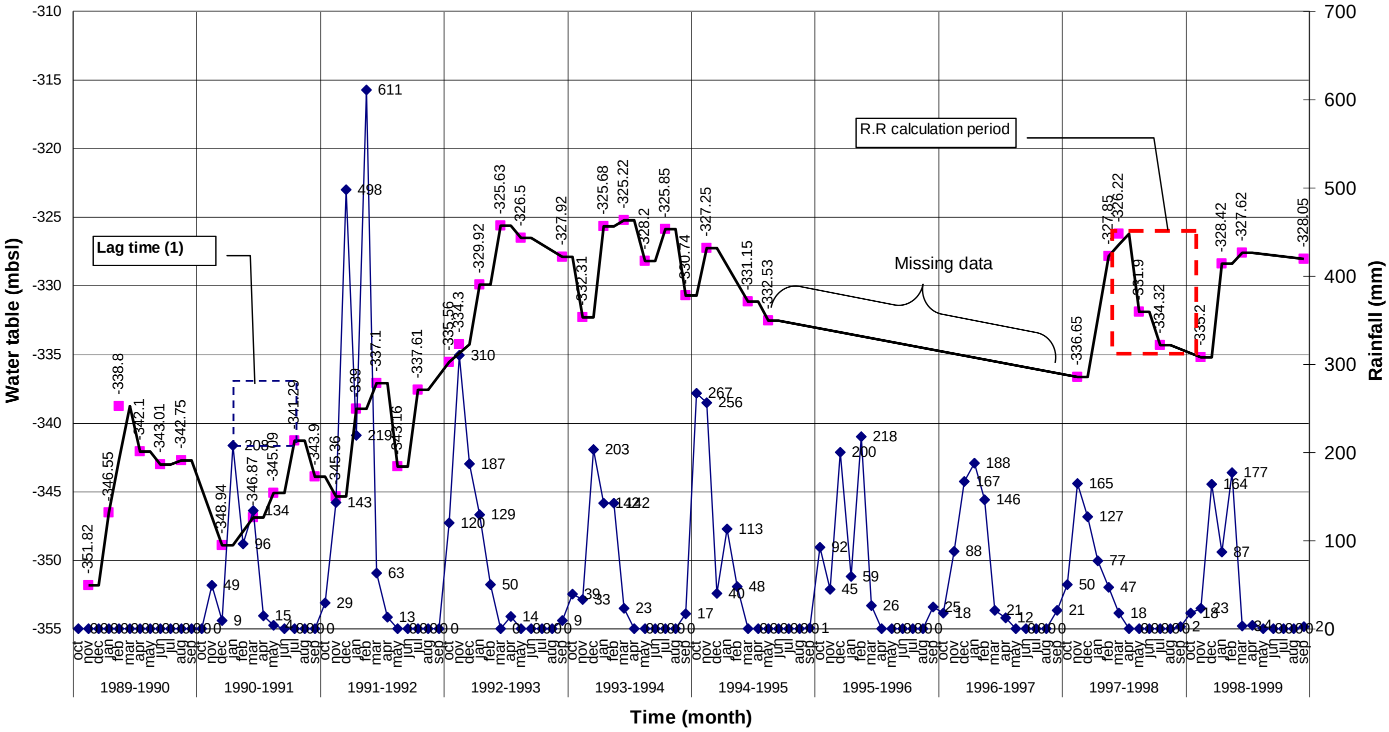

Figure 5.1.9 groundwater table hydrograph of the well 19-14/019.

8) Well 19-14/037T:

This well sited in the core area of Jericho field, it lays 1,500 m to the south of Wadi Newe'mah and 1,920 m to the north of Wadi Al-Quilt. The depth of this well reaches 83 m (Fig. 5.1.1). The R.R value is 6.6 * 10^{-4} m/h in average, so it indicates the inter-fingering of Lisan and Samra formations. The lag time is estimate to be 165 days in average (Fig. 5.1.10)

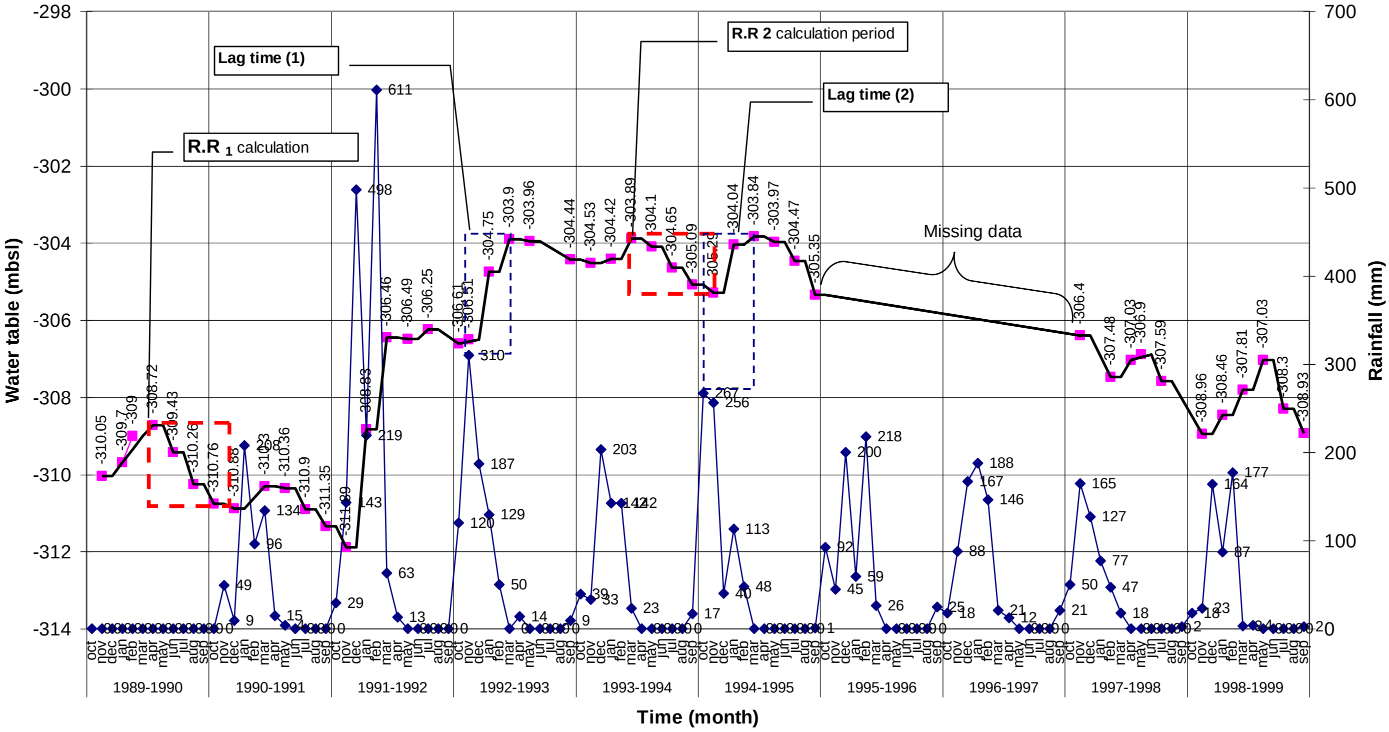

Figure 5.1.10 groundwater table hydrograph of the well 19-14/037T.

9) Well 19-14/064:

The depth of this well reaches 90 m, and it located by 2,500 m to the north of Wadi Al – Qilt. Samra formation is the outcropping formation (Fig. 5.1.1), and R.R value is 4.0 * 10^{-3} m/h indicate good connection between Samra coarse gravel member (Begin, 1974). The average lag time is 195 days. (Fig. 5.1.11).

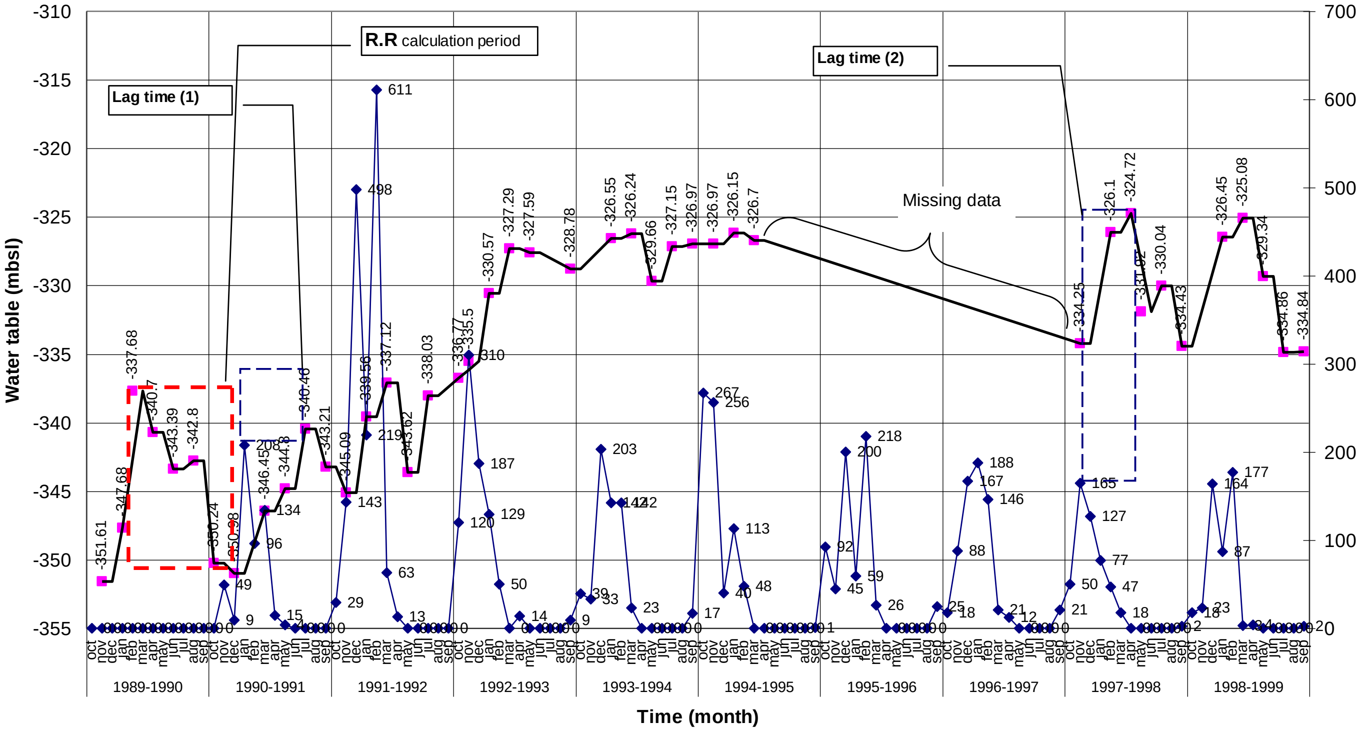

Figure 5.1.11 groundwater table hydrograph of the well 19-14/064T.

10) Well 19-14/066:

This well locates by 1,500 m to the north of Wadi Al-Qilt. It sited within the outcropping of the Samra formation. The hydrograph behavior is highly similar to well no. 19-14/064 hydrograph. The R.R value is 3.9 * 10^{-3} m/h, and the lag time is 210 days (Fig. 5.1.12). This value is very close to the value of well no. 19-14/066 indicating the same recharge pathway.

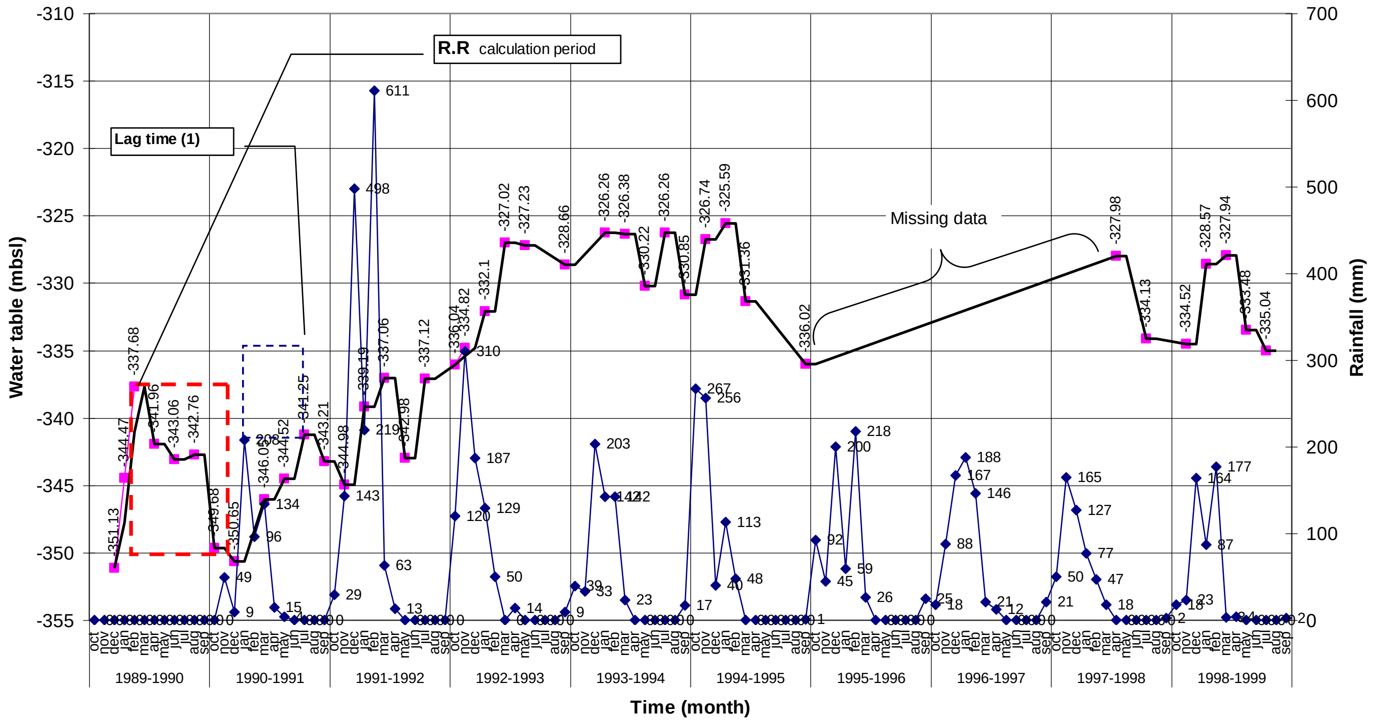

Figure 5.1.12 groundwater table hydrograph of the well 19-14/066.

11) Well 19-14/080:

This well is located in the Lisan outcropping area. It is sited 2,645 m to the north of the wadi. General view of the water table fluctuation hydrograph shows no clear groundwater peak. Rainfall peaks (Fig. 5.1.13) did not reflected by peak. The R.R value is the lowest 1.7 * 10^{-4} m/h, which means that the well lithology is mainly composed of marl – clay layers of Lisan formation. Very long average lags time of 410 days due to long distance from the wadi, and the marl – clay layers.

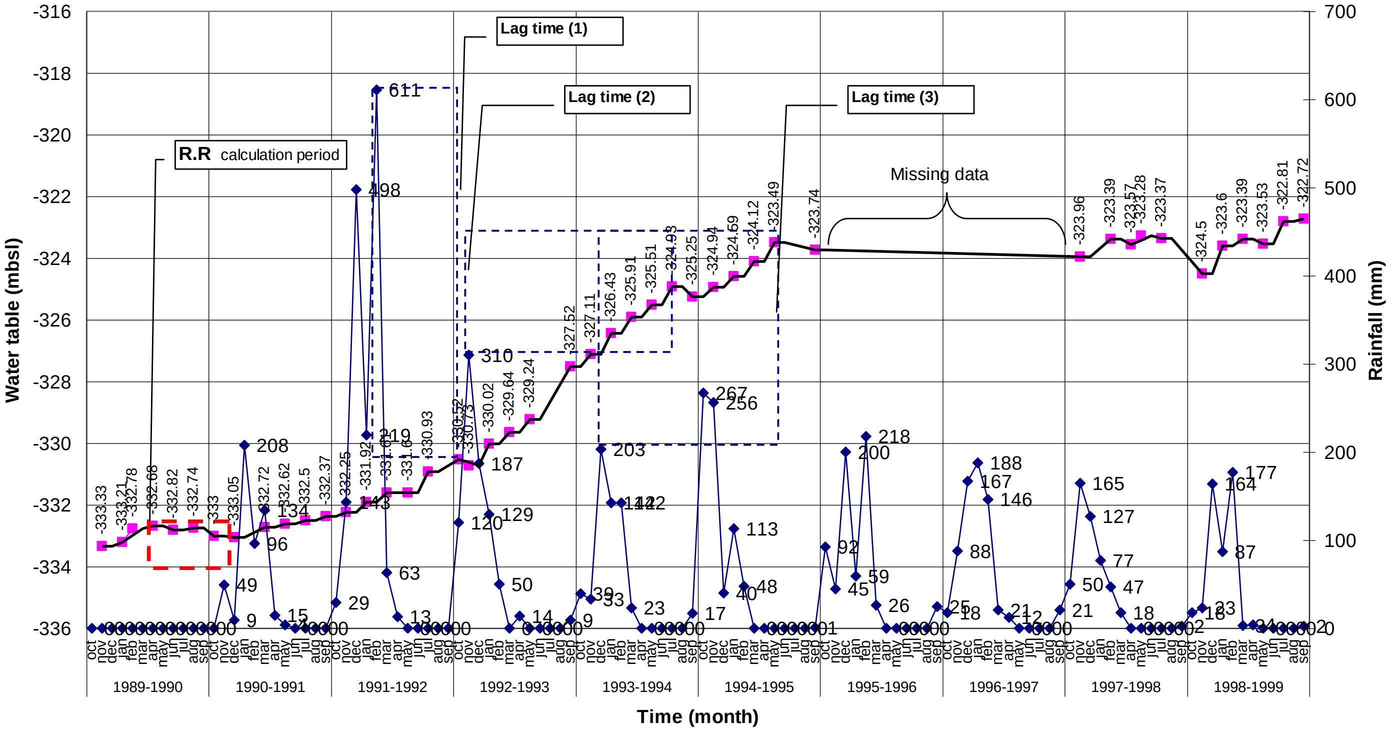

Figure 5.1.13 groundwater table hydrograph of the well 19-14/080.

12) Well 19-14/081:

It is locates in Samra formation outcropping (Fig. 5.1.1) Very good fluctuation in water table, long distance from Wadi Al-Qilt 3,040 m. The R.R with the value 5.4 * 10^{-4} m/h was grouped in the Lisan stratification aquifer. The estimated lag time was 180 day (Fig. 5.1.14). The low value of R.R is related to the inter-tanging phenomenon of Lisan and Samra formations.

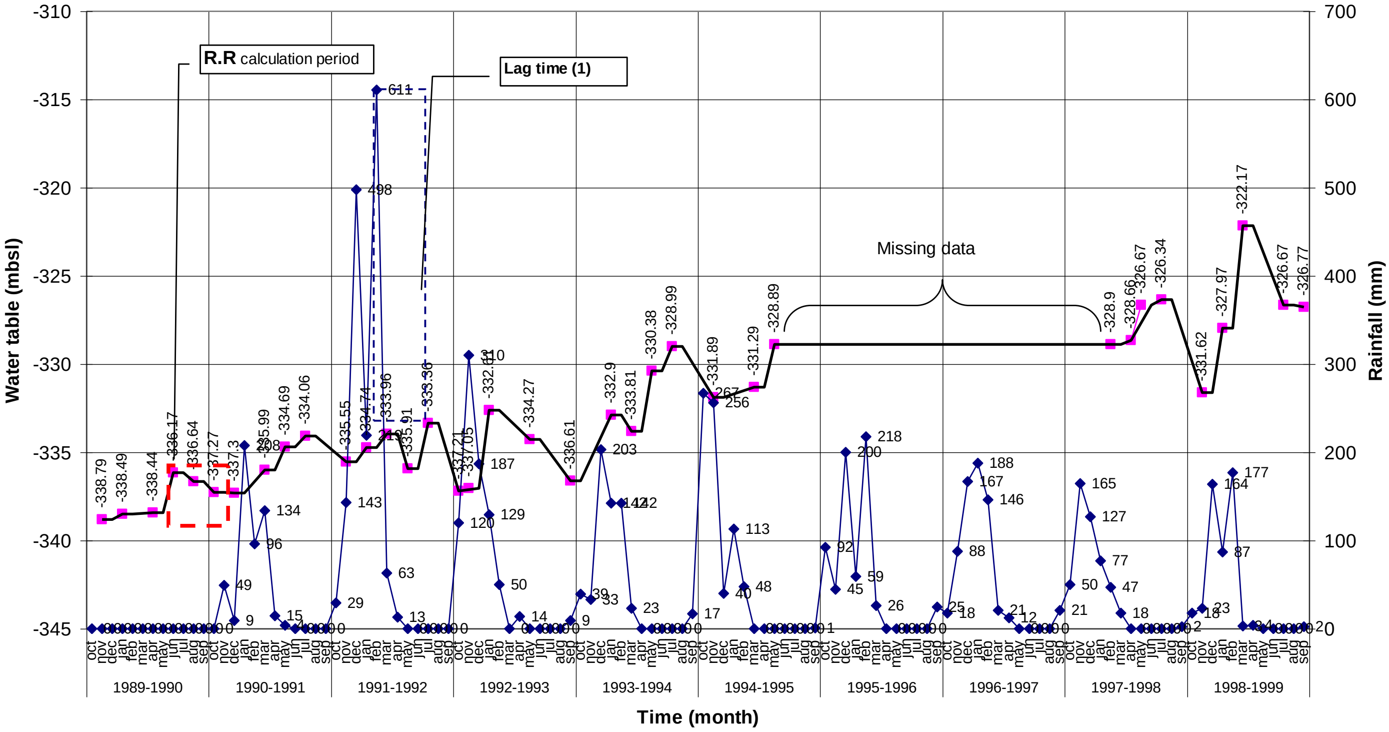

Figure 5.1.14 groundwater table hydrograph of the well 19-14/081.

13) Well 19-14/098:

This well is located about 2,190 m to the north of Wadi Al-Qilt (Fig. 5.1.1). It lies in the Lisan outcropping formation. The R.R value is calculated to 7.6 * 10^{-4} m/h indicating high Lisan lithology. The average lag time was 260 days (Fig. 5.1.15). The low R.R and high lag time reflecting the Lisan and Samra inter-tanging.

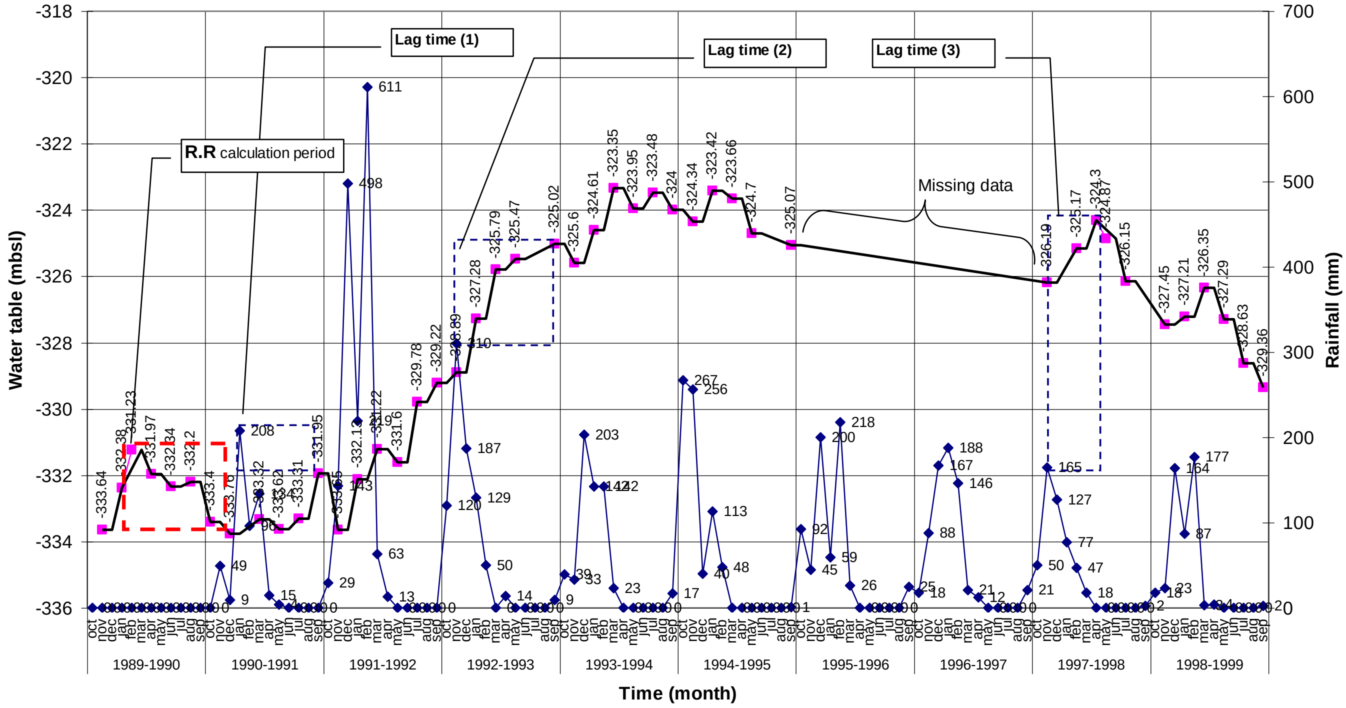

Figure 5.1.15 groundwater table hydrograph of the well 19-14/098.

5.2 Geo-electrical sounding

In order to support the main investigation idea, geophysical techniques was used intensively. Electrical sounding is chosen to explore the geological and lithological sitting of Jericho area. This technique is very useful to identify the lithological and geological characteristics of the underground.

The geo – electrical investigation of the Plio – Pleistocene gravel aquifer consists of seven geo-electrical profiles, which are accomplished and labeled form A – A' to G – G' (Fig. 5.2.1). Each profile composed of a group of vertical electrical sounding (VES) measuring points (Table 5.2.1).

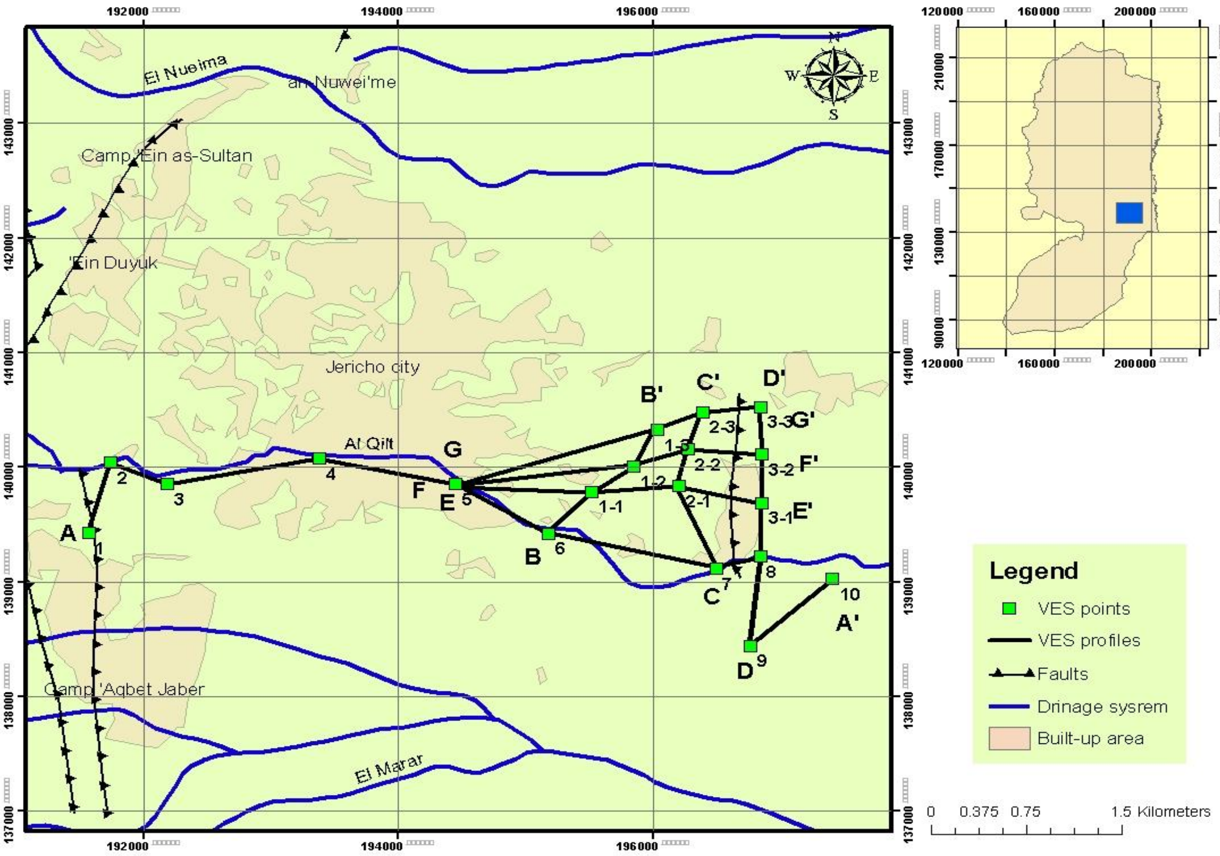

Figure 5.2.1 location of geo-electrical sounding profiles.

The total points of the all profiles are 19 VES points (Table 5.2.1). The minimum investigation depth is 75 m at the measuring point (8) along profile (A), and the maximum depth is 201 m at the measuring point (9) at profile (A).

These profiles explore the vertical lithological successive compositions in each measuring points. The horizontal lithological changes are explored in the profile mode. Each profile buildup by a numbers of VES measuring points in correlation with each others one by one mode. All profile locations are mapped in (Fig. 5.2.1).

Table 5.2.1 vertical electrical sounding points

VES Points	East	North	Ground elevation	Groundwater table
1	191570	139421	-220	-295
2	191745	140039	-230	-295
3	192191	139851	-233	-295
4	193382	140072	-245	-295
5	194450	139849	-265	-310
6	195180	139418	-279	-333
7	196496	139112	-300	-351
8	196842	139220	-315	-353
9	196767	138437	-307	-356
10	197410	139020	-320	-359
1-1	195520	139759	-280	-337
1-2	195839	139992	-289	-341
1-3	196029	140337	-290	-342
2-1	196193	139854	-295	-340
2-2	196279	140173	-297	-343
2-3	196374	140492	-292	-344
3-1	196848	139690	-307	-352
3-2	196839	140095	-304	-348
3-3	196839	140518	-305	-344

The relation between electrical resistivity and lithological compositions are describing in (Table 5.2.2), electrical resistivity values are compared with the results which obtained by (Avihu, 1979) in Arava area south of Palestine

Table (5.2.2): lithological description of electrical resistivity values.

Lithology	**Electrical Resistivity**	
	Arava* *Ω.m*	***Jericho*** *Ω.m*
Gravel	98 – 110	100 – 200
Limestone	150	100 – 150
Chalk	------	40 – 80
Sand + silt	34 – 53	70-30
Marl	5 – 15	20 – 40
Marl + clay	5 – 10	10 – 30
Saline water	Less than 4.0	Less than 1.0

(-----): data not available. *: Avihu, 1979.

5.2.1 Electrical sounding and lithology profiles description:

1) Profile (A – A'):

This profile starts from the outlet of Wadi Al-Qilt and ends in the area of Ketf Alwad in the eastern sides of Jericho city (Fig. 5.2.1). This profile composed of 10 VES points directed east – west. The total length of the profile is 7,723 meter. The measuring VES points is labeled from 1 to 10, the points 1, 2, 7, and 9 located out side of the wadi stream pathway, where's the points 3, 4, 5, 6, 8 and 10 locate inside the wadi stream pathway (Fig. 5.2.1).

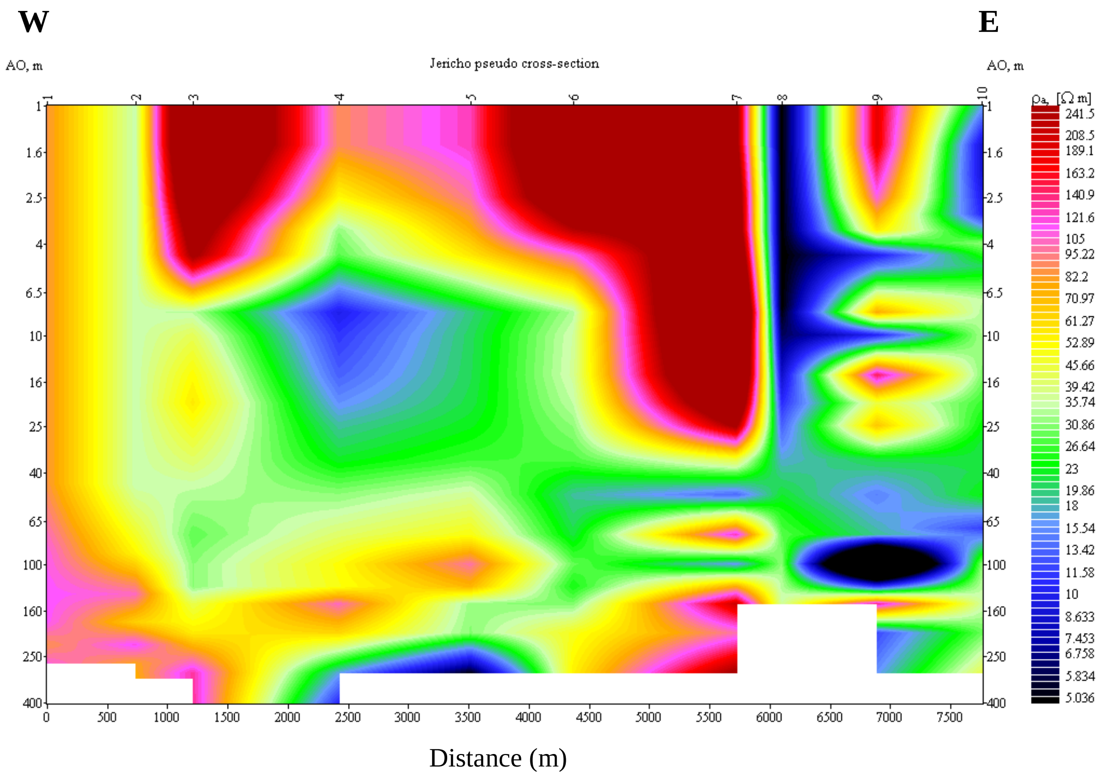

Figure 5.2.2a (A – A') electrical sounding profile.

The maximum depth was reached in point (9) and the minimum depth reached in point (8). 10,045 Ω.m was the maximum resistivity value; it was measured at a depth of about 2 m. the lowest resistivity value was less than 1 Ω.m, it was measured in point 4 at 96 m depth, also it was measured in points (5) and (10) at 75 m, 119 m depth respectively . (Fig. 5.5.2a). Litological characteristics are illustrating in (Fig. 5.2.2b) and describe in (Table. 5.2.3).

2) Lithology of profile (A – A'):

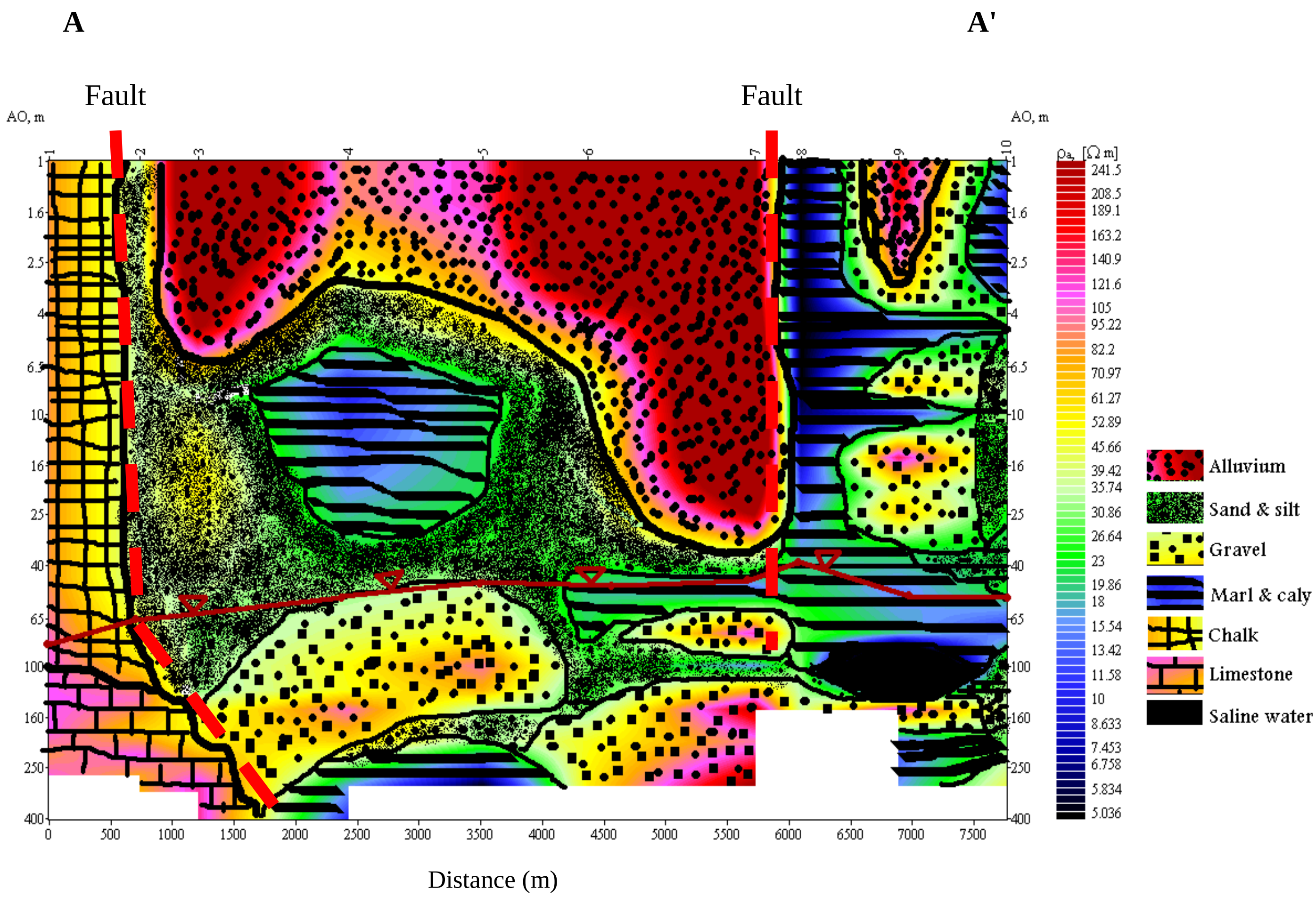

Figure 5.2.2b lithology of the electrical profile (A – A').

Table (5.2.3) Lithological description of A – A' profile.

Point-ID	ρ (Ω.m)	Depth (m)	Lithology	Potential use for water
1	40-80	0-100	Chalk	Aquicluds
	100-150	100-150	Limestone	Aquifer
2	70-30	0-90	Silt - Sand	Semi aquifer
	100-150	90-250	Limestone	Aquifer
3	150-300	0-6.5	Alluvium	Top soil
	70-30	6.5-110	Silt - Sand	Semi aquifer
	100-150	110-250	Limestone	Aquifer
4	150-300	0-4	Alluvium	Top soil
	70-30	4-6.5	Silt - Sand	Semi aquifer
	30-10	6.5-30	Marl + clay	Aquicluds
	70-30	30-50	Silt - Sand	Semi aquifer
	100-200	50-170	Gravel	Aquifer
	70-30	170-200	Silt - Sand	Semi aquifer
	30-10	200-250	Marl + clay	Aquicluds
5	150-300	0-5	Alluvium	Top soil
	70-30	5 8	Silt - Sand	Semi aquifer
	30-10	8 20	Marl + clay	Aquicluds
	70-30	20-50	Silt - Sand	Semi aquifer
	100-200	50-160	Gravel	Aquifer
	70-30	160-200	Silt - Sand	Semi aquifer
	30-10	200-250	Marl + clay	Aquicluds
6	150-300	0-6.5	Alluvium	Top soil
	70-30	6.5-40	Silt - Sand	Semi aquifer
	30-10	40-70	Marl + clay	Aquicluds
	70-30	70-120	Silt - Sand	Semi aquifer
	100-200	120-200	Gravel	Aquifer
7	150-300	0-30	Alluvium	Aquifer
	70-30	30-50	Silt - Sand	Semi aquifer
	30-10	50-65	Marl + clay	Aquicluds
	100-200	65-100	Gravel	Aquifer
	70-30	100-120	Silt - Sand	Semi aquifer
	100-200	120-180	Gravel	Aquifer
8	30-10	0-100	Marl + clay	Aquicluds
	70-30	100-110	Silt - Sand	Semi aquifer
	100-200	110-150	Gravel	Aquifer
9	150-300	0-3	Alluvium	Top soil
	100-200	3 4	Gravel	Aquifer
	30-10	4-6.5	Marl + clay	Aquicluds
	100-200	6.5-9	Gravel	Aquifer
	30-10	9 11	Marl + clay	Aquicluds
	100-200	11 30	Gravel	Aquifer
	30-10	30-70	Marl + clay	Aquicluds
	>1	70-130	Saline water	Aquifer
	100-200	130-160	Gravel	Aquifer
	30-10	160-200	Marl + clay	Aquicluds
10	30-10	0-3	Marl + clay	Top soil
	100-200	3-4.5	Gravel	Aquifer
	70-30	4.5-25	Silt - Sand	Semi aquifer
	30-10	25-70	Marl + clay	Aquicluds
	100-30	70-150	Gravel + marl + clay	Aquicluds
	30-10	150-180	Marl + clay	Aquicluds

1) Profile (B – B'):

This profile located in the middle of Jericho field area (Fig. 5.2.1). The length of this profile is 1,290 m; it was directed north – south. Four (VES) points are composed the profile which are labeled (6), (1 – 1), (1 – 2), and (1 – 3). The measurement starts from the Wadi center to the middle of Jericho field. The maximum depth reached was 150 m, and was reached by point 6. The shallow depth was at point (1 – 3) which reached 80 m.

S **N**

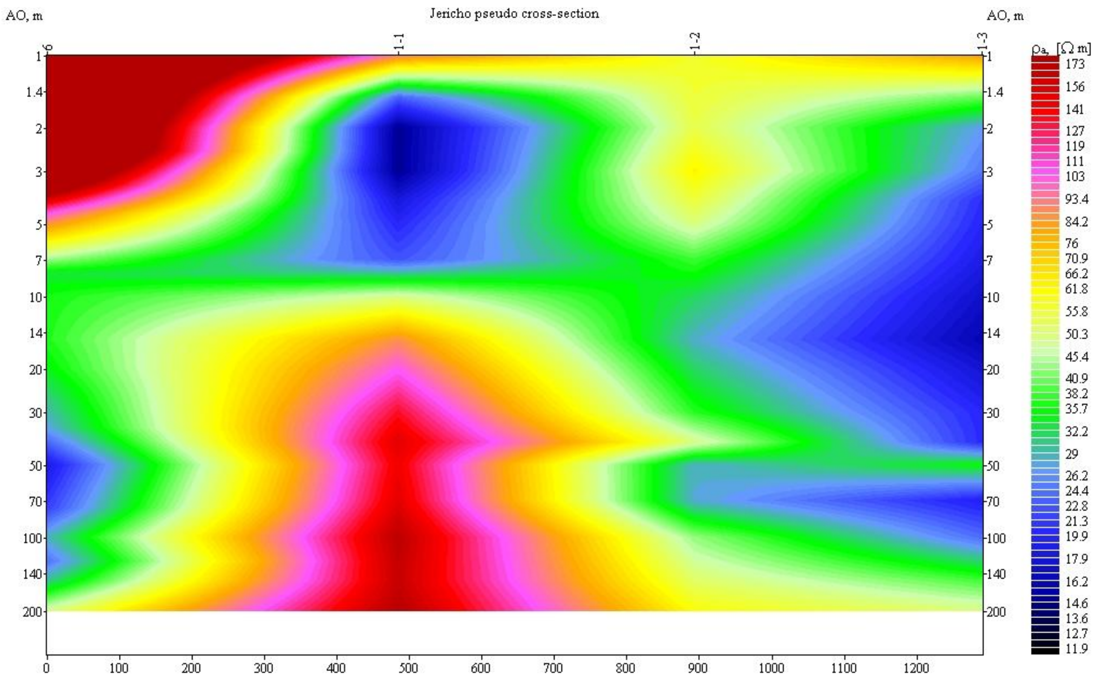

Distance (m)

Figure 5.2.3a (B – B') electrical sounding profile.

The maximum resistivity values (ρ) was measured at point (1 – 1), with 4,670 Ω.m at 4 m depth. The lowest (ρ) values were measured at point (1 – 3) at a subsurface depth of 0.5 m. The distribution electrical resistivity among (B – B') profile contains many different features. P values are greater tan 200 Ω.m under the point 6, it reached about 4 m depth, also there are such values under the point (1 – 1) at a depth ranging between 15 m to about 200 m.(Fig. 5.2.3a)

Distinguished low (ρ) values located in the subsurface area of the point (1 – 1) and along the point (1 – 3), it reached about 100 m depth. There are intermediate (ρ) values ranging between 45 Ω.m to 75 Ω.m. this feature located at 5 m depth under the point (1 – 2). (Fig. 5.2.3a)

2) Lithology of profile (B – B'):

Alluvium deposits located just before the wadi in point 6, it reached about 5m in depth. Sand – Silt layers located beneath the alluvium. Thickness ranging from 2 – 4 meter. Marl – clay layers located below the sand – silt layers, its thickness ranging between 7 – 30 maters. Moreover, thick sand – silt layers located at 20 m depth with 15 m thickness in average. Gravel mass located in point (1 – 1) with 60 m depth. (Fig. 5.2.3b)

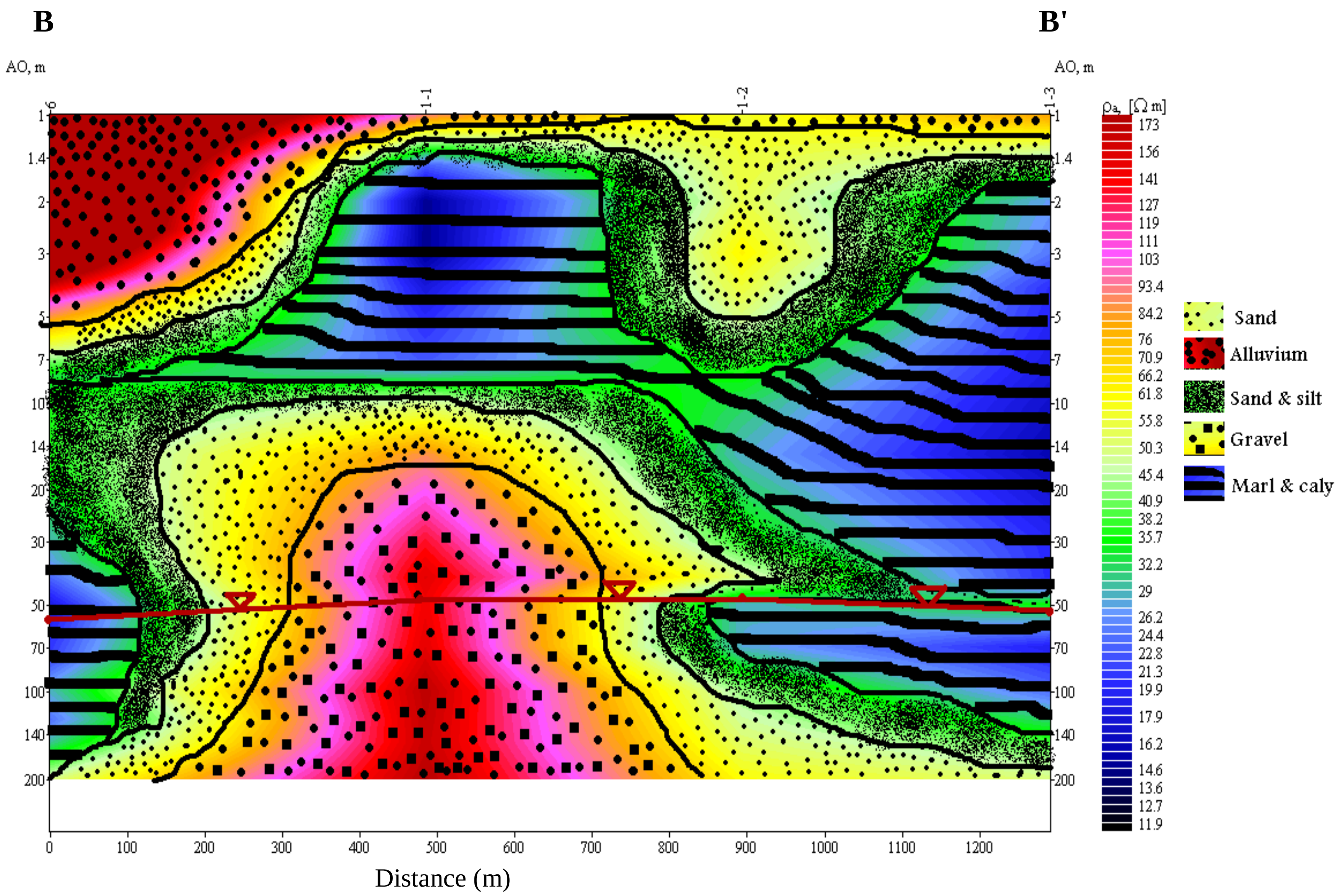

Figure 5.2.3b lithology of the electrical profile (B – B').

Table (5.2.4) Lithological description of (B – B').

Point-ID	ρ (Ω.m)	Depth (m)	Lithology	Potential use for water
6	100-250	0-4	Alluvium	Top soil
	150-80	4 6	Sand	Aquifer
	70-30	6 25	Sand + silt	Semi aquifer
	30-15	25 140	Marl + clay	Aquiclude
(1-1)	150 300	0-1	Alluvium	Top soil
	70-30	1 2	Sand + silt	Semi aquifer
	30-15	2 7	Marl + clay	Aquiclude
	70-30	20 7	Sand + silt	Semi aquifer
	150-250	20-140	Gravel	Aquifer
(1-2)	90-30	0-8	Silt + sand + alluvium	Top soil + sediments
	30-15	8 25	Marl + clay	Aquiclude
	70-30	25-50	Silt + sand	Semi aquifer
	30-15	50-80	Marl + clay	Aquiclude
	70-30	80-200	Silt + sand +clay	Aquiclude
(1-3)	100-150	0-2	Alluvium + sand	Top soil
	30-15	2 48	Marl + clay	Aquiclude
	70-30	48-52	Silt + sand	Semi aquifer
	30-15	52-140	Marl + clay	Aquiclude
	70-30	140-200	Silt + sand	Semi aquifer

1) Profile (C – C'):

This profile is locates in front of profile (B –B'), the total length of the profile is 1,455 m directed north – south. It is composed of 4 VES measuring points, which labeled (7), (2 – 1), (2 – 2), and (2 – 3). the maximum depth was 200 m reached in point 7, and the minimum depth was 80 m reached in point (2 – 1). The highest (ρ) value was measured to 14,400 Ω.m at 1 m depth, and the lowest (ρ) value (less than 1 Ω.m) was measured at 65 m and 80 m depth in point (2 – 1).

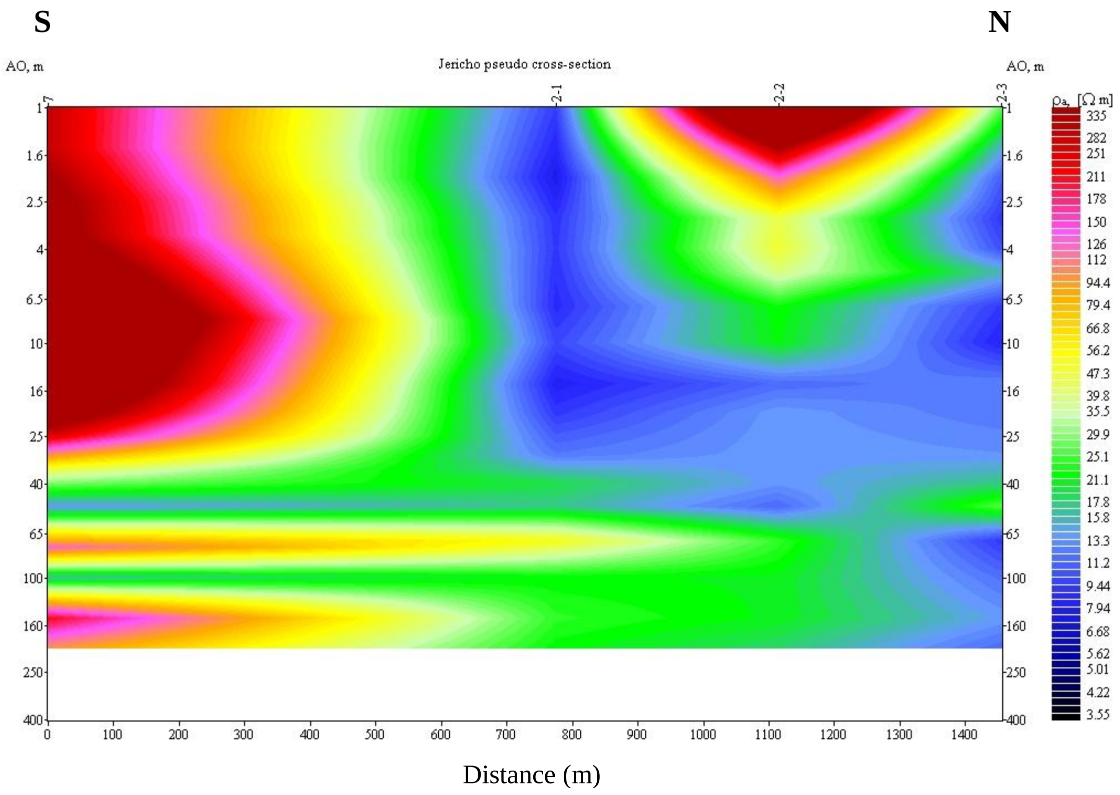

Figure 5.2.4a (C – C') electrical sounding profile.

(ρ) Values distribution buildup the following distinguished features:

1- High values (more than 200 Ω.m) located in firstly in the measuring point (7), it is starting from the surface and reached about 30 m depth, the second feature located in the measuring point (2-2), starting from the surface and ending in about 2 m depth.(Fig. 5.2.4a). Another high values of (ρ) located at 150 m depth in the measuring site (7).

2- Low (ρ) values located between the measuring points (2 – 1), (2 – 2), and (2 – 3), it shows some type of vertical feature extending from the surface to about 30 m depth. Also in the measuring point (1 – 3) there is some kind of successive features of low (ρ) values (less than 10 Ω.m) reaching a 43 m depth. (Fig. 5.2.4a). Another horizontal low values located between the measuring points (2 – 1), (2 – 2), and (2 – 3) at a depth ranging between 8 and 25 m. this low (ρ) values ranging between (10 – 1) Ω.m.

3- Intermediate (ρ) values located between the measuring points (7) and (2 – 1), (ρ) values featured a horizontal structure. It is located between 55 m and 80 m depth. (ρ) Values of this feature ranging between (30 – 150) Ω.m. Also this (ρ) values located in the measuring point (2 – 2) between 2 m and 6 m depth. (Fig. 5.2.4a)

2) Lithology of profile (C – C'):

Close to the wadi there is alluvium mass reached a thickness between 7 – 15 meters in the upper part of the profile. Gravel lenses located near the wadi in point (7), it range between 20 – 30 meter in thickness. Marl – clay layers could be seen in the points (1 – 2), (2 – 2), and (2 – 3). (Fig. 5.2.4b)

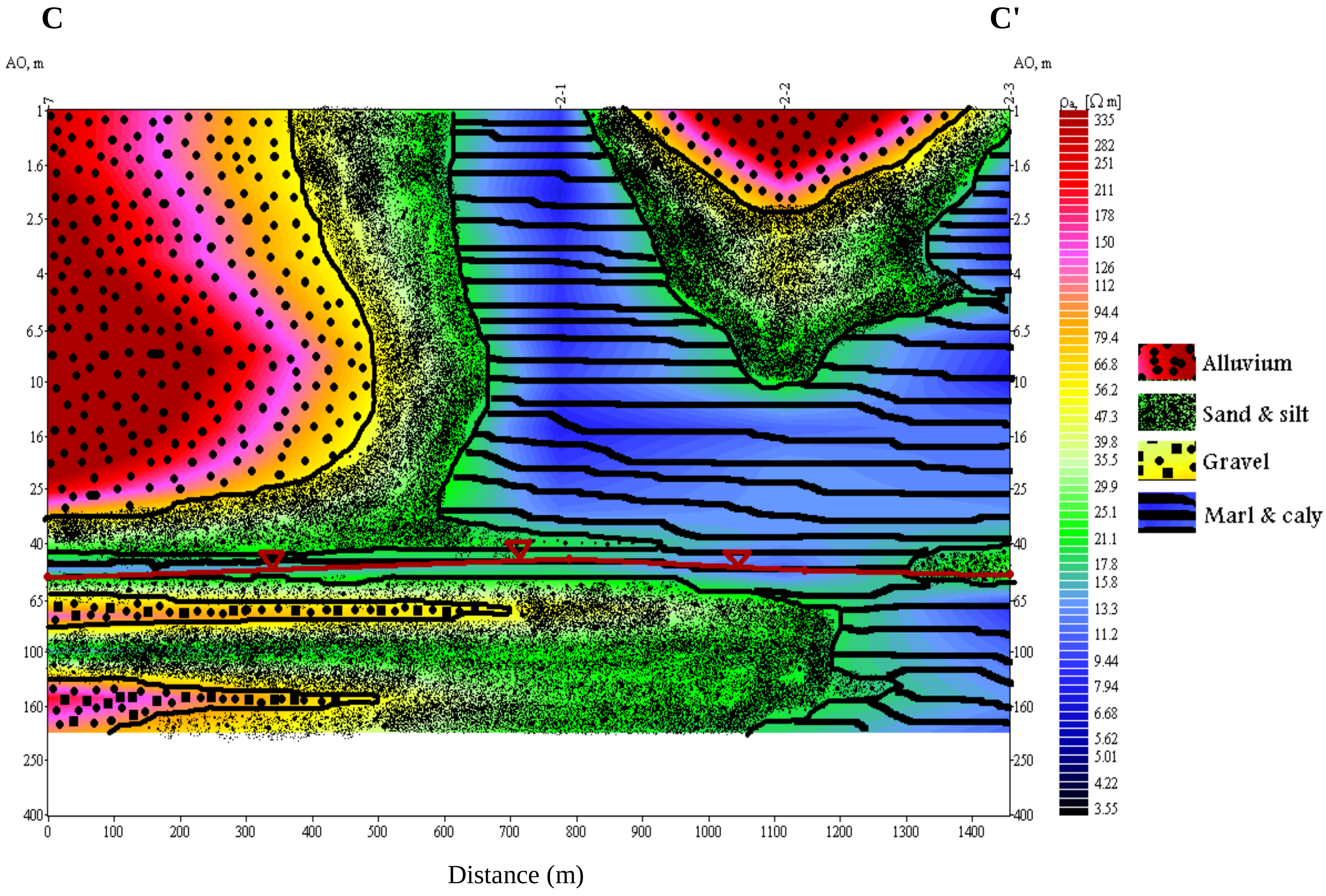

Figure 5.2.4b lithology of the electrical profile (C – C').

Table (5.2.5) Lithological description of (C – C').

Point-ID	**ρ (Ω.m)**	**Depth (m)**	**Lithology**	**Potential use for water**
7	300-150	0-30	Alluvium	Aquifer
	70-30	30-45	Silt + sand	Semi aquifer
	30-10	45-55	Marl + clay	Aquiclude
	70-30	55-60	Silt + sand	Semi aquifer
	100-200	60-75	Gravel	Aquifer
	70-30	75-130	Silt + sand	Semi aquifer
	100-200	130-170	Gravel	Aquifer
(2-1)	15-10	0-38	Marl + clay	Aquiclude
	50-30	38-43	Silt + sand	Semi aquifer
	15-10	43-50	Marl + clay	Aquiclude
	50-30	50-60	Silt + sand	Semi aquifer
	100-150	60-68	Gravel	Aquifer
	50-30	68-170	Silt + sand	Semi aquifer
(2-2)	150-300	0-2	Alluvium	Top soil
	70-30	2 11	Silt + sand	Semi aquifer
	30-10	11 65	Marl + clay	Aquiclude
	70-30	65-170	Silt + sand	Semi aquifer
	30-10	170-180	Marl + clay	Aquiclude
(2-3)	70-30	0-1.5	Silt + sand	Top soil
	30-10	1.5-5	Marl + clay	Aquiclude
	70-30	5 6	Silt + sand	Semi aquifer
	70-10	6 40	Marl + clay	Aquiclude
	70-30	40-60	Silt + sand	Semi aquifer
	30-10	60-170	Marl + clay	Aquiclude

1) Profile (D – D'):

This profile located to the east of profile (C – C'), it is 2,184 m long, this profile composed of 5 VES measuring points, 3 of them (3 – 1), (3 – 2), and (3 – 3) located to the north of Wadi Al-Qilt (Fig. 5.2.1), the VES measuring points (9) and (8) located south of the Wadi. The maximum depth was reached in the measuring point (9), and the lowest depth was reached in the measuring point (8).

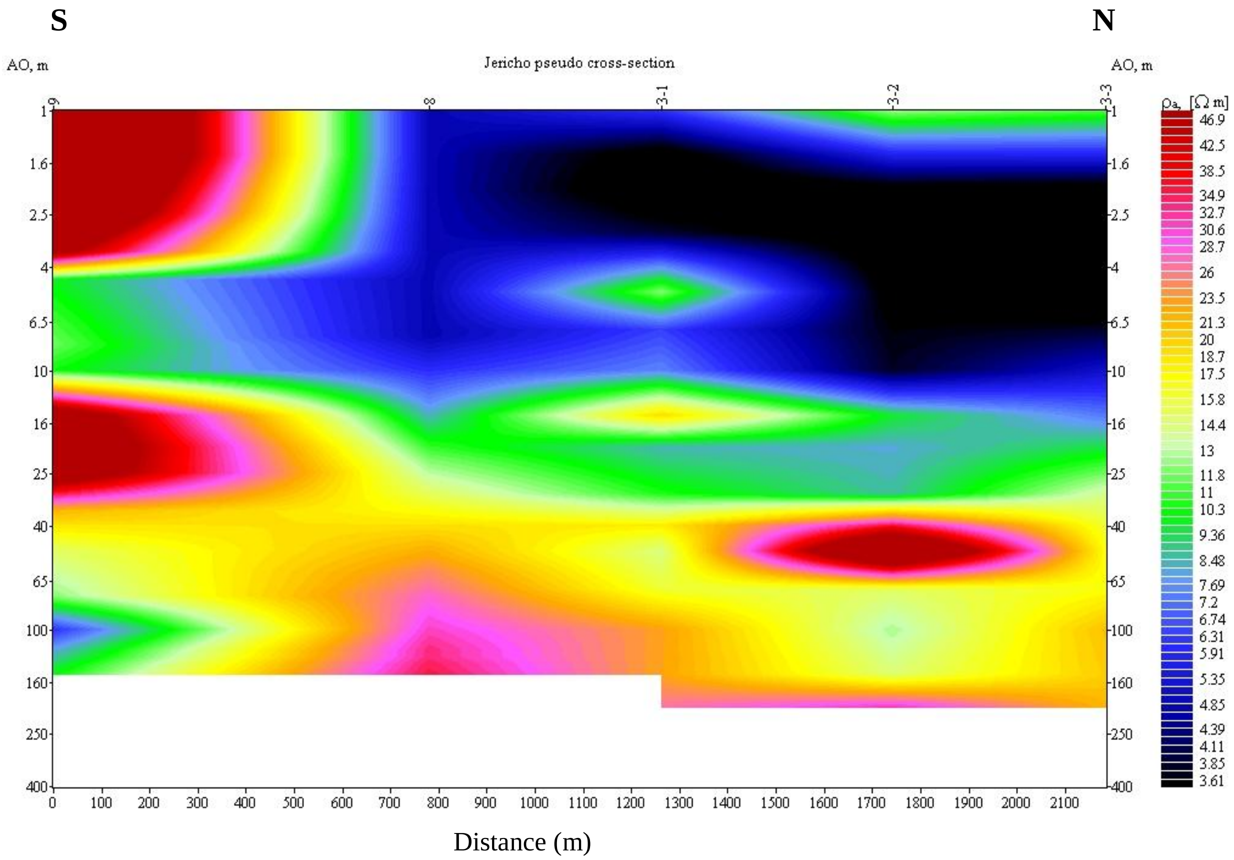

Figure 5.2.5a (D – D') electrical sounding profile.

Deep looking to the electrical resistivity profile (D – D') shows the following features:

1- the maximum (ρ) values was recorded in the VES measuring point (9) at a depth rang between 3,5 m and 4.5 m, this (ρ) values recorded more than 200 Ω.m. it has some type of horizontal extension toward the VES measuring point (8). (Fig. 5.2.5a).

2- A distinguished low resistivity body extending horizontally allover the profile at a different depth. (Fig. 5.2.5a). this low (ρ) values (less than 10 Ω.m) continuously extending form the surface of the measuring points (8), (3 – 1), (3 – 2), and (3 – 3), it is ranging between the surface to about 30 m depth in the above points, also it is connected to the same (ρ) values in the measuring point (9) at a depth ranging between (4 – 12) m. (Fig. 5.2.5a)

3- Another (ρ) values located along the profile at a depth ranging between 12 – 60 m in point (9), and located at a depth between (30 – 100) m at the rest of the profile. This (ρ) ranging between 15 Ω.m to 100 Ω.m.

4- There are a significant low (ρ) values located within the previous values ((ρ) = (10 – 100) Ω.m). This low (ρ) values is less than 15 Ω.m, it is located in the measuring points (3 – 1) and (3 – 2) at a depth ranging between 40 m to 70 m in point (3 – 1) and between 70 m to 150 m in the point (3 – 2). (Fig. 5.2.5a).

2) Lithology of profile (D – D'):

Alluvium deposits located near the wadi at point (9), it is 4 m depth. Marl – clay layers are dominant among the profile to a depth of 10 – 25 meters. Gravel mass located in point (9) with 25 m thickness. Nevertheless, another gravel lenses appears at point (3 – 2) with 30 m depth. Sand – silt layers located under the marl – clay layers, thickness is ranging between 20 – 30 meters. Again, gravel layers appear under the sand – silt layers with a thickness ranging between 20 – 40 meters. (Fig. 5.2.5b)

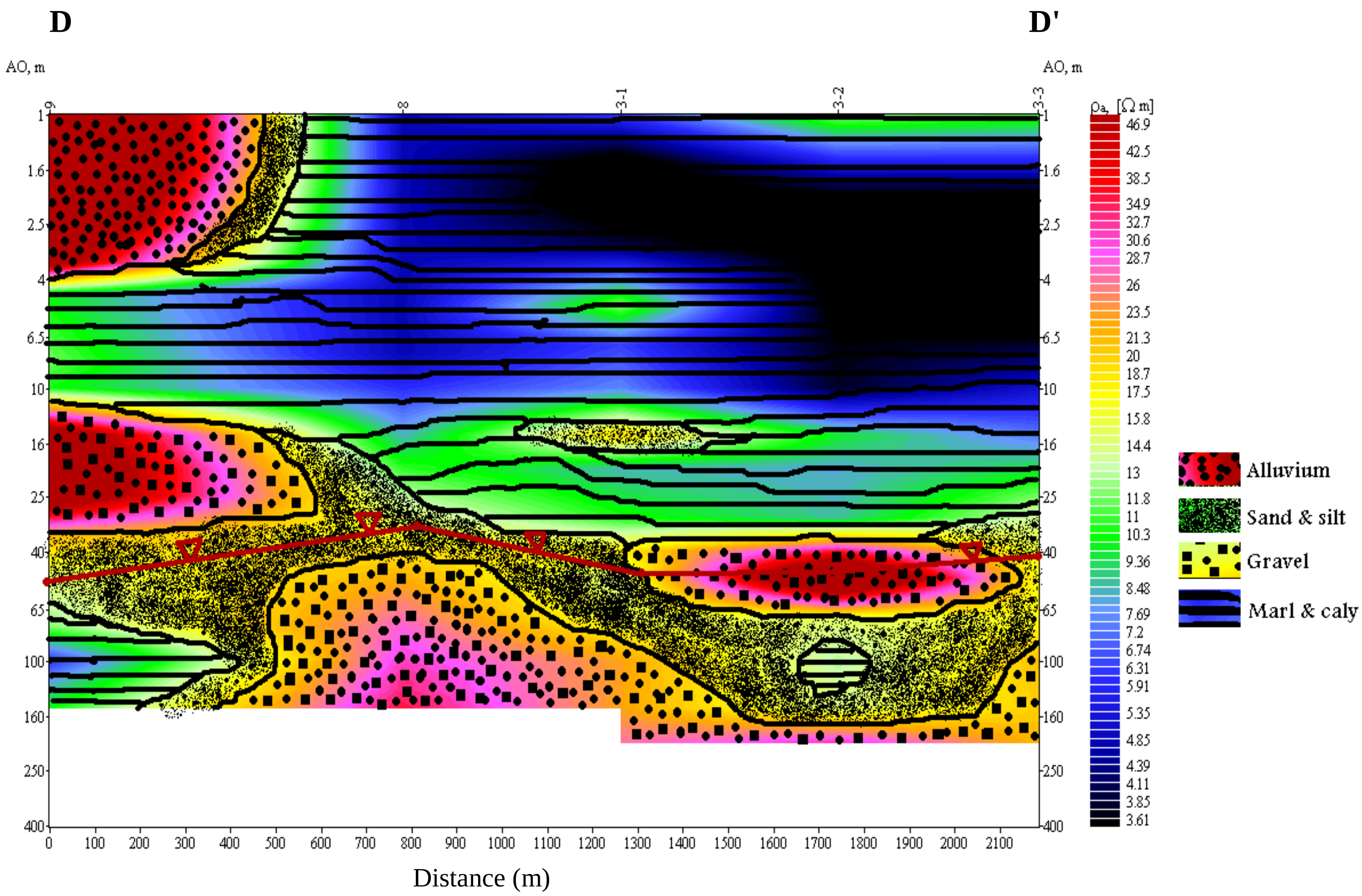

Figure 5.2.5b lithology of the electrical profile (D – D').

Table (5.2.5) Lithological description of D – D'.

Point-ID	**ρ (Ω.m)**	**Depth (m)**	**Lithology**	**Potential use for water**
9	150-300	0-4	Alluvium	Top soil
	20-10	4 11	Marl + clay	Aquiclude
	100-200	11 30	Gravel	Aquifer
	50-30	30-60	Silt + sand	Semi aquifer
	30-10	60-130	Marl + clay	Aquiclude
8	20-10	0-20	Marl + clay	Aquiclude
	50-30	20-45	Silt + sand	Semi aquifer
	100-30	45-130	Gravel + Marl + clay	Aquiclude
(3-1)	20-8	0-14	Marl + clay	Aquiclude
	50-30	14-20	Silt + sand	Semi aquifer
	20-10	20-42	Marl + clay	Aquiclude
	50-30	42-75	Silt + sand	Semi aquifer
	100-30	75-130	Gravel + Marl + clay	Aquiclude
(3-2)	20-8	0-40	Marl + clay	Aquiclude
	100-200	40-60	Gravel	Aquifer
	50-30	60-80	Silt + sand	Semi aquifer
	25-10	80-120	Marl + clay	Aquiclude
	50-30	120-165	Silt + sand	Semi aquifer
	100-30	168-180	Gravel + Marl + clay	Aquiclude
(3-3)	20-8	0-28	Marl + clay	Aquiclude
	50-30	28-70	Silt + sand	Semi aquifer
	100-30	70-180	Gravel + Marl + clay	Aquiclude

1) Profile (E – E'):

The resistivity data within this profile is composed by correlating the electrical resistivity data of the point (5), (1 -1), (2 – 1), and (3 – 1). The total length of this profile reached 2,422 m and it is directed west – east (figure 5.2.1). The minimum (ρ) values (less than 1 Ω.m) was recorded at point (3 – 1) at 3.5 m depth. Maximum (p) value (4,670 Ω.m) was recorded at point (1 – 1), it is located at 4 m depth.

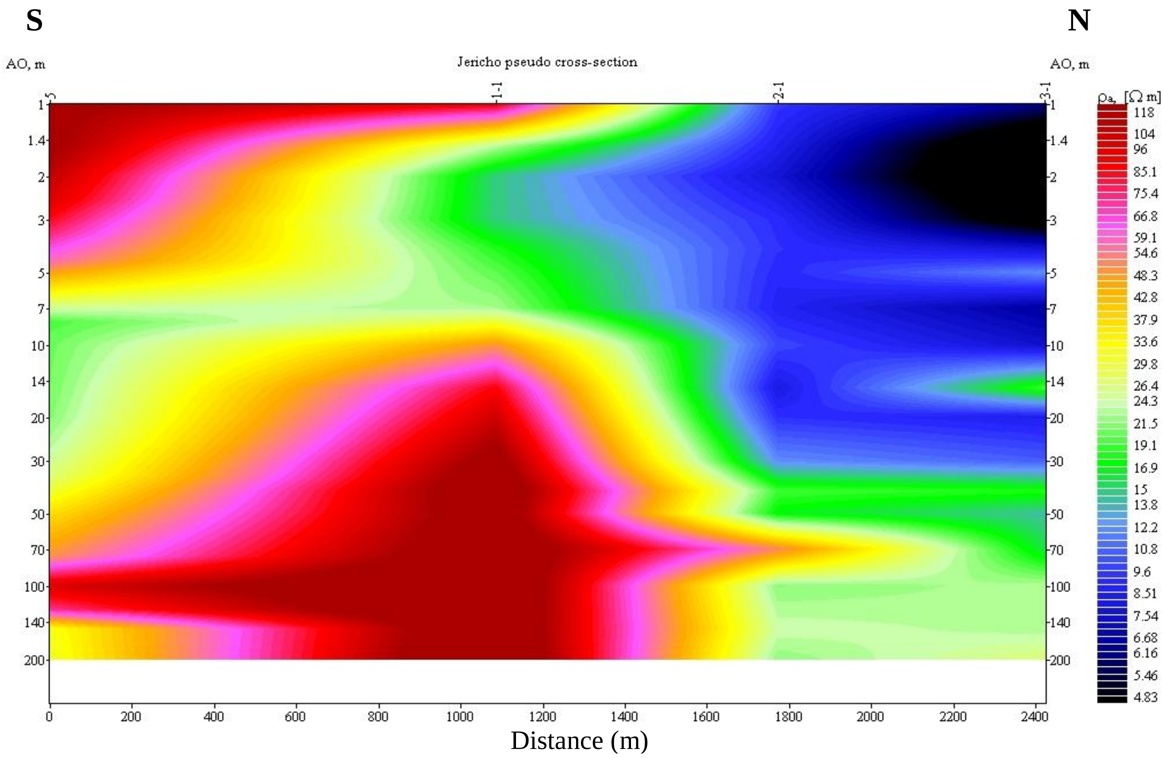

Figure 5.2.6a (E – E') electrical sounding profile.

Three distinguished features were identifying within this profile. The electrical resistivity features of this profile are described as the following:

1- Low resistivity values (ρ) were located between the points (1 – 1), (1 – 2), and (3 – 1) at (1.5 m to 3.5 m) in point (1 – 1), this (ρ) values located in points (2 – 1) and (3 – 1) from the surface to 35 m depth. (ρ) Values ranging between 15 Ω.m to less than 1 Ω.m.

2- High (ρ) values located in tow places in this profile, first one located between the points 5 and (1 – 1). It is starts from the surface to about 6 m depth at point 5. Whereas it reached almost 1.5 m in point (1 - 1). The values of (ρ) ranges between 40 Ω.m to more than 300 Ω.m. (Fig. 5.2.6a). The second distinguished feature located in point (1 – 1) at 20 m to 100 m depth. It has some type of horizontal extension towered the point (5) at a depth interval ranges between (80 – 130) m.

3- Intermediate (ρ) values distributed allover the profile at different depths, it is located at a depth ranges between (6 – 40) m in point (1 – 1), in point (2 – 1) and (3 – 1) it located between (60 – 100) m depth. (Fig. 5.2.6a). The value of this (ρ) ranges between 20 Ω.m and 40 Ω.m.

2) Lithology of profile (E – E'):

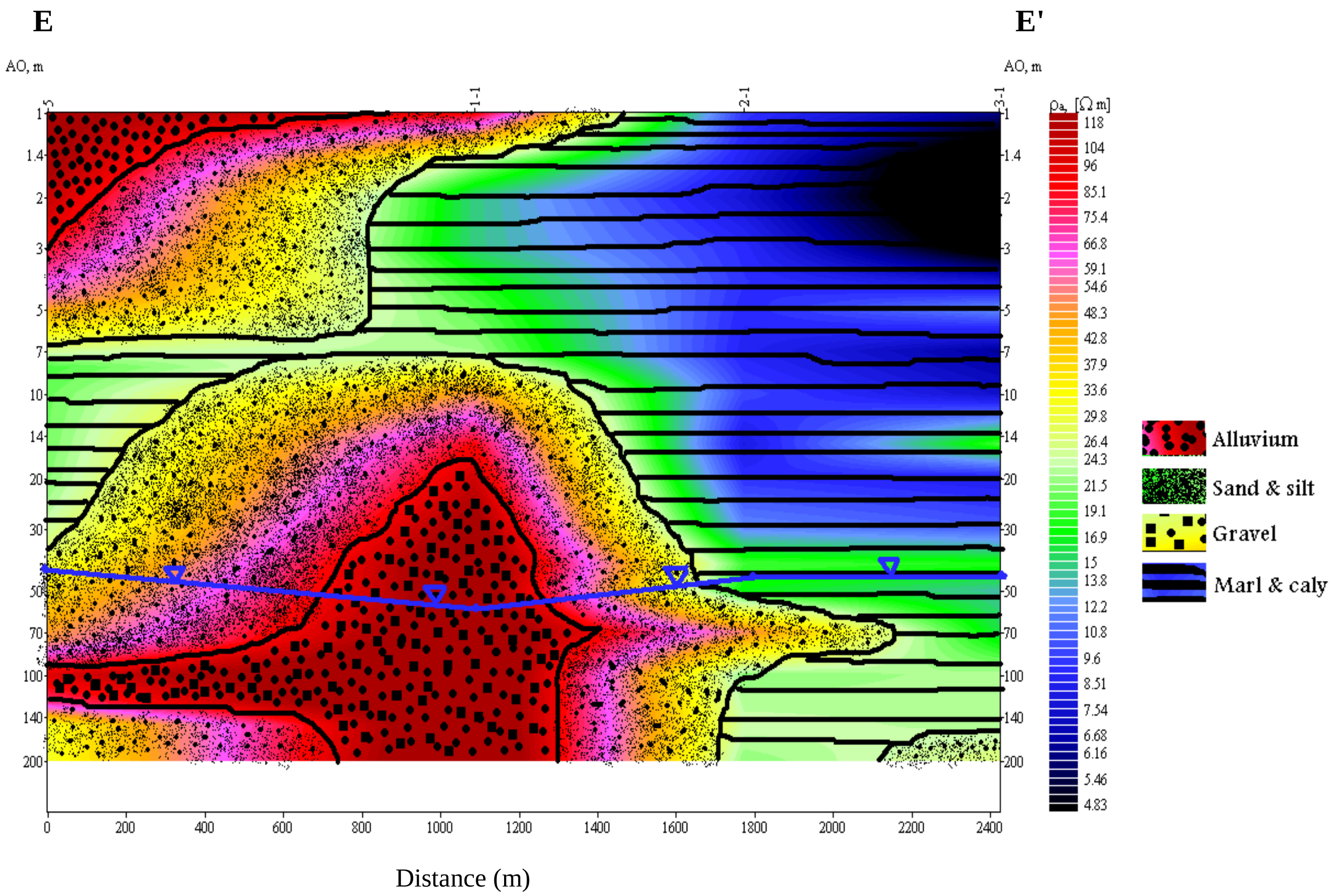

Figure 5.2.6b lithology of the electrical profile (E – E').

Alluvium deposits in dominant next to the wadi at point (5) with 5 m depth. 4 m of sand – silt layers located beneath the alluvium. Marl – clay layers mostly located in points (2 – 1) and (3 – 1) along the profile. Different sand – silt layers located under the marl – clay, it reached about 20 – 30 meters in thickness. Finally, gravel mass located in point (5) and (1 – 1) with 30 – 60 meters thickness (Fig. 5.2.6b).

Table (5.2.6) Lothological description of (E – E') profile.

Point-ID	**ρ (Ω.m)**	**Depth (m)**	**Lithology**	**Potential use for water**
5	150-300	0-3	Alluvium	Top soil
	70-30	3 7	Silt + Sand	Semi aquifer
	30-10	7 35	Marl + clay	Aquiclude
	70-30	35-80	Silt + Sand	Semi aquifer
	100-200	80-110	Gravel	Aquifer
	70-30	110-200	Silt + Sand	Semi aquifer
(1-1)	70-30	0-1.5	Silt + Sand	Top soil
	30-10	1.5-8	Marl + clay	Aquiclude
	70-30	8 18	Silt + Sand	Semi aquifer
	100-200	18-150	gravel + silt	Aquifer
(2-1)	30-10	0-50	Marl + clay	Aquiclude
	70-30	50-90	Silt + Sand	Semi aquifer
	30-10	90-150	Marl + clay	Aquiclude
(3-1)	30-10	0-150	Marl + clay	Aquiclude
	70-30	150-180	Silt + Sand	Semi aquifer

1) Profile (F – F'):

This profile located between the tow (E – E') and (G – G') (Fig. 5.2.1). It is directed west – east. This profile is composed of 4 VES measuring points. The total length of the profile was 2,417 m. the maximum depth 150 m reached in point (5), and the minimum depth was 100 m reached in the other profile point (1 – 2), (2 – 2), and (3 – 2).

S **N**

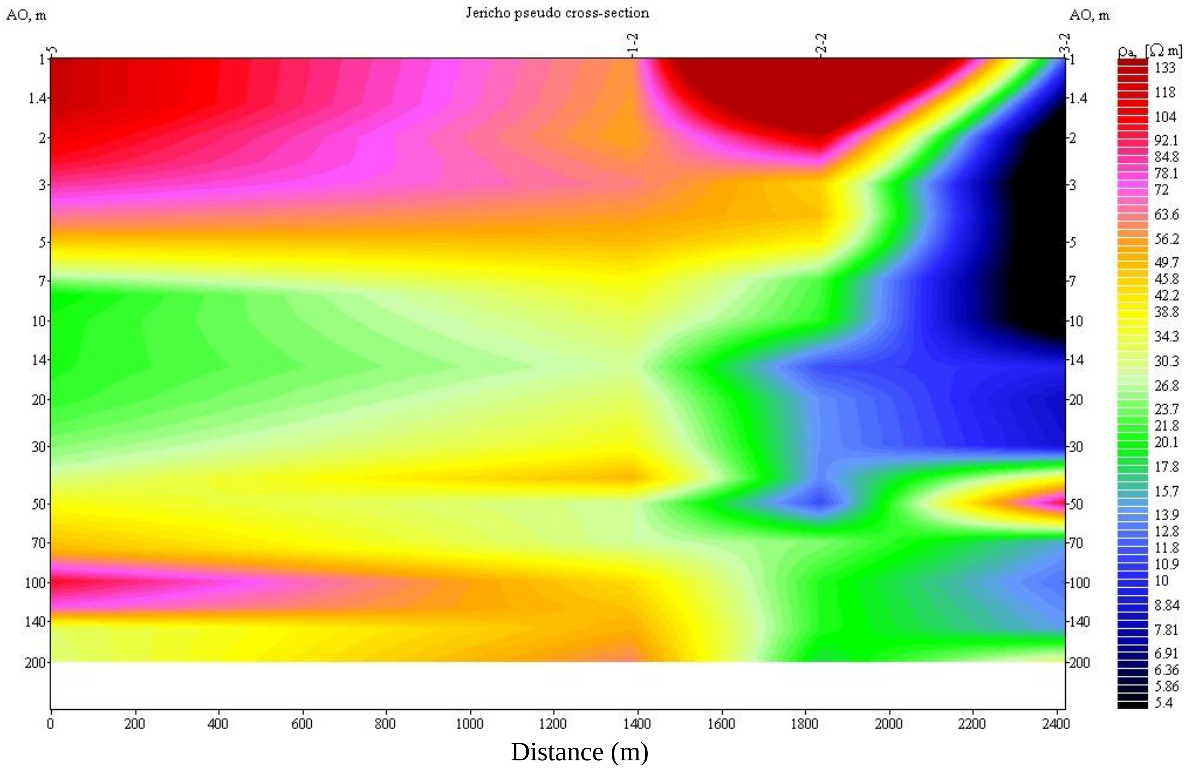

Figure 5.2.7a (F – F') electrical sounding profile.

By carefully looking into this profile, 3 types of (ρ) values could be categorized:

1- High (ρ) values ranging between 100 Ω.m to more than 200 Ω.m. this values located between the measuring points (5), (1 – 2), and (2 – 2), it is extended vertically from the surface to about 4 m depth. Also it appears in points (5) and (1 – 2) in horizontal manner at a depth ranging between (80 – 130) m. nonetheless, there is another feature characterized by the same (ρ) values located in point (3 – 2) at 50 m depth. (figure (5.2.7a)

2- Intermediate rang of (ρ) values (20 Ω.m – 100 Ω.m). tow different features copy this resistivity values, the first one located between 7 m and 70 m depth, across the points (5) and (1 – 2), in point (2 – 2) it appears in tow depths, which are (7 – 14) m and (70 – 100) m depth.

3- Low (ρ) values (less than 15 Ω.m). this values located between the measuring points (2 – 2) and (3 – 2), it is appear at a depth ranging between (14 – 50) m in point (2 – 2), it extending vertically from the surface to about 35 m depth in point (3 – 2). Also it appear in point (3 – 2) in 100 m depth. Figure (5.2.7a)

2) Lithology of profile (F – F'):

Alluvium deposits located near the wadi in point (5), also it located 2 km faraway from the wadi at point (2 – 2) with 3 m depth. Sand – silt layers located beneath the alluvium with 4 – 7 meter thickness along the profile, (figure 5.2.7b). Marl – clay layers are dominant at points (2 – 2) and (3 – 2). Moreover, sand – silt layers located beneath the marl – clay, it has a thickness between 35 – 70 meters. Two gravel mass located at 100 m depth at point (5), the other located 50 m depth at point (3 – 2). (Fig. 5.2.7b)

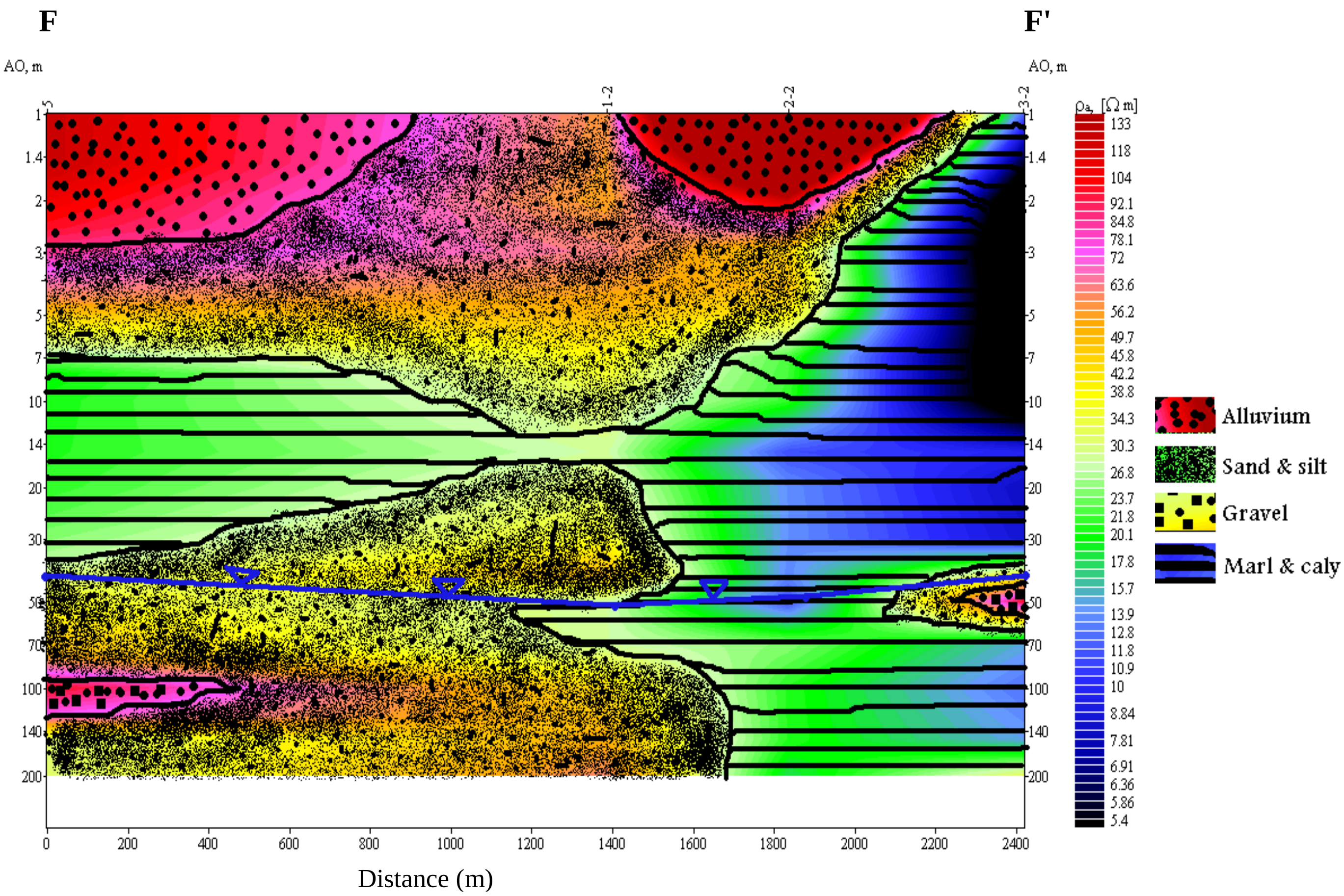

Figure 5.2.7b lithology of the electrical profile (F - F).

Table (5.2.7) Lithological description of (F – F').

Point-ID	P (Ω.m)	Depth (m)	Lithology	Potential use for water
5	150-300	0-3	Alluvium	Top soil
	70-30	3 7	Silt + sand	Semi aquifer
	30-10	7 35	Marl + clay	Aquiclude
	70-30	35-90	Silt + sand	Semi aquifer
	100-200	90-120	Gravel	Aquifer
	70-30	120-180	Silt + sand	Semi aquifer
(1-2)	70-30	0-13	Silt + sand	Top soil
	30-10	13-16	Marl + clay	Aquiclude
	70-30	16-50	Silt + sand	Semi aquifer
	30-10	50-75	Marl + clay	Aquiclude
	70-30	75-180	Silt + sand	Semi aquifer
(2-2)	150-300	0-2	Alluvium	Top soil
	70-30	2 7	Silt + sand	Semi aquifer
	30-10	7 180	Marl + clay	Aquiclude
(3-2)	30-10	0-35	Marl + clay	Aquiclude
	70-30	35-45	Silt + sand	Semi aquifer
	100-200	45-55	Gravel	Aquifer
	70-30	55-65	Silt + sand	Semi aquifer
	30-10	65-180	Marl + clay	Aquiclude

1) Profile (G – G'):

This farthest profile for Wadi Al-Qilt. (G – G') profile is composed of 4 VES measuring points. The total length of the profile is 2,503 m; it is directed west – east.

S **N**

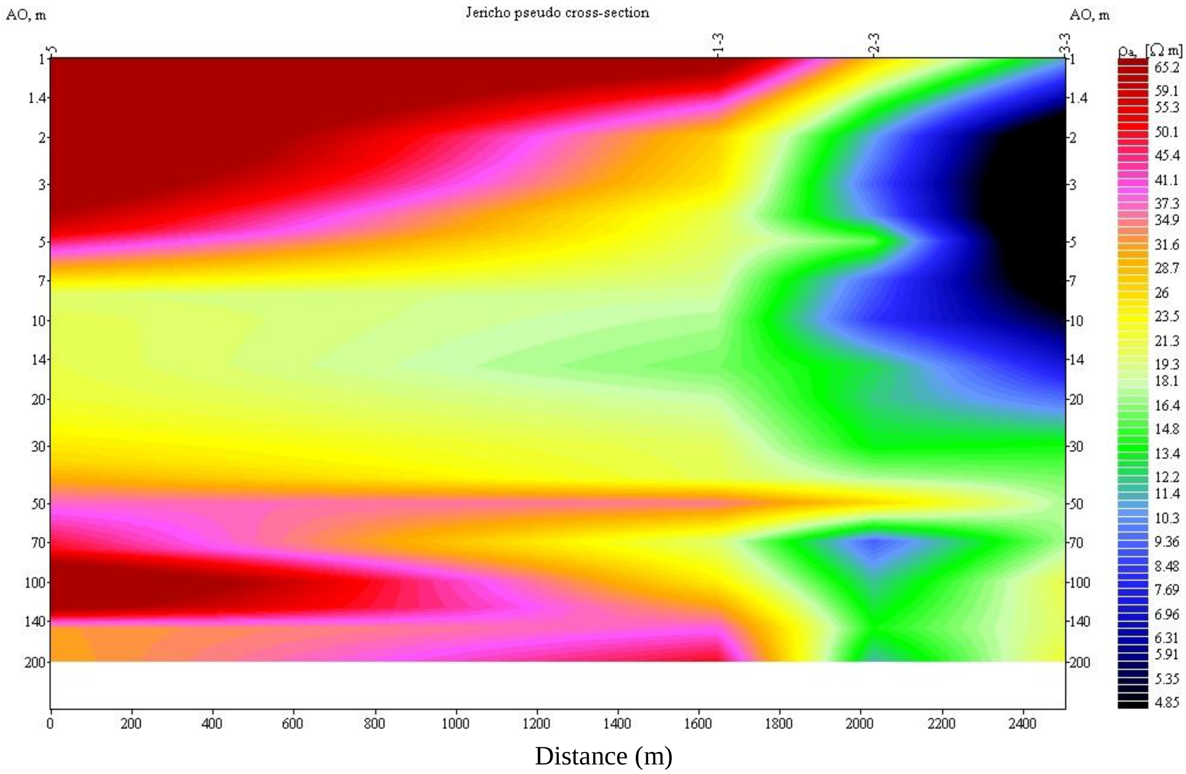

Figure 5.2.8a (G – G') electrical sounding profile.

There are three ranges of (ρ) values, the distribution of (ρ) values are describe below:

1- High (ρ) values ranging between 100 Ω.m to more than 200 Ω.m. this (ρ) values located horizontally between the points (5) and (1 – 3) at a depth ranges between (0 – 6) m in point (5) and (0 – 1.5) m in point (1 – 3). Another feature copy the same (ρ) values, it is located in point (5) at 100 m depth. (Fig. 5.2.8a)

2- Intermediate (ρ) values ranging between 20 Ω.m and 100 Ω.m. it mostly extending horizontally at points (5) and (1 – 3). In point (5) it located at a depth ranges between 7 m and 35 m in point (1 – 3). It is located between 3 m and 40 m depth. The same (ρ) values are coped in point (3 – 3) at a depth ranges between (70 – 100) m.

3- Low (ρ) values (less than 20 Ω.m), this values located on tow distinguished features. (Fig. 5.2.7). The first one could be viewed in point (2 – 3) at a depth ranging between (70 – 100) m. the second one could be viewed in point (3 – 3) at a depth ranging between (1 – 25) m. (Fig. 5.2.8a)

2) Lithology of profile (G – G'):

Alluvium deposits located near the wadi in point (5) at 3 m depth, it reached point (1 – 3) at about 1 m depth. Sand – silt layers are dominants in the profile with a 50 m thickness in average. Gravel mass located in point (5) at 100 m depth with 40 m thickness. Marl – silt layers located in point (2 – 3) and (3 – 3), it is founded in depths of the profile. About 20 m of marl – clay layers located at point (1 – 3) at 15 m depth.

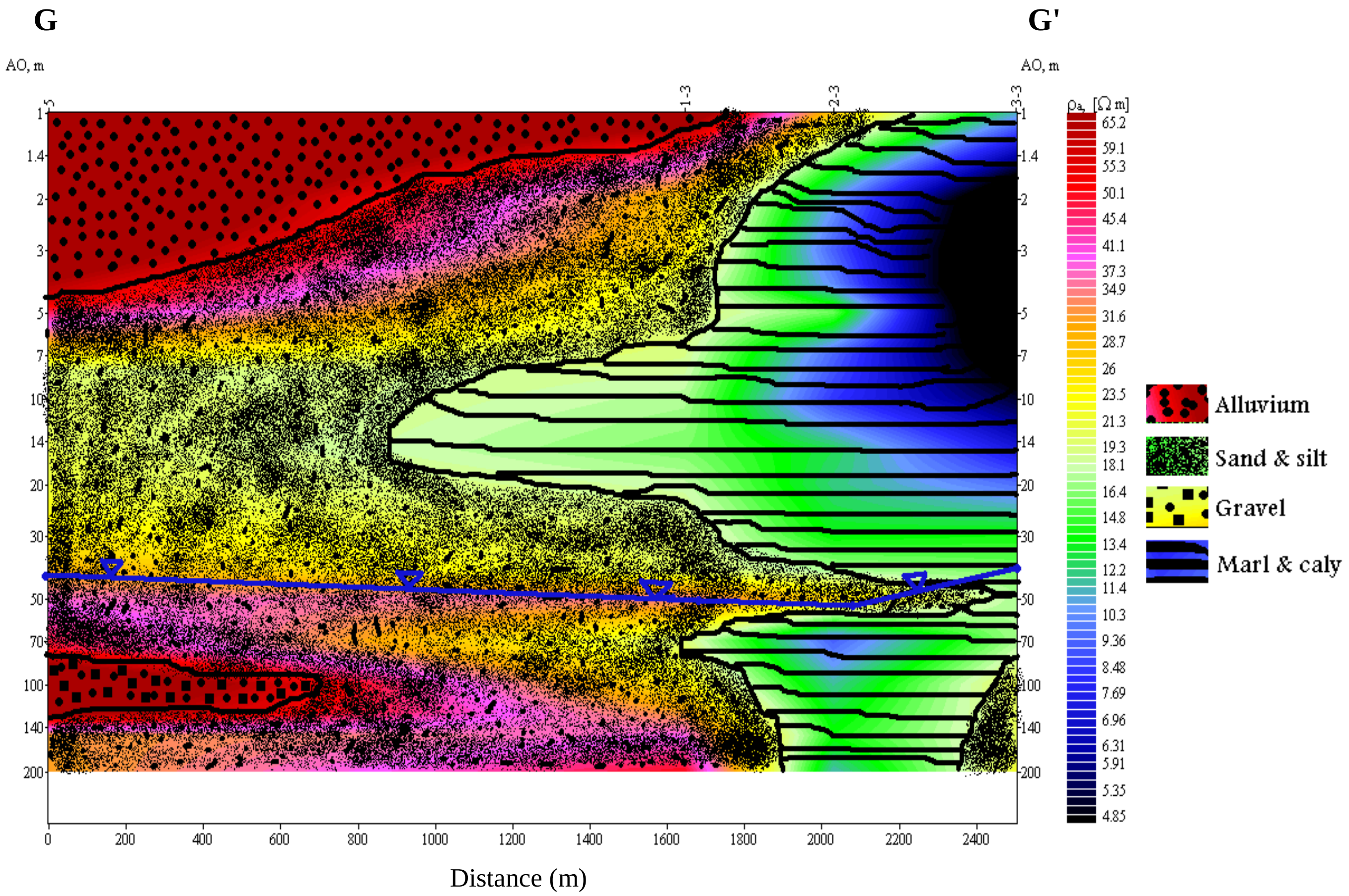

Figure 5.2.8b lithology of the electrical profile (G – G').

Table (5.2.8) Lithological description of G – G'.

Point-ID	ρ (Ω.m)	Depth (m)	Lithology	Potential use for water
5	100-250	0-4	Alluvium	Top soil
	70-30	4 75	Silt + sand	Semi aquifer
	100-200	75-125	Gravel	aquifer
	70-30	125-180	Silt + sand	Semi aquifer
(1-3)	100-250	0-1	Alluvium	Top soil
	70-30	1 7	Silt + sand	Semi aquifer
	30-10	7 25	Marl + clay	Aquiclude
	70-30	25-75	Silt + sand	Semi aquifer
	30-10	75-85	Marl + clay	Aquiclude
	70-30	85-180	Silt + sand	Semi aquifer
(2-3)	70-30	0-1.5	Silt + sand	Top soil
	30-10	1.5-40	Marl + clay	Aquiclude
	70-30	40-60	Silt + sand	Semi aquifer
	30-10	60-180	Marl + clay	Aquiclude
(3-3)	30-8	0-75	Marl + clay	Aquiclude
	70-30	75-180	Silt + sand	Semi aquifer

5.3 Soil analysis:

5.3.1 Soil permeability

Soil sieve analysis was accomplished in 10 sites along Wadi Al-Qilt, staring form the out let of the wadi and ending the area of Ketf Al-wad. The distance between each sampling site was about 600 m. the total distance of Wadi Al-Qilt pathway (between sample (1) and sample (10)) was 6,066 m. (Fig. 5.3.1); results of soil samples were arranged in (Table. 5.3.1).

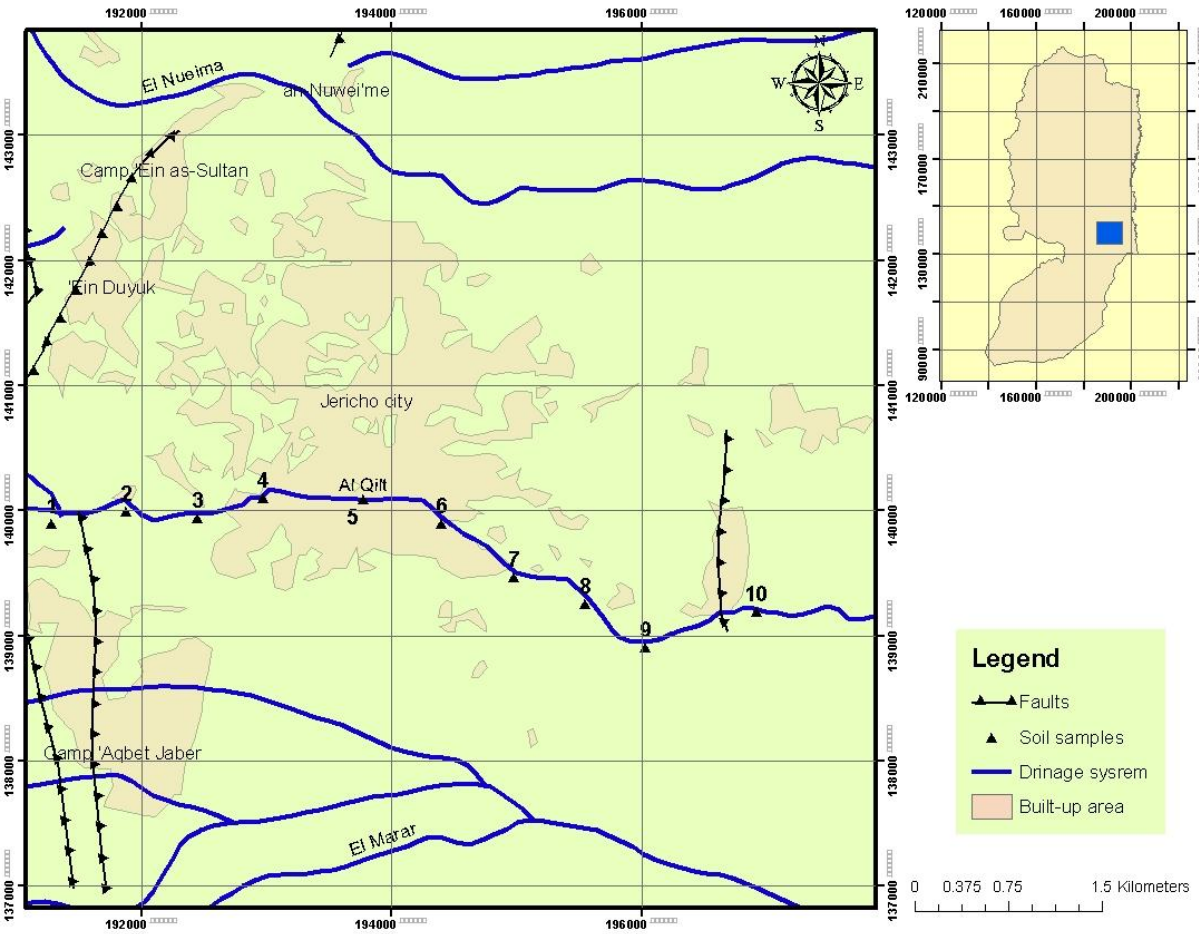

Figure 5.3.1 Wadi sediments samples location.

Samples were taken from the top soil surface of Wadi Al-Qilt. The average sampling depth was about 40 cm. sieve analysis was accomplished for the 10 soil samples. The results of the sieve analysis are listed in (Table. 5.3.1).

Table 5.3.1 sieve analysis results:

Sample ID			Sieve diameter (mm)										
	East	North	2.000	1.600	1.000	0.710	0.500	0.250	0.200	0.160	0.090	0.075	0.063
1	191283	139899	1.6	46.1	135.8	105.4	76.5	58.5	13.5	12.9	15.8	4.7	29.2
2	191875	139998	1.3	44.8	120.0	100.7	60.7	61.4	12.0	7.5	15.4	25.4	50.9
3	192444	139944	1.0	38.9	135.9	97.4	62.4	55.4	13.9	12.3	14.2	19.1	50.5
4	192968	140104	0.0	4.3	7.8	18.9	41.3	100.3	49.3	100.5	81.4	36.0	60.2
5	193772	140089	0.8	20.1	63.8	52.8	100.3	19.5	69.2	19.2	40.2	46.0	68.1
6	194395	139899	0.5	17.5	120.6	87.3	76.8	57.2	47.8	33.3	25.5	14.4	19.1
7	194979	139466	0.9	12.9	102.5	94.0	83.0	114.9	18.4	11.2	20.3	12.5	29.4
8	195549	139254	0.7	14.2	125.6	73.6	80.6	53.2	33.6	53.0	25.7	18.6	21.7
9	196027	138912	1.0	13.2	55.2	35.0	59.6	57.6	47.3	58.4	32.8	54.1	85.8
10	196915	139193	0.5	17.2	49.2	30.7	66.2	74.0	70.3	44.3	22.1	34.8	90.7

Permeability was calculated in reference with three empirical formula, Breyer, Hazan, and Kozeny equations. The permeability was chosen according to the formula applicability. Hazen equation is applicable for sediments with coefficient of uniformity less than 5 ($U<5$) and effective grain size between 0.1 and 3 mm ($0.1mm<d_{10}<3mm$), Konezy equation is applicable for coarse sand, and Brayer equation is applicable for $1<U<20$ and $0.06<U<0.6$ which makes it useful for analyzing heterogeneous porous media. Grain size distribution curve is used to determine the d_{60} and d_{10} values. Grain size distribution curves are illustrated in Appendix A. (Neven, 1997).

Table 5.3.2 permeability of the soil samples.

Sample ID	East	North	D_{60}	D_{10}	U	$K_{(Br)}$ m/s	$K_{(Hz)}$ m/s	$K_{(Ko)}$ m/s
1	191283	139899	1.000	0.180	5.556	3.268E-04	4.683E-04	6.293E-04
2	191875	139998	0.950	0.170	5.588	2.911E-04	4.177E-04	5.613E-04
3	192444	139944	1.000	0.200	5.000	4.129E-04	5.781E-04	7.769E-04
4	192968	140104	0.230	0.090	2.556	9.581E-05	1.171E-04	1.5732E-04
5	193772	140089	0.610	0.082	7.439	6.343E-05	9.718E-05	1.306E-04
6	194395	139899	0.880	0.200	4.400	4.244E-04	5.781E-04	7.769E-04
7	194979	139466	0.800	0.230	3.478	5.892E-04	7.646E-04	1.027E-03
8	195549	139254	0.840	0.180	4.667	3.395E-04	4.683E-04	6.293E-04
9	196027	138912	0.420	0.069	6.087	4.705E-05	6.881E-05	9.247E-05
10	196915	139193	0.430	0.068	6.324	4.530E-05	6.683E-05	8.981E-05

$K_{(Br)}$: permeability after Breyer. $K_{(Hz)}$: permeability after Hazen. $K_{(Ko)}$: permeability after Kozeny.

Breyer empirical formula was chosen for the above reasons, Surface permeability is varying along the wadi, it is began with 3.268E-04 m/s in the outlet area at point (1), and it still in the same domain in the points (2) and (3), it decrease in site (4) and (5) and then it again increase in the sampling points (6), (7), (8). Surface permeability decrease again in sampling points (9) and (10). (Fig.5.3.2)

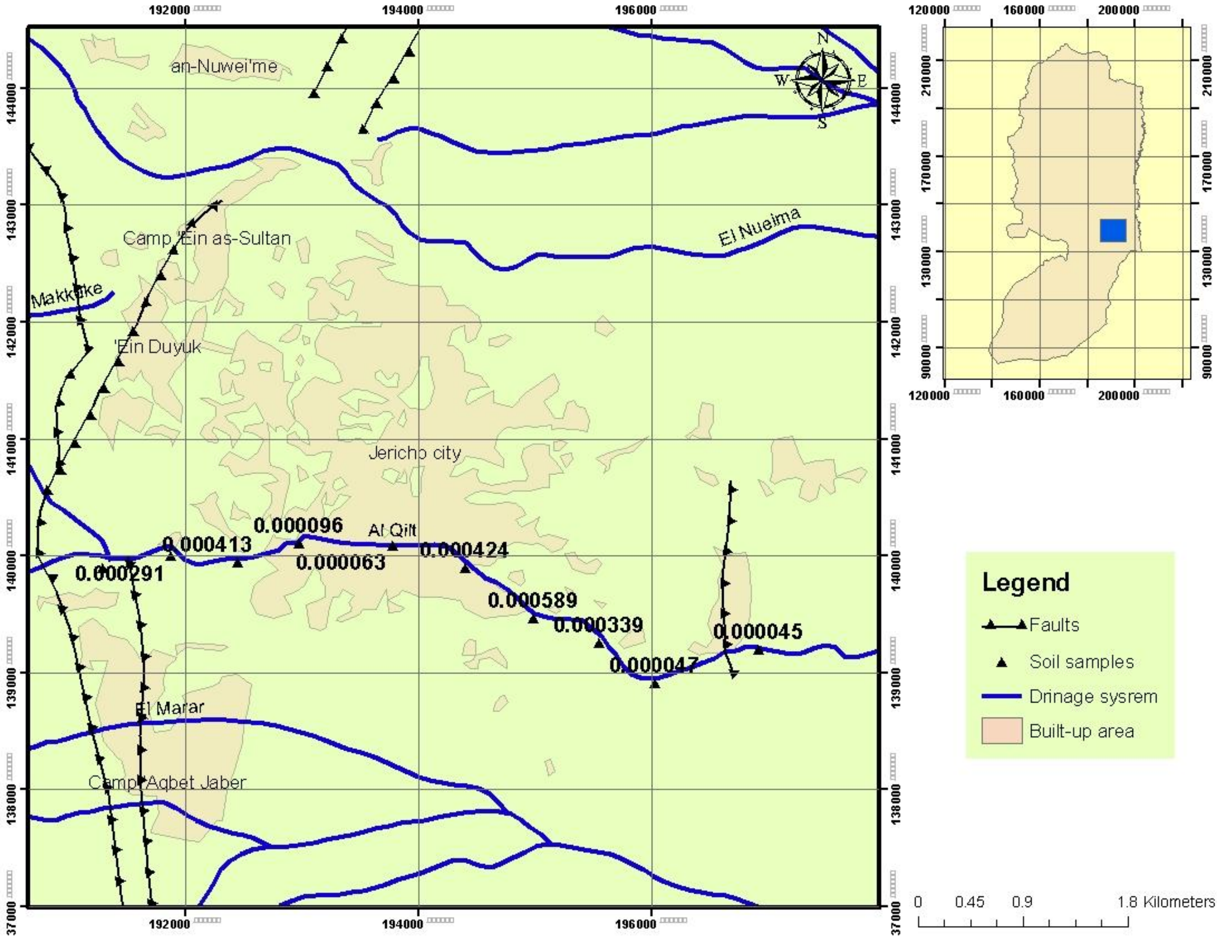

Figure 5.3.2 permeability distribution along the surface of Wadi Al-Qilt.

5.3.2 Soil texture

Soil texture classification was performing for the 10 soil samples. USDA classification scheme was used in soil classification (USDA, 1993). Samples (9) and (4) were consider as clay soils, sample (10) consider as clay loam soil, samples (8) and (5) are considered as sandy clay loam soils. Whereas the rest samples ((1), (2), (3), (6), and (7)) are considered as sandy loam soils. (Fig. 5.3.3)

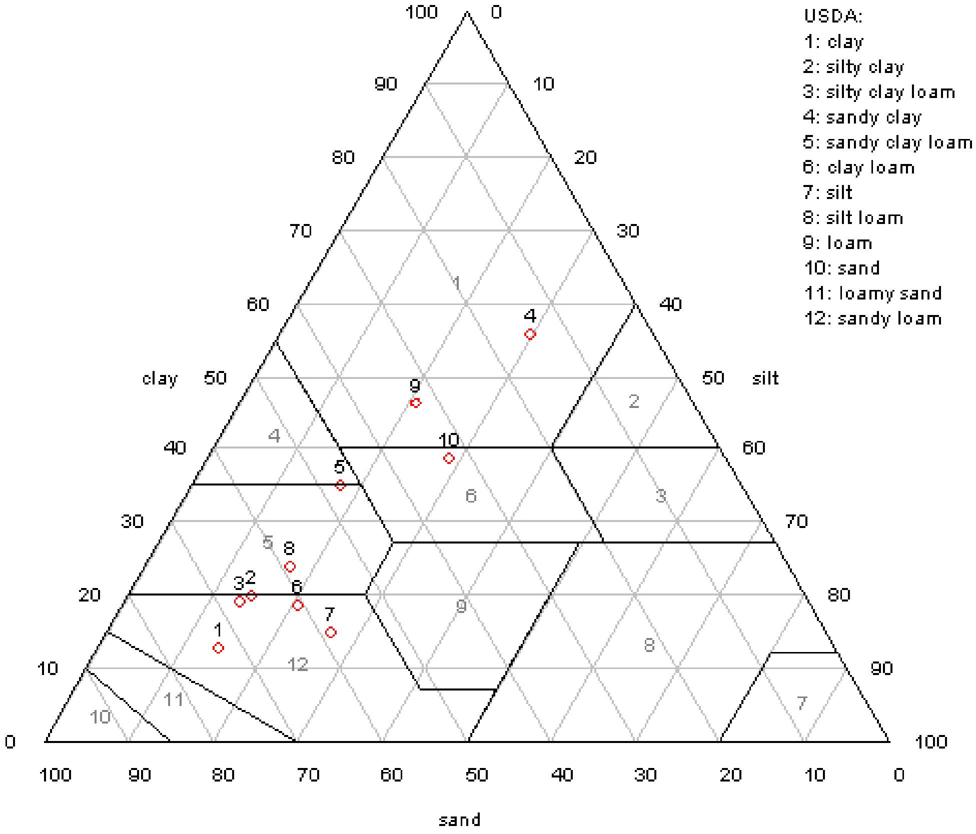

Figure 5.3.3 texture classification for Wadi Al-Qilt sediments samples.

Table 5.3.3 permeability and texture of the soil samples.

Sample ID	**East**	**North**	**$K_{(Br)}$ m/s**	**Soil texture**
1	191283	139899	3.268E-04	Sandy loam
2	191875	139998	2.911E-04	Sandy loam
3	192444	139944	4.129E-04	Sandy loam
4	192968	140104	9.581E-05	Clay
5	193772	140089	6.343E-05	Sandy clay loam
6	194395	139899	4.244E-04	Sandy loam
7	194979	139466	5.892E-04	Sandy loam
8	195549	139254	3.395E-04	Sandy clay loam
9	196027	138912	4.705E-05	Clay
10	196915	139193	4.530E-05	Clay loam

5.4 Groundwater Water quality

Groundwater chemistry is introduced to clarify the water – rocks interactions. Groundwater chemical analysis for 34 well is obtained form (PWA, 2008). It is distributed allover Jericho area. (Fig. 5.4.1). This data included the electrical conductivity (EC), chloride concentration, Sulfate concentration, and Sodium concentration.

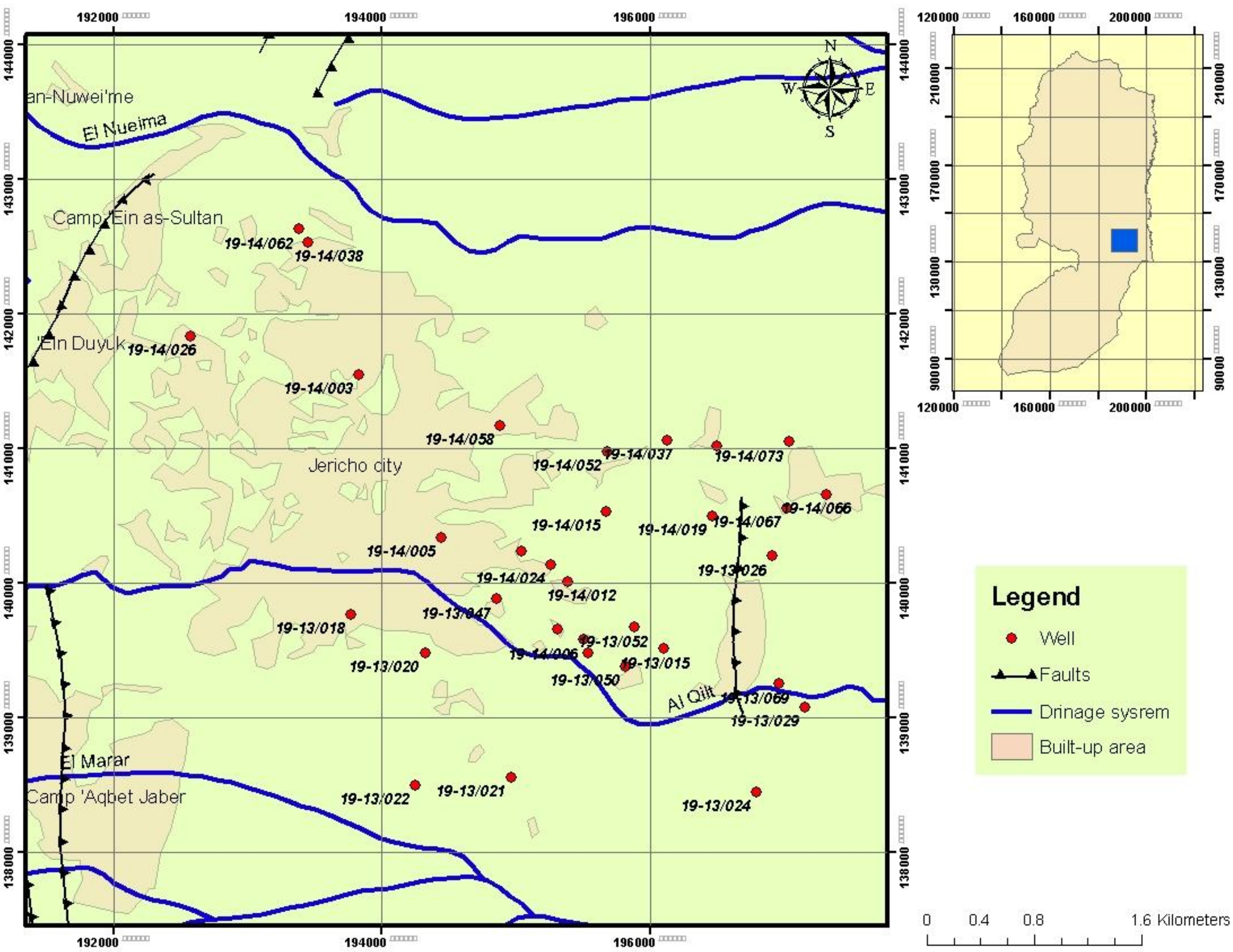

Figure 5.4.1 location of the groundwater analyzed wells.

High variation located among the chemical analysis data. Chloride concentration founded in the ranges between (38.4 - 2425.0) mg/l, also there area a huge variation in the sulfate and sodium concentrations, sulfate ranges between (19.0 – 600.1) mg/l, sodium concentration ranges between (25.5 – 920.1) mg/l. Nevertheless, EC ranges between (480 – 6846) µS/cm, chemical analyses were arranged in (Table 5.4.1).

Table 5.4.1 chemical analysis of the selected groundwater wells.

Date	Well ID	East	North	Elevation	Depth	EC	pH	Temp	Cl^-	SO_4^{2-}	Na^+
		(m)	(m)	(m.b.s.l)	(m)	(µS/cm)		°C	mg/l	mg/l	mg/l
5/12/2007	19-13/006	195500	139580	-278.99	80	2495	6.7	22.4	645.7	187.3	265.2
5/12/2007	19-13/015	196100	139510	-292.69	63	2115	7.1	23.9	500.0	54.2	240.1
5/12/2007	19-13/018	193770	139770	-260.00	90	2325	7.2	25.1	190.0	124.8	136.2
5/12/2007	19-13/020	194320	139480	-270.00	83	1579	7.0	22.3	405.0	161.8	222.0
5/12/2007	19-13/021	194960	138560	-279.00	72	2997	7.3	22.4	685.5	100.0	314.4
5/12/2007	19-13/022	194250	138500	-272.00	81	2150	7.4	26.0	470.0	250.3	280.0
5/12/2007	19-13/024A	196785	138449	-306.85	75	3430	6.9	24.0	793.1	600.1	350.1
5/12/2007	19-13/026A	196900	140200	-233.00	90	2825	7.1	25.0	685.6	180.3	284.2
5/12/2007	19-13/026B	195680	140980	-240.00	84	2140	7.4	25.6	480.5	120.2	110.2
5/12/2007	19-13/029	197150	139080	-310.00	130	3580	7.2	22.1	840.6	403.0	380.1
5/12/2007	19-13/047	194850	139880	-278.30	74	1342	6.9	22.0	245.3	65.9	172.5
5/12/2007	19-13/048	195310	139660	-285.00	57	1436	6.9	22.0	438.2	112.3	179.7
5/12/2007	19-13/049	195530	139480	-290.00	70	2949	7.2	24.0	121.0	64.0	214.0
5/12/2007	19-13/050A	195810	139380	-290.00	100	1927	7.0	22.9	453.6	80.3	220.1
6/1/2008	19-13/052	195880	139670	-289.00	120	3255	6.9	19.8	1030.1	309.3	407.2
6/1/2008	19-13/069	196950	139250	-315.00	132	4070	7.1	25.0	1040.0	108.3	618.1
6/1/2008	19-14/003	193830	141550	-256.00	120	3220	7.0	26.0	857.9	64.0	289.1
6/1/2008	19-14/005	194440	140340	265.44	65	1050	7.0	23.8	124.3	41.7	145.6
6/1/2008	19-14/006	195500	139580	-278.99	80	1835	7.0	23.0	350.7	163.1	176.2
6/1/2008	19-14/012	195380	140010	-282.00	79	823	7.2	13.8	103.5	55.1	95.0
6/1/2008	19-14/015	195670	140530	-285.00	93	2355	6.7	22.0	554.6	70.3	238.1
6/1/2008	19-14/019	196460	140500	-291.85	67	3995	6.8	22.0	980.4	369.1	395.2
6/1/2008	19-14/020	196490	141020	-295.00	60	3940	7.2	23.4	1490.2	154.2	400.2
6/1/2008	19-14/023	195040	140240	-295.00	60	1380	6.9	21.6	270.5	51.3	145.2
6/1/2008	19-14/024A	195260	140140	-280.00	65	4370	7.1	24.2	943.8	590.2	369.0
6/1/2008	19-14/026A	192573	141834	-233.47	85	1143	6.9	22.8	118.0	19.0	71.0
8/3/2008	19-14/037	196120	141060	-287.30	83	3623	7.0	24.5	883.6	156.2	249.0
8/3/2008	19-14/038	193450	142530	-244.00	110	2230	7.0	25.5	495.0	52.3	167.0
8/3/2008	19-14/052	195680	140980	-282.00	82	2930	7.3	26.0	685.3	90.0	285.0

8/3/2008	19-14/058	194880	141170	-270.00	63	480	7.6	21.0	38.4	23.8	25.5
8/3/2008	19-14/062	193380	142630	-240.00	120	2025	7.1	25.0	490.1	50.2	258.5
8/3/2008	19-14/066	197310	140660	-309.88	33	5840	6.8	25.0	1692.0	290.1	801.3
8/3/2008	19-14/067	197010	140560	-308.00	73	6846	6.8	25.0	2425.0	188.3	920.1
8/3/2008	19-14/073	197030	141050	-305.00	80	4050	6.9	24.7	1355.0	143.2	479.1

Source: (PWA, 2008).

ArcGIS 9.2 was used to generate contour maps for Chloride, Sulfate, Sodium, and EC. Chloride concentration contoured in (Fig 5.4.2), chloride concentrations increased toward the east, this increase is due to the absorption of sodium by clay minerals (Jundi, 2005), clay minerals founded mostly in the Lisan formation which clarify the distribution manner of the high chloride values.

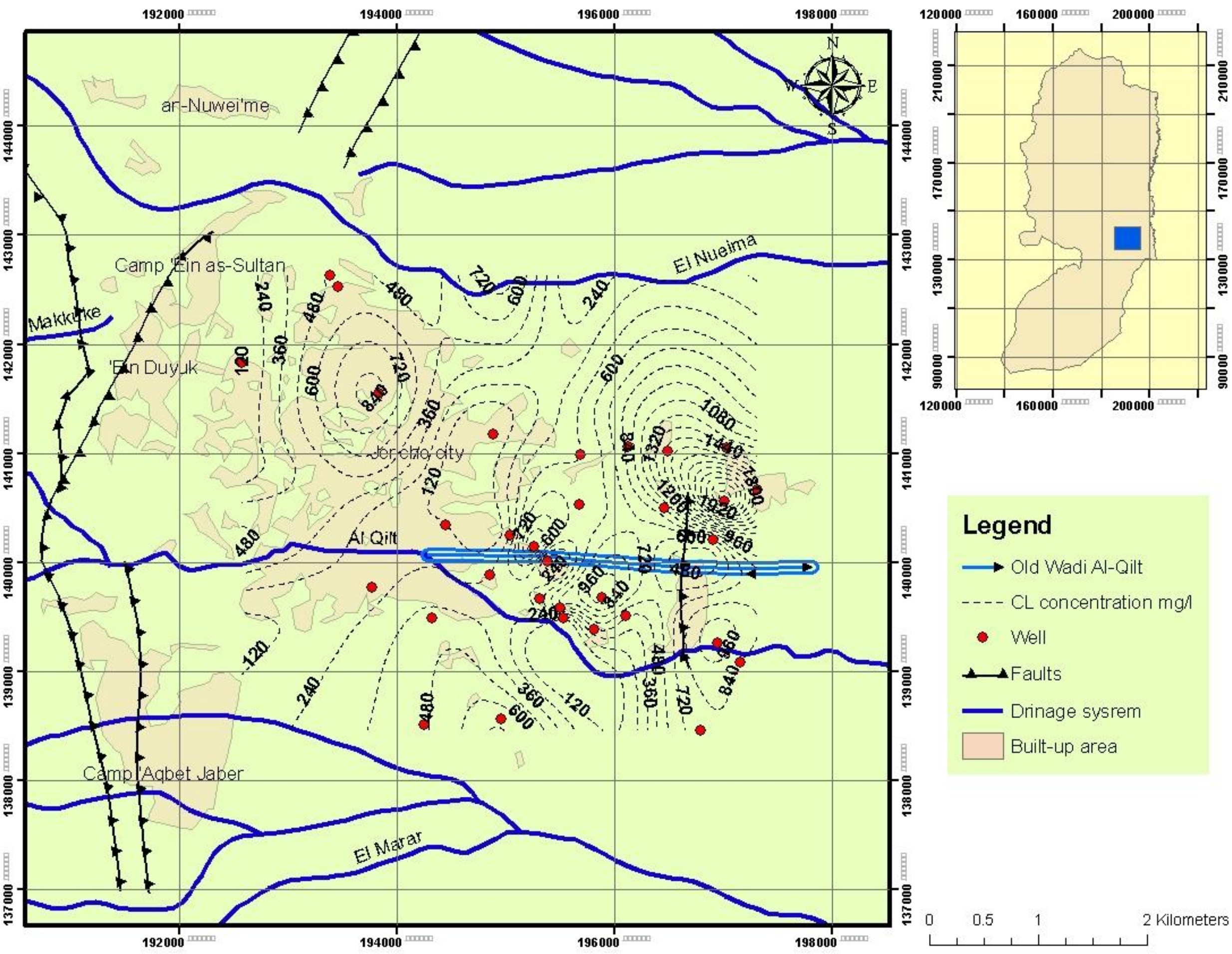

Figure 5.4.2 groundwater Chloride contour map.

The sulfate distribution is note illustrated in the same way of the chloride distribution; it is increased toward the east. (Fig 5.4.3), and groundwater sulfate increase due the dissolution of evaporates salts (Gypsum) form Lisan Formation, the effect of fresh water which comes from the infiltration of Wadi Al-Qilt runoff is clear shown in both sides of the of the Wadi.

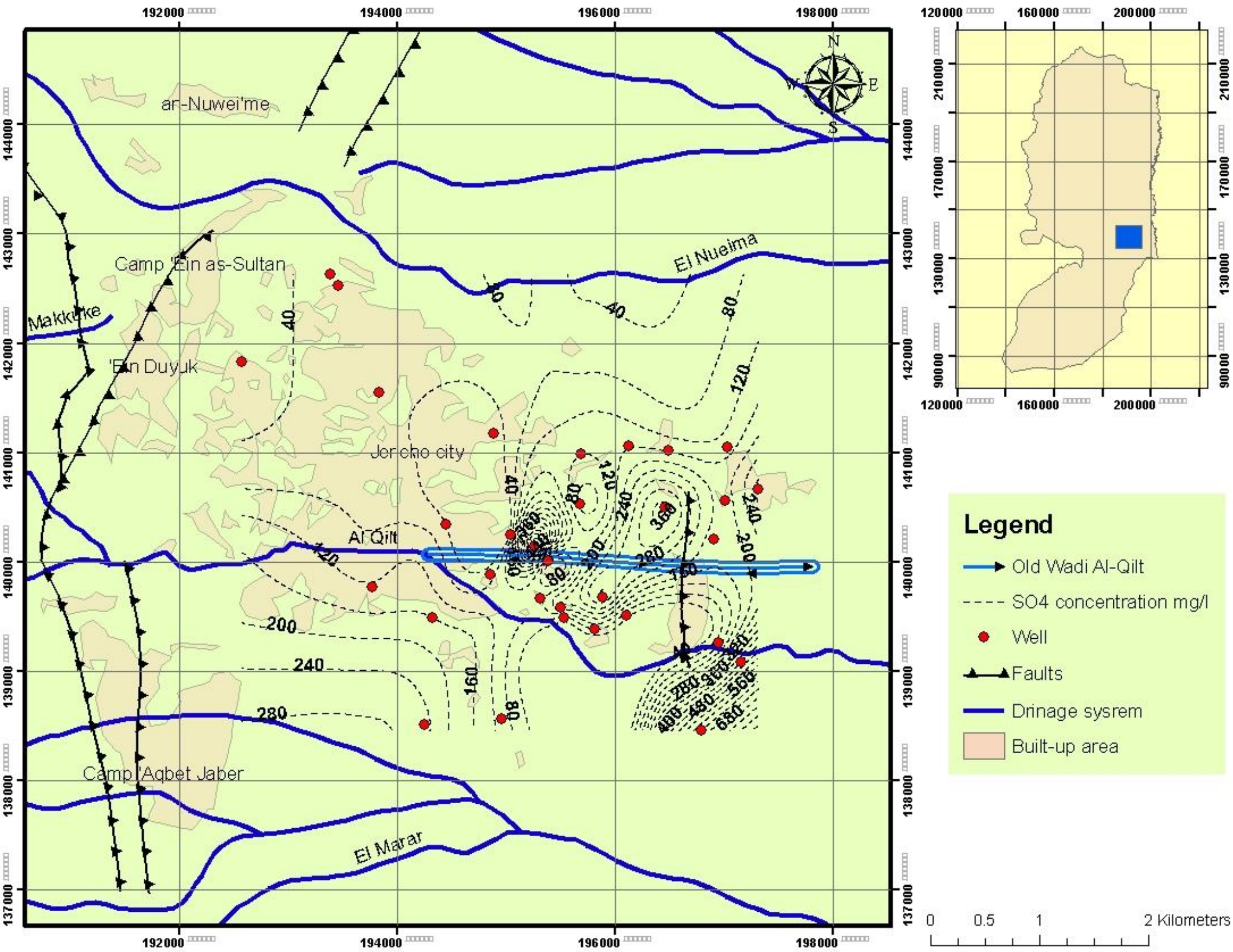

Figure 5.4.3 groundwater Sulfate contour map.

Sodium concentrations distributed in the same way of chloride behave. It is increased toward the east. (Fig. 5.4.4), it is comes from the mixing of the up conning of the deep brine water with the fresh Pleistocene groundwater (Nasser ed Din, 1999) Nonetheless, the salt dissolution of Lisan Halite is another geochemical factor rise up the concentration of Sodium in the groundwater. (Jundi, 2005)

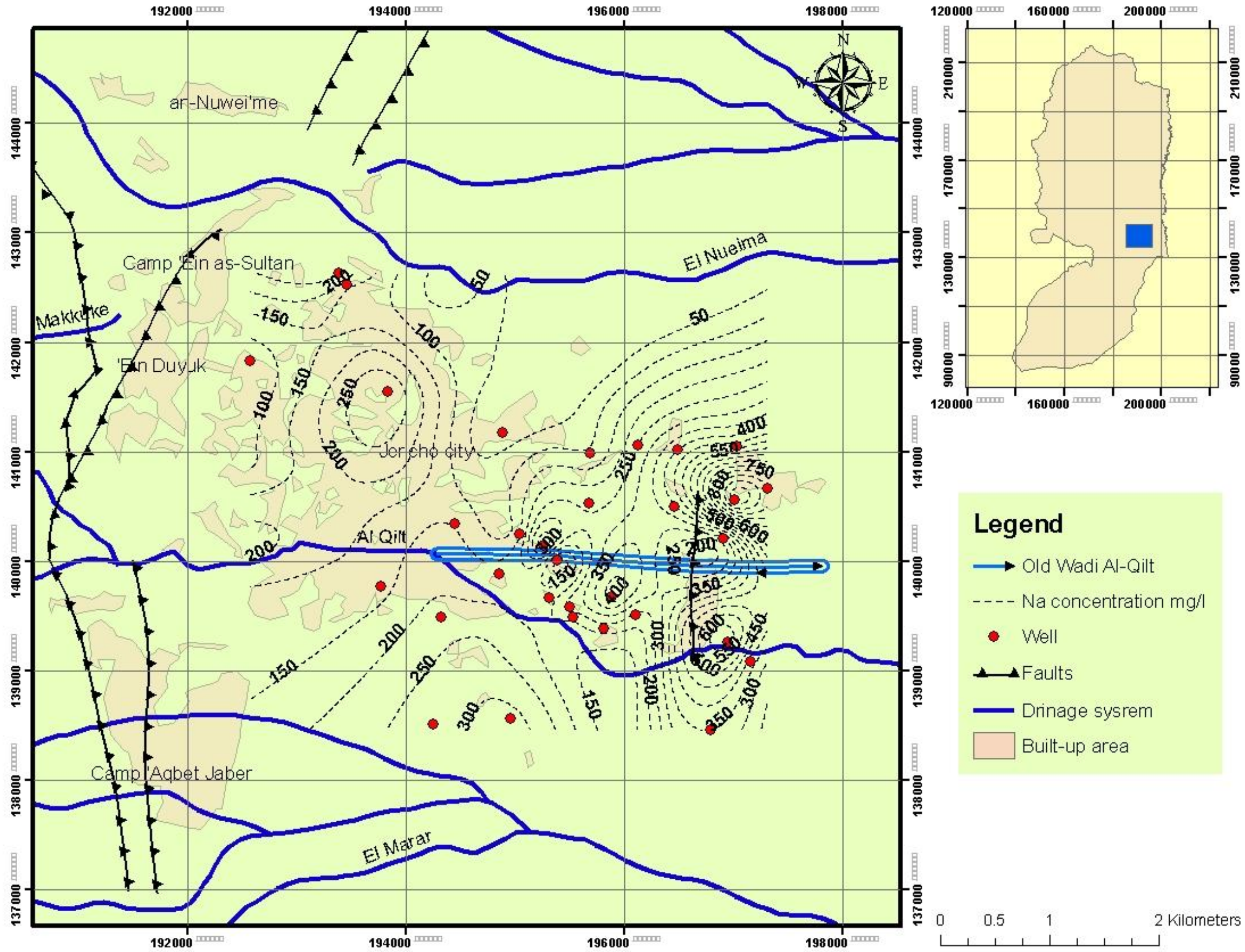

Figure 5.4.4 groundwater Sodium contour map.

Contour map 5.4.5 shows a general electrical conductivity (EC) increase toward the east, also the effect of freshwater which come form Wadi Al-Qilt infiltrated runoff is evidently show. The values of EC are decreased along the Wadi.

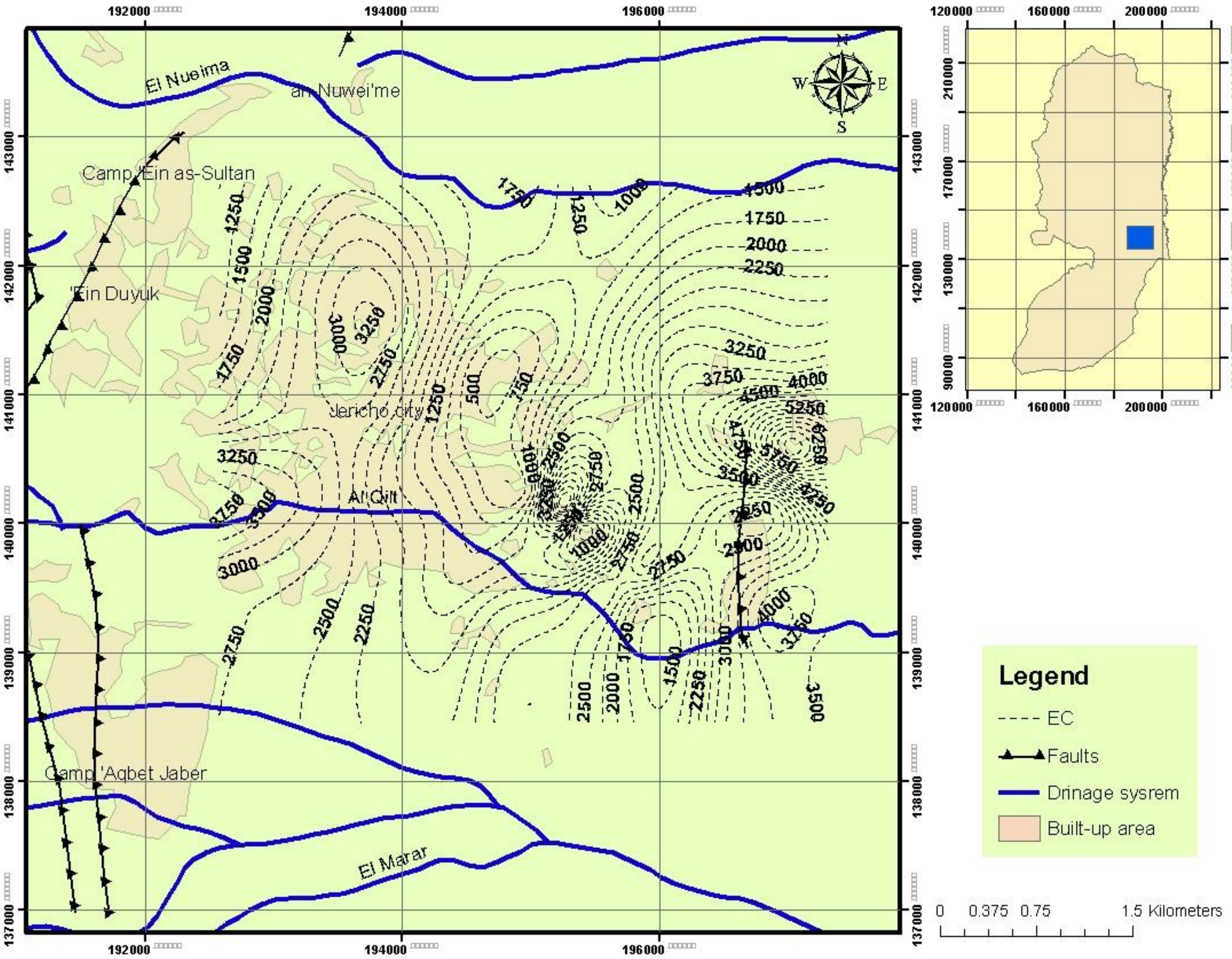

Figure 5.4.5 electrical conductivity contour map.